STATIONARY WAVES AND ANTIDUNES IN ALLUVIAL CHANNELS

Thesis by

John Fisher Kennedy

In Partial Fulfillment of the Requirements

For the Degree of

Doctor of Philosophy

California Institute of Technology

Pasadena, California

1960

ACKNOWLEDGEMENTS

The writer would like to express his appreciation for the guidance and assistance offered by Professor Norman H. Brooks throughout the course of this investigation.

The writer is also indebted to Professor Vito A. Vanoni for valuable criticism of many aspects of the research.

The laboratory investigation was carried out with the aid of the Agricultural Research Service of the U. S. Department of Agriculture, Contract 12-14-100-995(41).

During the academic year 1959-60, the writer carried on the research with the aid of the Corning Glass Works Foundation Fellowship in Engineering.

For their assistance in typing and preparing the figures for this thesis, the writer would like to extend his gratitude to Mr. Carl Eastvedt, Miss Evangeline Gibson, Mrs. Barbara Hawk, and Mr. Robert C. Y. Koh.

ABSTRACT

A theoretical and laboratory investigation was made of antidunes and associated stationary waves. The objectives were to determine the factors involved in the formation of antidunes, the characteristics of the stationary waves, and the effects of antidunes and waves on the friction factor and sediment transport capacity of streams.

In the potential flow solution for flow over a wavy bed it was hypothesized that the flow shapes the erodible sand bed by scour and deposition to conform to a streamline of the flow configuration for which the energy is a minimum. Under this hypothesis, flow over antidunes is the same as the segment of flow above an intermediate streamline of the fluid motion associated with stationary gravity waves (waves with celerity equal and opposite to the flow velocity) in a fluid of infinite depth. For a velocity V the wave length, λ, is given by

$$\lambda = \frac{2\pi V^2}{g}$$

and waves break when their height reaches 0.142λ. Laboratory and field data for two-dimensional antidunes confirmed these relations.

Forty-three experimental runs in laboratory flumes were made for different depths and velocities and bed sands of two different sizes (0.55 mm and 0.23 mm). No general criterion for the formation of antidunes or the occurrence of breaking waves could be formulated because of inadequate knowledge of the complex sediment transport phenomenon. Qualitatively, it was found that for a given sand, the critical Froude number for the occurrence of breaking waves decreased as the depth was increased. Over a certain range of depth and velocity it was found that the flow formed waves and antidunes or was uniform depending on whether or not the flow was disturbed to form an initial wave. Waves that did not break had no measurable effect on the transport capacity or friction factor, but breaking waves increased both of these quantities.

TABLE OF CONTENTS

Chapter		Page
1.	INTRODUCTION	1
1-1	Stationary Waves and Antidunes in Alluvial Channels	1
1-2	Historical Background	4
1-3	Purpose and Scope of this Investigation	10
2.	ANALYTICAL CONSIDERATIONS	12
2-1	Equations of Flow over a Deformable Wavy Bed	13
2-2	Flow over a Rigid Wavy Bed	15
2-3	Form of the Bed Profile	18
2-4	Velocity-Wave Length Relation for Flow over Antidunes	19
2-5	Breaking of Stationary Waves	24
2-6	Movement of Antidunes	25
2-7	Velocity-Wave Length Relation for Three-Dimensional Waves	27
2-8	Summary	29
3.	APPARATUS AND PROCEDURE	31
3-1	The 40-foot Recirculating, Tilting Flume	31
3-2	The 60-foot Recirculating, Tilting Flume	38
3-3	Experimental Procedure	42
3-4	Temperature Control	44
3-5	Discharge Measurements	45
3-6	Movable Carriages	46
3-7	Determination of Water Surface Elevation and Water Surface Slope	48
3-8	Measurement of Bed Elevation	53
3-9	Computation of Depth, Mean Velocity, and Slope of the Energy Gradient	55
3-10	Measurement of Total Sediment Load	61
3-11	Wave Length Measurement	67
3-12	Photographs	68
3-13	Calculation of Bed Shear and Friction Factor	69
3-14	Reproducibility	73
3-15	Sand Characteristics	75
4.	EXPERIMENTAL RESULTS	80
4-1	General Outline of Experiments	80
4-2	Some General Features of High Velocity Flow over a Sand Bed	81
4-3	Observations of Bed and Water Surface Configurations	93
4-4	Hydraulic and Sediment Transport Characteristics of the Laboratory Streams	128

Chapter Page

5. DISCUSSION OF RESULTS 143

5-1 Velocity-Wave Length Relation 143
5-2 Discussion of the Mechanism of Antidune Formation and Growth 146
5-3 Criteria for the Formation of Antidunes and Breaking Waves 150
5-4 Discussion of Gilberts' Experiments and Langbein's Criterion for Antidunes 153
5-5 Effect of Waves on Sediment Transport Rate 156
5-6 Stationary Waves of Finite Amplitude 157
5-7 Antidunes and Stationary Waves in Natural Streams 158

6. SUMMARY OF CONCLUSIONS 164

APPENDIX. Summary of Notation 168

REFERENCES 171

CHAPTER 1

INTRODUCTION

1-1. Stationary Waves and Antidunes in Alluvial Channels

Consider the steady, uniform flow of water over a bed of sand. If the sand bed was flat when the flow was started, one might expect, without prior experience in the matter, that the bed would remain flat. That such is not the case is well known. When the flow velocity is great enough to move the individual sand grains, but smaller than another limiting value which will be discussed presently, the bed deforms into irregular features called dunes which are familiar to everyone who has ever looked closely at a bed of a natural alluvial stream, drifting sand, or wind-blown snow. The salient features of dunes are their arrangement, which may be quite irregular for the individual dunes but periodic in the statistical sense; their movement, which is almost always in the direction of flow; and the flow separation which frequently occurs at the downstream edge of each dune.

When the velocity is increased until the Froude number (based on the depth of flow) approaches unity, the water surface becomes somewhat unstable, and even very small disturbances give rise to rather large surface waves. If dunes are still present, the dunes interact with the water surface and a stationary surface wave is formed above each dune, as shown in figure 1-1.

For most sand sizes there exists a limiting value of velocity above which the dunes disappear and the bed becomes flat. The velocity at which this occurs depends on the depth of flow and the characteristics of the sand. If the character of the sand is such that the bed has

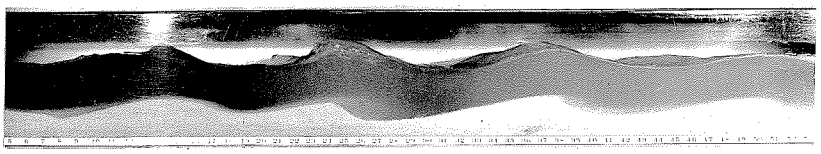

Fig. 1-1. Side view of flow over dunes which interact with the free surface. Run 5-3, flow depth = 0.245 ft, mean velocity = 2.18 ft/sec, Froude number = 0.776, wave length = 1.00 ft, mean sand size = 0.549 mm. Flow from left to right.

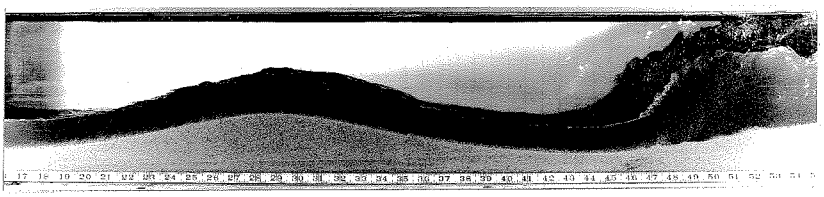

Fig. 1-2. Side view of flow over a wavy sand bed. Note breaking wave at right. Run 5-14, flow depth = 0.123 ft, mean velocity = 4.65 ft/sec, Froude number = 2.34, wave length = 2.65 ft, mean sand size = 0.549 mm. Flow from left to right.

achieved the flat condition and if surface waves occur, the perturbation velocities associated with the waves act on the bed to form regular two-dimensional waves of sand as shown in figure 1-2. Successive sand waves are generated from a flat bed and form trains of three or more waves which grow in amplitude and often become so high that the surface waves break, as the wave at the right in figure 1-2 has just done. The agitation accompanying the breaking usually obliterates the sand waves and the bed again becomes flat. The cycle of wave initiation, growth, and breaking is then repeated, each cycle taking about 1 to 3 minutes in the flume depending of the character of the sand and the flow parameters. The sand waves will often spontaneously diminish in amplitude and the bed will again become flat without the surface waves having broken.

The two types of bed features just described which strongly interact with the free surface are called antidunes. Antidunes are here defined as any disturbances on the bed of an alluvial channel which are periodic or nearly so, and which are strongly coupled with stationary free-surface waves. Under this definition, dunes are a type of antidune when they interact with the free surface, as in figure 1-1. The surface water waves which form above antidunes are called stationary waves* because they move very slowly if at all.

---

* The surface waves accompanying antidunes have been called standing waves by other authors (1, 2). However, by usage, the term standing wave has come to be associated with surface waves which are not propagated and whose surface elevation is harmonic in time at a fixed location (3), although Milne-Thomson (4) uses both terms in connection with this phenomenon. Such waves accompany surface disturbances in closed basins. The surface waves accompanying antidunes will be called stationary waves by this writer since this term describes them more precisely.

Antidunes and stationary waves are frequently observed in natural alluvial rivers and streams. They are most common in steep streams which carry large loads of sediment. The stationary waves often have heights of several feet and wave breaking causes severe local scour which can endanger bridge piers. In the last 60 years, numerous field, laboratory, and theoretical studies have been made of the mechanics of alluvial streams with dunes and flat beds and the understanding of their behavior has steadily improved. However, no comprehensive study has been made of antidunes and their effects on channel roughness and the sediment transport capacity of streams.

Antidunes and stationary waves in alluvial channels and their occurrence, behavior, and effects constitute the subject of this investigation. They will be more fully described in the next section which quotes several historical descriptions of the phenomenon.

1-2. Historical Background

Apparently the first description of antidunes published in English was presented by Cornish (5) in 1899. In a paper presented to the Royal Geographical Society, Cornish proposed the name "kumatalogy" for the study of waves and wave-structures of the atmosphere, hydrosphere, and lithosphere. Cornish felt that it would be advantageous to group all wave phenomena together and treat them as a single subject. In describing the behavior of streams "which plough their way through sandy beaches to the sea", Cornish observed that such streams often had surface waves. He then went on to describe the waves as follows:

> The water-wave was really controlled by a submerged sand-wave, the up-stream flank of which was exposed to a heavy shower of sand from the turbid water. The stream being

> shallow and its surface in waves, the crest of the water-wave was pushed up-stream as the up-stream flank of the sand-wave received additions of material. The scour of the water was thereby deflected, and the lee slope of the sand-hill moved up-stream, although every particle of sand and every particle of water travelled down-stream. (pp. 625-626)

Cornish presented a photograph of stationary waves in a stream and a sketch which illustrated his description of the mechanism of upstream movement.

In 1908 while discussing a paper presented by Owens (6), also before the Royal Geographical Society, Cornish presented his observations "made in streams in which the ordinary or best-known ripples had been replaced by those which move upstream" (p. 421). In reply to Cornish, Owens stated that he too had observed the same type of stream behavior:

> I may say that I have observed the peculiar sand-waves which he (Cornish) referred to, and, roughly speaking--I did not get an accurate measurement--I thought their formation began at about 3 feet per second. The small ordinary ripples were swept away, and suddenly a large wave, of about 3 feet from crest to crest and about 2 inches high, was suddenly formed; and it travelled up against the stream, as distinct from the small ripples, by the transference of sand from the front of one to the back of the other. (p. 424)

The first description of the antidune regime of flow in the American literature was given by Murphy (7) in 1910. Murphy worked with G. K. Gilbert during the course of the laboratory investigation which was reported by Gilbert (8) in 1914*. The project was sponsored

---

* Actually, a large part of the laboratory investigation was carried out by Murphy. Gilbert became ill while the investigation was in progress and was forced to withdraw from it. Murphy prepared a preliminary report on the investigation and is credited with many of the conclusions. However, Gilbert published the final report.

by the U. S. Geological Survey and carried out at the University of California at Berkeley from 1907 to 1909. While the investigation was still in progress, Murphy published several short articles which reported some of the findings of the Berkeley investigation. He presented the following description of the disappearance of dunes and the appearance and behavior of sand waves:

> The form of the dunes became less distinct and at a little greater velocity they disappeared, leaving the sand surface even and the water surface above it waveless. This condition of waveless surface flow continued while the sand slope increased from about 0.9% to 1.6% ... . For higher slopes the sand surface formed into waves. These waves were from 2 to 3 ft in length from crest to crest, extended the width of the trough and some were .05 ft in height from crest to trough of wave. ... These sand waves travel slowly upstream, the sand being scoured from the down-stream face ... and deposited on the up-stream face (of the next wave) ... . Some of these waves remain for two minutes but generally not longer than one minute. The velocity is greater in the wave trough than in the vicinity of the crest and the motion of the grains at the crest is very complex, some of them jumping almost to the surface. (p. 580)

It remained for Gilbert (8) to call the sand waves which move upstream antidunes* "because they are contrasted with dunes in their direction of movement; they travel against the current instead of with it" (p. 31). Gilbert presented a description of antidunes and stationary waves which contained the essential elements of the accounts presented by Cornish, Owens, and Murphy. He then went further and described some details which had not been previously reported:

> Not only is a row of antidunes a rhythm in itself, but it goes through a rhythmic fluctuation in activity, either oscillating about a mean condition or else developing

---

* Note that the word antidunes, as coined by Gilbert, is not hyphenated.

> paroxysmally on a plane stream bed and then slowly declining. Paroxysmal increase starts at the downstream end of a row and travels upstream, gaining in force for a time, and the climax is accompanied by a combing of wave crests. (p. 32)

Further on, quoting Murphy directly*, Gilbert gave the first complete description of the breaking of the stationary waves:

> A white cap forms on the surface of the water when the larger waves disappear. Sometimes, two or more will disappear at once and leave the surface without waves for a distance of 10 feet or more. (p. 32)

In describing the "rhythm in the flow of water", Gilbert again spoke of the wave breakings as occurring when "a master wave, with curling crest, rushes through the trough from end to end" (p. 243).

Gilbert went on to explain the formation of antidunes as occurring when

> the restraint (due to the bed and water surface) is overpowered, and a diversified but systematic arrangement of flow lines develops, which carries with it systematic diversity of both water surface and channel bed and gives the antidune phase" (p. 34).

The argument is not at all clear. Further on (p. 243) he elaborated on the mechanism involved in the formation and growth of the antidunes and the breaking of the stationary waves, but did not clarify his argument. Gilbert was quite intrigued with the "rhythm of motion" and believed that antidunes were subject to analytical treatment, but did not pursue such a treatment because it was not within the scope of his investigation.

With the publishing of Gilbert's work, workers in the field of river hydraulics became more conscious of the different regimes of

---

* Gilbert did not cite the work of Murphy which he quoted. It was probably the preliminary report which Murphy prepared.

river flow and descriptions of the behavior of natural stream started appearing more frequently. An example of such a description of the antidune regime of flow is found in a paper presented by Pierce (9) in 1916 in which he reported on the behavior of the San Juan River near Bluff, Utah:

> Only on heavily loaded silt streams is ... antidune movement seen at its best. The visible surface effect of this collective movement is commonly known as the "sand wave".* In appearance the sand waves much resemble the waves thrown up by a stern-wheel river steamboat. On the wide, shallow sections of San Juan River sand waves may usually be seen below the riffles at medium stages. In the deeper sections they appear at their best development on rapidly rising stages ... . The usual length of the sand waves, crest to crest, on the deeper sections of the river is 15 to 20 feet, and the height, trough to crest, is about 3 feet. However, waves of a height of at least 6 feet were observed. The sand waves are not continuous, but follow a rhythmic movement. Their appearance as seen on the lower San Juan is as follows: At one moment the stream is running smoothly for a distance of perhaps several hundred yards. Then suddenly a number of waves, usually from 6 to 10, appear. They reach their full size in a few seconds, flow for perhaps two or three minutes, then suddenly disappear. Often, for perhaps a minute before disappearing, the crests of the waves go through a combing movement, accompanied by a roaring sound. On first appearance, it seems that the wave forms occupy fixed position, but by watching them closely, it is seen that they move slowly upstream. In the narrow parts of the stream the waves may reach nearly the width of the river, but in the wider parts, they occupy smaller proportional widths. Usually they are at right angles to the axis of the stream, but at some places, particularly in the wider parts of the river, they may suddenly assume a diagonal position, moving rather rapidly across the stream in the direction toward which the upstream side of the wave has turned. (pp. 42, 43)

Pierce's description of the phenomenon is generally very clear and

---

* Pierce referred to the surface wave as a "sand wave". This is somewhat confusing since the term sand wave is also associated with the waves of sand on the bed. In this work, the term sand wave has the latter meaning. The surface water waves are called stationary waves.

quite accurate.

The first attempt at an analytical treatment of antidunes was made by Langbein (10) in 1942. Using dimensional analysis and the results of Gilbert's experiments, he delineated the transitions from dunes to flat bed and from flat bed to antidunes on a plot of Froude number (based on hydraulic radius) versus the product of velocity and hydraulic radius. A different relation was obtained for three of the different sands used by Gilbert. Langbein's criterion will be discussed in section 5-4. He was also the first to point out that there is some disagreement on the rate and direction of movement of antidunes.

Recently, various laboratory investigators have mentioned antidunes as being the regime of flow which they did not investigate because the highly unsteady nature of the flow made the depth, velocity, etc., difficult to measure. Vanoni and Brooks (1) made such an observation in 1957:

> If the velocity is increased still further to reach a critical Froude number of around 0.8, standing surface waves start to form and are reinforced by long wavelength undulations of the bed. When the velocity is increased so that the Froude number exceeds 1.0, the surface waves become exceedingly high, as do the corresponding undulations of the bed; occasionally the surface waves break and the peaks of the corresponding waves in the bed are rapidly scoured. This condition is characterized by rapid and convulsive changes in the bed configuration. These waves on the bed are often called anti-dunes. Because of the unstable nature of the flow no experiments in this regime were carried on, although it is a spectacular demonstration experiment. Unlike supercritical flow of clear water, the flow never becomes stable again as the Froude number is further increased (unless all the bed sand is carried into suspension). (p. 44)

Vanoni and Brooks' statement that "the flow never becomes stable again" is not strictly correct, as will be discussed in chapter 4.

1-3. Purpose and Scope of this Investigation

The purpose of this investigation was to conduct a laboratory and theoretical study of the occurrence, behavior, and effects on the friction factor of antidunes and the stationary waves which accompany them. The laboratory research consisted of 30 runs in a recirculating flume 10.5 inches wide and 40 feet long, and 13 runs in a recirculating flume 33.5 inches wide and 60 feet long. In each run, equilibrium flow was established over a bed of sand and the flow depth, water discharge, energy grade line slope, and mean sediment concentration in the flow were measured. The depth of flow ranged from 0.074 to 0.356 feet and the velocity was varied to give a Froude number range of about 0.75 to 2.25. Two different sands were used. The theoretical study is concerned with an analysis of the stationary waves which form and their breaking, and the movement of the antidunes.

In chapter 2, the theoretical study of the problem is presented. Chapter 3 describes the apparatus, procedure, and sand used and discusses the analysis of laboratory data. In chapter 4 the experimental results are presented and compared with the theoretical results. The fifth chapter explains some of the experimental observations, discusses Langbein's criterion and presents the limited amount of data which is available from natural streams. The results are summarized in chapter 6.

Symbols will be defined where they first appear and are summarized in the appendix. Tables, figures, and equations are numbered separately for each chapter; the number before the dash denotes the chapter and the number following the dash gives the number of the item

in the chapter. The reference numbers used in the text refer to the numbered items in the reference list which follows the appendix.

CHAPTER 2

ANALYTICAL CONSIDERATIONS

Water flowing over antidunes has two interfaces: one with air at the free surface and one with sand at the bed. A solution describing the flow must satisfy the dynamic condition at the free surface (constant pressure), kinematic conditions at both surfaces (velocity tangent to interface), and, together with the law governing the interaction of the sand and water, must satisfy the continuity of sand motion. This physical law relating the movements of the sand and water is unknown.

In his 1956 survey of the problem of wind generation of water waves, Ursell (11) opens with the statement that "wind blowing over a water surface generates waves in the water by a physical process which cannot be regarded as known" and concludes that "the present state of our knowledge is profoundly unsatisfactory". Such is the case in a problem where the laws governing the motion of the fluids on either side of the interface can be expressed mathematically as the Navier-Stokes equations. In the problem at hand, neither the laws governing the interaction of the water and sand nor the laws governing the motion of the sand are known. Furthermore, the behaviors of the two interfaces are strongly coupled and the phenomenon is inherently nonlinear. Thus it would be indeed optimistic to expect a complete solution to be forthcoming.

In this chapter, the equations governing the flow over a wavy, deformable bed will be formulated and the special case of a fixed wavy bed will be solved. This solution together with physical arguments will

be used to deduce the relation between the flow velocity and the wave length of the surface waves (and thus of the antidunes also). The breaking of the stationary waves and motion of the antidunes will be analyzed. Finally, the velocity-wave length relation will be considered for stationary waves and antidunes which are not of the two-dimensional form.

In the analytical considerations of waves presented in this investigation, linearized formulations will be used. Thus the squares of the perturbation velocities will be taken as small so the nonlinear terms can be neglected, and the boundary conditions will be satisfied on the undisturbed positions of the interfaces.

2-1. Equations of Flow over a Deformable Wavy Bed

The water flow will be treated as irrotational. Then the velocity, $\vec{q}$, can be expressed as the gradient of a potential function, ϕ

$$\vec{q} = \nabla \phi . \tag{2-1}$$

Since the fluid is incompressible, the divergence of $\vec{q}$ is zero and hence

$$\nabla^2 \phi = 0 \tag{2-2}$$

is the equation which must be satisfied in the region $-d < y < 0$, where y is the vertical coordinate, with $y = 0$ being the mean water surface, and d is the depth (see figure 2-1). It will be convenient to divide ϕ into two parts,

$$\phi = Vx + \overline{\phi} \tag{2-3}$$

where

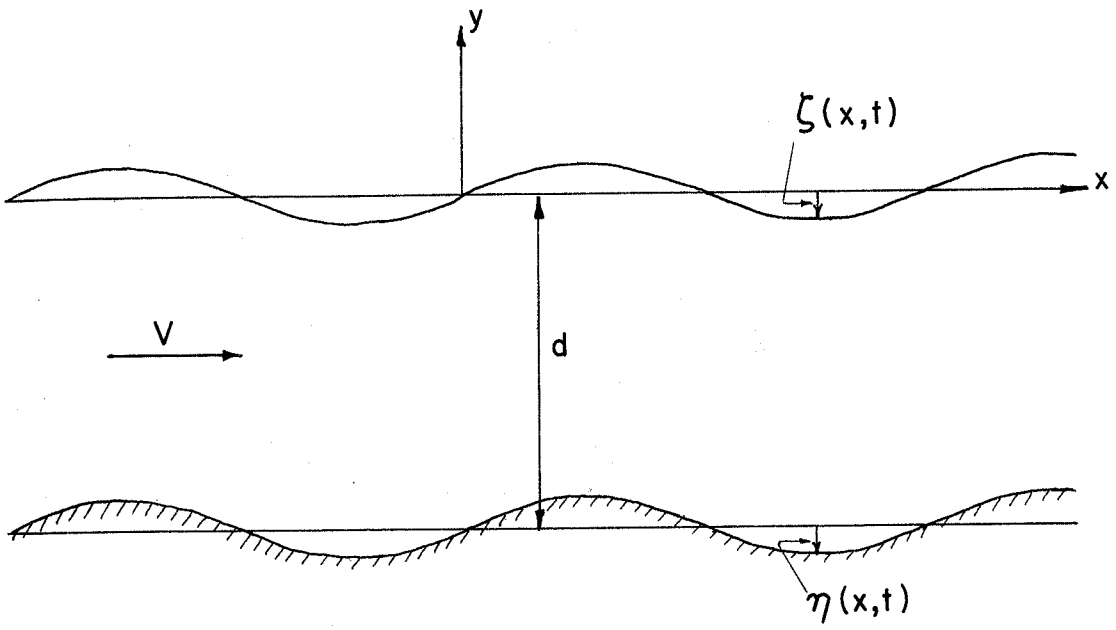

Fig. 2-1. Definition sketch of flow over a wavy bed.

$\overline{\phi}$ = potential of the perturbation velocities

V = mean velocity = $\frac{q}{d}$

q = water discharge per unit width of stream

d = mean depth.

$\overline{\phi}$ must also satisfy equation 2-2.

The profiles of the wavy bed and free surface will be denoted by $\eta(x, t)$ and $\zeta(x, t)$ respectively. The kinematic boundary condition at the free surface is

$$V\zeta_x + \zeta_t = \overline{\phi}_y(x, 0, t) \qquad (2\text{-}4)$$

and the dynamic condition (Bernoulli's equation) is

$$g\zeta + \overline{\phi}_t(x, 0, t) + V\overline{\phi}_x(x, 0, t) = 0 \qquad (2\text{-}5)$$

where the subscripts denote partial differentiation and g is the gravitational constant. The kinematic condition at the sand bed is

$$V \eta_x + \eta_t = \overline{\phi}_y(x, -d, t). \tag{2-6}$$

The remaining condition involves the continuity equation for the sand transport,

$$\frac{\partial G(x)}{\partial x} + \beta \eta_t = 0 \tag{2-7}$$

where

$G(x)$ = local rate of sediment transport per unit width on a weight basis (e.g., lb/ft-sec).

β = bulk specific weight of sand in bed.

The last condition (equation 2-7) introduces another unknown, $G(x)$, which necessitates another equation. This equation is the relation between $G(x)$ and the flow parameters and sand characteristics

$$G(x) = G(d, V, \text{fluid properties, sand characteristics}). \tag{2-8}$$

Herein lies the stumbling block, for the physical law which equation 2-8 expresses is unknown.

2-2. Flow over a Rigid Wavy Bed

Although the general problem of flow over a deformable bed cannot now be solved, certain aspects of the behavior of antidunes and their stationary waves can be obtained from the solution for flow over a fixed wavy bed. The solution of this problem can be obtained directly in the following way. Consider the simple harmonic wave train shown in figure 2-2a moving from right to left in a fluid of depth H. The celerity, c, of such a wave is given by Milne-Thomson (4) as

$$c^2 = \frac{g}{k} \tanh kH \tag{2-9}$$

where

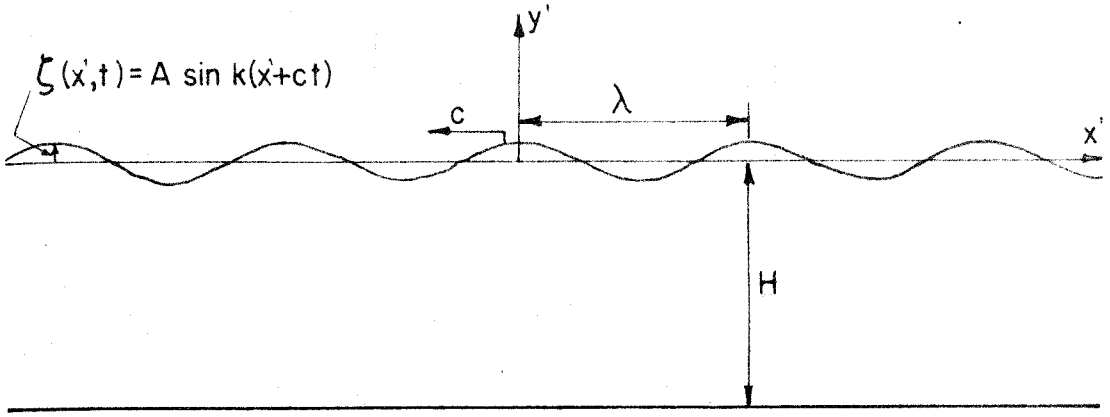

(a) Translational gravity waves moving from right to left.

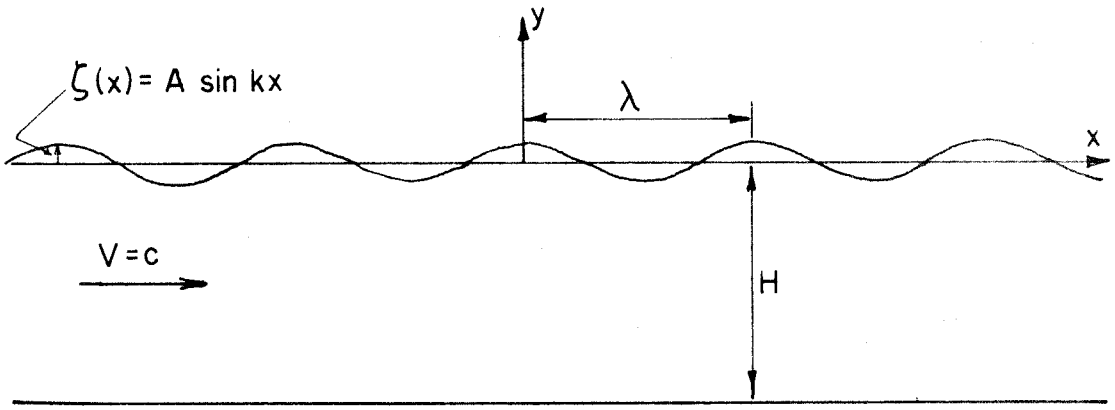

(b) Stationary gravity waves. The wave train of figure (a) has been brought to rest by imposing a velocity V = c on the fluid.

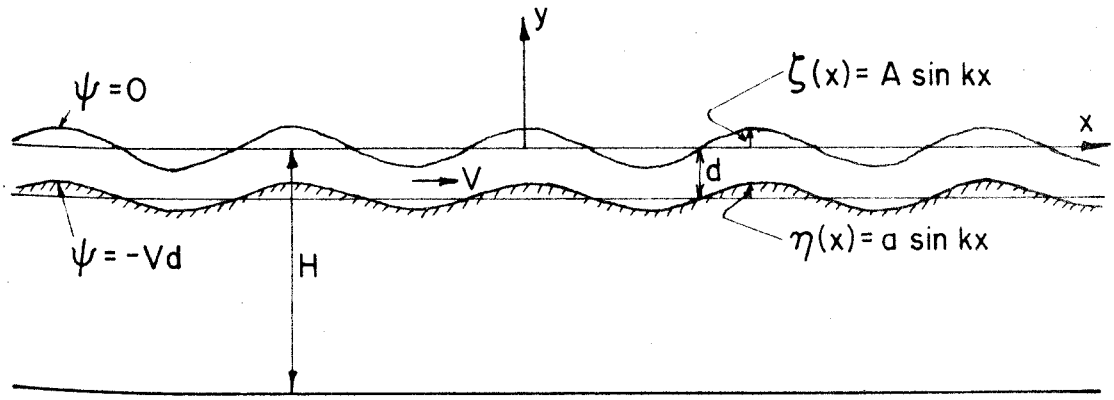

(c) Flow over a rigid wavy bed. A streamline of the flow shown in figure (b) has been replaced by a rigid boundary.

Fig. 2-2. Steps in the development of the equations for flow over a rigid wavy bed.

$k = \frac{2\pi}{\lambda}$ = wave number

λ = wave length.

Denote the stream function by ψ and the complex potential by

$$f(z,t) = \phi + i\psi. \tag{2-10}$$

For this flow the complex potential is (see Milne-Thomson (4), p. 376)

$$f = \frac{cA}{\sinh kH} \cos k(z' + iH + ct) \tag{2-11}$$

where A is the wave amplitude. The problem can be reduced to one of steady motion by taking the axes as moving with the waves. This is accomplished by substituting $z - ct$ for z'. If a velocity $V = c$ is then superposed on the whole system (figure 2-2b) the wave profile will be brought to rest and the water will have a mean velocity V in the x direction. This is the desired flow and its complex potential is given by

$$f = Vz + \frac{AV}{\sinh kH} \cos k(z + iH). \tag{2-12}$$

When the real and imaginary parts of equation 2-12 are separated, the velocity potential and stream function can be expressed as

$$\phi = Vx + \frac{AV}{\sinh kH} \cosh k(y + H) \cos kx \tag{2-13}$$

$$\psi = Vy - \frac{AV}{\sinh kH} \sinh k(y + H) \sin kx. \tag{2-14}$$

The flow is now steady and any streamline can be considered as a fixed bed, as shown in figure 2-2c. Equations 2-13 and 2-14 describe the flow in the interval $-d < y < 0$. This flow is the top part of the simple train of gravity waves in a fluid of depth H. The waves have been

brought to rest by superposing on them a velocity equal and opposite to the wave celerity.

From equation 2-9 it may be noted that since $c = V$,

$$V^2 = \frac{g\lambda}{2\pi} \tanh \frac{2\pi H}{\lambda}. \qquad (2\text{-}15)$$

Thus λ depends only on V and H and is independent of d. The higher order solution for the case of finite A/λ can be obtained by replacing f of equation 2-11 (which is, after the transformations, the harmonic term of equation 2-12) by the complex potential of a wave of finite amplitude.

2-3. Form of the Bed Profile

The relation between the form of the bed profile and water surface profile can be obtained directly from equation 2-14. The equation of the bed profile is $\eta(x)$ and its position is $y = -d + \eta(x)$. The total flow over the wavy bed is $V d$. Thus, the wavy bed is the streamline $\psi = -V d$. If these values of y and ψ are substituted into equation 2-14, the result is

$$-V d = V[-d + \eta(x)] - \frac{A V}{\sinh k H} \sinh k(H - d) \sin k x. \qquad (2\text{-}16)$$

Note that using $y = -d$ instead of $y = -d + \eta(x)$ in the hyperbolic sine term is consistent with the linearized theory. From equation 2-16,

$$\eta(x) = \frac{A \sinh k(H - d)}{\sinh k H} \sin k x.$$

Thus the bed profile $\eta(x)$ is also sinusodial with a different amplitude, a, given by

$$a = \frac{A \sinh k(H - d)}{\sinh k H}. \qquad (2\text{-}17)$$

Equation 2-17 can be simplified with the aid of equation 2-15 to yield

$$\frac{a}{A} = \left(1 - \frac{g}{V^2 k} \tanh k d\right) \cosh k d. \qquad (2\text{-}18)$$

Actually, the complete mathematical solution includes the case in which the bed and water surface are 180^{o} out of phase as well as the case in which they are in phase. In the former case, $d > H$ and the solution in the interval between the horizontal bottom and the wavy bed $(-d < y < -H)$ is the analytic continuation of the complex potential (equation 2-12). This case will not be considered here because of its obvious dissimilarity to flow over antidunes.

2-4. Velocity-Wave Length Relation for Flow over Antidunes

As will be discussed in chapter 4, an antidune is formed when the free surface of a stream is disturbed provided, the depth, velocity, and transport characteristics of the bed material are within certain limits. This disturbance can be externally induced, can result from the presence of dunes or other antidunes, or can arise spontaneously as a stationary wave. The disturbance causes local scouring downstream from which deposition occurs and an antidune results. Immediately downstream from this antidune, another antidune is formed by the same process. This mechanism continues to form successive antidunes until it is interrupted by the breaking of a stationary wave or the spontaneous disappearance of the antidunes.

It was shown in the two preceeding sections that for a given velocity, there is an infinite number of wave lengths which will yield a solution compatible with the boundary conditions. These wave lengths are a function only of H and V and are the solutions to

$$V^2 = \frac{g\lambda}{2\pi} \tanh \frac{2\pi}{\lambda} H, \qquad H > d. \tag{2-15}$$

The question that will now be considered is whether there is a preferred wave length for each depth and velocity. The complete answer to this question lies in the unattainable solution to the problem formulated in section 2-1. The alternative is to ignore the details of the sediment transport for the moment and assume that the fluid flow pattern will impose itself on the sand bed and form the desired boundary configuration by suitable scour and deposition. Attention can then be focused on the fluid motion in determining the preferred wave length.

It is here hypothesized that the flow will seek out the wave length for which fluid motion described by equation 2-12 will have the minimum energy in the interval $-d < y < 0$. The problem now consists of determining the value of H for which the energy of the flow is a minimum.

The potential energy per wave length, P, is simply due to the water which is displaced from the wave trough to the wave crest. If ρg is the unit weight of the water,

$$P = \frac{\rho g}{2} \int_0^{\lambda} \eta^2 \, dx$$

$$= \frac{\rho g}{2} \int_0^{\lambda} A^2 \sin^2 k x \, dx$$

$$= \frac{1}{4} \rho g A^2 \lambda. \tag{2-19}$$

The average potential energy per unit area, $\overline{P}$, is

$$\overline{P} = \frac{1}{4} \rho g A^2 \tag{2-20}$$

and is independent of λ and thus of H. Thus only the kinetic energy must be considered in determining the minimum total energy.

The kinetic energy per wave length, T, is

$$T = \frac{\rho}{2} \int_{-d}^{0} \int_{0}^{\lambda} \left[\left(\frac{\partial \phi}{\partial x} \right)^2 + \left(\frac{\partial \phi}{\partial y} \right)^2 \right] dx\, dy.$$

Introducing ϕ from equation 2-13 and carrying out the integration the result is

$$T = \frac{1}{2} \rho V^2 \lambda d + \frac{\rho \lambda k A^2 V^2}{8 \sinh^2 k H} \left[\sinh 2kH - \sinh 2k(H - d) \right]. \quad (2\text{-}21)$$

The first term on the right is simply the kinetic energy due to the translational velocity of the fluid and is independent of H. The second term represents the kinetic energy due to the perturbation velocities. Substituting for V^2 from equation 2-15, equation 2-21 becomes

$$T = \frac{1}{2} \rho V^2 \lambda d + \frac{\rho \lambda g A^2}{4} \left[1 - \frac{\sinh 2k(H - d)}{\sinh 2kH} \right]$$

and the average kinetic energy per unit area, $\overline{T}$, is

$$\overline{T} = \frac{1}{2} \rho V^2 d + \frac{\rho g A^2}{4} \left[1 - \frac{\sinh 2k(H - d)}{\sinh 2kH} \right]. \quad (2\text{-}22)$$

Note that if $H = d$, the second term on the right reduces to the kinetic energy of a simple harmonic wave.

Equation 2-22 shows that for all values of d the kinetic energy (and thus the total energy) of the flow approaches its minimum value as H goes to infinity. Thus, under the hypothesis that wave length selected by the system is that which corresponds to the minimum energy for a given amplitude, the perturbation velocities accompanying the

flow over antidunes are the same as those of a gravity wave in a fluid of infinite depth. This is possible even though the actual depth, d, is relatively small because the flow can deform the boundary to conform to a streamline of such a wave. The resulting velocity-wave length relation given by equation 2-15 is

$$V^2 = \frac{g\lambda}{2\pi} \tag{2-23}$$

since $\tanh kH$ approaches unity as H goes to infinity.

The fact that the minimum energy of the flow over a wavy bed corresponds to the case $H = \infty$ can be deduced directly from physical considerations. The total kinetic energy of a simple harmonic wave is given by Milne-Thomson (4) as

$$T = \frac{1}{4} \rho g \lambda A^2 \tag{2-24}$$

and is independent of the depth, H, to the virtual bottom. If $H = d$ all of the kinetic energy is included in the region of flow, $-d < y < 0$. As H is increased, T remains constant but some of the kinetic energy is accounted for by the perturbation velocities below the region of interest, i.e. $y < -d$. Thus as the virtual bottom is lowered, the total kinetic energy remains constant but is spread over a wider region so that the kinetic energy in the region of interest, $-d < y < 0$, decreases and approaches a minimum as H goes to infinity.

The solution based on the minimum energy assumption shows that there is a single wave length for each velocity. However, it is theoretically possible for all admissible wave lengths to exist simultaneously on a rigid wavy bed. If the exciting disturbance contains all

frequencies $\omega = \frac{2\pi V}{\lambda}$ where λ is any solution of

$$V^2 = \frac{g\lambda}{2\pi} \tanh \frac{2\pi H}{\lambda}, \quad H > d, \tag{2-15}$$

it might be expected that all modes would be excited. The bed form would then consist of a superposition of the bed forms of all wave lengths and would be a complex, intricate pattern consisting of many individual undulations of different amplitudes and wave lengths. Such a pattern would not seem compatible with the sediment transport phenomenon in the antidune regime where no flow separation occurs downstream from the bed features. In this regime, the sediment in transport is swept along at such high velocities that it is impossible for the differential scour and deposition to result in features which are not regular and periodic. The transport phenomenon can, however, cause bed features which are periodic and smooth.

In this regard, the theoretical work of Vitousek (12) should be mentioned. Vitousek sought a solution to the problem of flow over a wavy bed which would satisfy the free surface boundary condition exactly. Using the inverse method of Lewy (13), Vitousek assumed that the free surface is a trochoid given parametrically by

$$x = \frac{\theta}{k} + A \sin \theta$$

$$y = h - A \cos \theta$$

where h is a constant. This is the form of a gravity wave of finite amplitude, as is discussed by Lamb (3). The waves of very small amplitude considered earlier are the special case of this form where $Ak \ll 1$. He then used Lewy's method to determine the complex

potential which satisfied the boundary conditions for a wave of length 2π. Midway through his solution he was forced to choose $2h = A^2 + 1$ in order to keep the solution in closed form. This choice of h is tantamount to choosing a velocity-wave length relation. Vitousek presented some numerical results based on his final solution which showed that this relation is the same as the velocity-wave length relation for a deep water gravity wave.* This is the same conclusion which was reached by the energy analysis of this section. Vitousek was unable to determine the form of the streamlines in the case $2h \neq A^2 + 1$. He stated, however, that his rough calculations gave a strong indication that the value $2h = A^2 + 1$ actually did yield a smoother and more regular bottom than did other values.

2-5. Breaking of Stationary Waves

It was observed that antidunes, once initiated, grow in amplitude until they reach some limiting value. Under certain conditions the stationary waves often break before the antidunes reach their limiting amplitude. The waves break toward the upstream direction which is the direction of the wave propagation relative to the water. In appearance, the breaking resembles that of ocean waves as they approach the shore.

In the preceding section it was shown from the minimum energy hypothesis that the waves which accompany antidunes can be considered

---

* The form of the free surface of the wave investigated by Vitousek is the same as that of Gerstner's trochoidal wave. However, the fluid motion accompanying Gerstner's wave is rotational. In Vitousek's solution, there are singularities which make the flow irrotational while still preserving the trochoidal form of the free surface. The location of the bed in Vitousek's solution must be such that the singularities are excluded from the region of interest.

as simple gravity waves in a fluid of infinite depth. The profile of such waves with finite amplitude has been investigated by Michell (14). He found that the maximum wave height (vertical distance from trough to crest) that can exist, $2A_c$, is

$$2A_c = 0.142\lambda. \tag{2-25}$$

2-6. Movement of Antidunes

In the descriptions of antidunes given in chapter 1, frequent mention was made of their growth and upstream movement. Their behavior cannot be fully analyzed until the sediment transport law is known. However, their direction of movement can be deduced if a reasonable transport law is assumed and used in connection with the solution for flow over a rigid wavy bed. It will be assumed that the antidunes move upstream and then shown that this movement is compatible with the solution presented in section 2-2 for flow over a rigid wavy bed if the rate of antidune movement, V_a, is small compared to the flow velocity, V. The solution which will be obtained is the same as that which would result if a velocity $V - V_a$ instead of V were superimposed on the translational waves discussed in section 2-2 in deriving the solution for flow over a fixed wavy bed.

At time t let the form of the bed be

$$\eta(x,t) = a \sin k(x + V_a t). \tag{2-26}$$

Then

$$\eta_t = k V_a a \cos k(x + V_a t). \tag{2-27}$$

Since t is arbitrary, $t = 0$ can be chosen and equation 2-27 becomes

$$\eta_t = k V_a a \cos kx. \tag{2-28}$$

It will now be assumed that the local rate of sediment transport is proportional to some power of the total horizontal velocity at the level of the bed. Thus

$$G(x) = m \left(\frac{\partial \phi}{\partial x}(x, -d) \right)^n$$

$$= m \left(V + \frac{\partial \overline{\phi}}{\partial x}(x, -d) \right)^n \tag{2-29}$$

where m and n are constants. The first term in parentheses represents the flow velocity and the second term represents the horizontal perturbation velocity at the level of the bed. If the squares and higher powers of the perturbation velocity are small and can be neglected compared to the flow velocity, a binomial expansion of equation 2-29 yields

$$G(x) = m V^n + m n V^{n-1} \frac{\partial \overline{\phi}}{\partial x}(x, -d). \tag{2-30}$$

As was discussed in section 2-1, the continuity of sand transport requires

$$G_x(x) + \beta \eta_t = 0. \tag{2-7}$$

Substituting equations 2-28 and 2-30 into equation 2-7 yields

$$\beta k V_a a \cos kx = -m n V^{n-1} \frac{\partial^2 \overline{\phi}}{\partial x^2}(x, -d), \tag{2-31}$$

where $\overline{\phi}$ is the second term on the right of equation 2-13. Substituting this value of $\overline{\phi}$ into equation 2-31 gives

$$V_a = \frac{m\,n\,V^n\,k\,A}{a\,\beta\,\sinh k\,H}\cosh k(H-d). \tag{2-32}$$

Substituting for a from equation 2-17,

$$V_a = \frac{m\,n\,V^n\,k}{\beta}\coth k(H-d). \tag{2-33}$$

For flow over antidunes, $H = \infty$ and equation 2-33 becomes

$$V_a = \frac{m\,n\,V^n\,k}{\beta}. \tag{2-34}$$

Since $m\,V^n$ is the mean rate of sediment transport, G, the final expression for the upstream rate of movement of the antidunes is

$$V_a = \frac{n\,G\,k}{\beta}. \tag{2-35}$$

Since V_a is independent of x and t and is positive, the original assumption that antidunes move upstream unchanged in form is correct under the assumed transport law (equation 2-29). However, equation 2-35 can be taken as qualitative only since the transport law on which it is based is only qualitatively correct.

The upstream movement is aided by the gravity force acting on the sand particles. On the upstream slopes of the antidunes, gravity hinders the movement of the particles. Conversely, on the downstream slopes the gravity force acts in the direction of movement. These effects act to decrease the sediment transport rate on the upstream slopes and increase it on the downstream slopes and thus increase the velocity of upstream movement of the antidunes.

2-7. Velocity-Wave Length Relation for Three-Dimensional Waves

In many of the flume experiments which are described in chapters

3 and 4, short-crested, three-dimensional stationary waves formed. Examples of these waves are shown in figures 4-10 and 4-13. Waves of this form are actually a superposition of two waves: a translational wave in the direction of flow and a standing wave normal to the flow. The celerity of the resulting wave is just equal to the flow velocity so the wave appears stationary. The antidunes accompanying these waves are also three-dimensional, as shown in figure 4-11. The characteristics and occurrence of these waves will be discussed in sections 4-2 and 4-3.

The solution of this problem is rather lengthy and will not be developed here. It is outlined by Lamb (Ref. 3, p. 440) and a detailed treatment of the problem is given by Fuchs (15). If the width of the channel is b and the second mode of vibration is excited in the transverse direction, the celerity of the waves according to Fuchs (15) is given by

$$c^2 = \frac{g\lambda}{2\pi}\sqrt{1 + \left(\frac{\lambda}{b}\right)^2}\ \tanh\left\{\frac{2\pi H}{\lambda}\left[1 + \left(\frac{\lambda}{b}\right)^2\right]\right\} \qquad (2\text{-}36)$$

where

λ = wave length in the direction of flow

b = wave length normal to direction of flow. This is also the width of the channel if the second mode in the transverse direction is excited.

H = distance to the horizontal bottom. This is the distance to the virtual bottom.

In section 2-4, it was shown from the minimum energy hypothesis that $H = \infty$ for flow over two-dimensional antidunes. It will be assumed that this same value of H applies to the case of the three-dimensional waves. This implies that the flow will shape the bottom to conform to

a stream surface of a wave in a fluid of infinite depth. If the wave is to be stationary, $c^2 = V^2$ and equation 2-36 becomes

$$V^2 = \frac{g\lambda}{2\pi}\sqrt{1 + \left(\frac{\lambda}{b}\right)^2}. \qquad (2\text{-}37)$$

Equation 2-37 shows that for a given velocity, the wave length of a three-dimensional wave is always less than that of a two-dimensional wave.

2-8. Summary

The linearized potential flow solution has been presented for flow over a fixed sinusodial bed with the bed and water surface in phase. It was found that such a flow is simply the flow above some intermediate streamline in the flow for a stationary wave train over a horizontal bed at depth H. For flow over a rigid wavy bed, λ is fixed and the depth, H, to the virtual bottom depends on the stream velocity according to the relation

$$V^2 = \frac{g\lambda}{2\pi} \tanh kH, \qquad H > d. \qquad (2\text{-}15)$$

In the case of flow over antidunes, neither λ nor H is fixed. If it is hypothesized that the value of λ which the system selects is that corresponding to the minimum energy, then $H = \infty$ and the velocity-wave length relation is

$$V^2 = \frac{g\lambda}{2\pi}. \qquad (2\text{-}23)$$

Thus the flow over antidunes may be considered as the top part of a stationary train of gravity waves in a fluid of infinite depth. An upstream movement of the antidunes is implied by this solution if the

local sediment transport rate is proportional to a power of the total local horizontal velocity at the level of the bed. The surface waves break when their height reaches the critical value given by

$$2A_c = 0.142\lambda. \qquad (2\text{-}25)$$

If three-dimensional stationary waves and antidunes form, their wave length is less than that given by the two-dimensional solution (equation 2-23).

CHAPTER 3

APPARATUS AND PROCEDURE

The principal items of apparatus in which the laboratory experiments were carried out were the 40-foot and the 60-foot recirculating, tilting flumes located in the Sedimentation Laboratory of California Institute of Technology. These flumes have been used in several previous sedimentation studies (1, 16, 17, 18, 19) and only slight modifications were necessary to adapt them to the current project.

Since the experimental procedure was improved during the conduct of the research, certain of the experimental techniques are not the same for all runs. These changes will be pointed out in appropriate sections. The flumes, their appurtenances and accessories, and the experimental procedure will be described and discussed in this chapter. The procedures used in the calculation of the energy grade line slope, depth, mean velocity, bed shear, and bed friction factor will also be described. Finally, the characteristics of the sand used will be presented.

3-1. The 40-foot Recirculating, Tilting Flume

The 40-foot tilting flume shown in figure 3-1 was used for Run Series 5 with the 0.549 mm sand and for Runs 4-1 and 4-24 through 4-38 with the 0.233 mm sand. In figure 3-1 the water flows from left to right in the open channel portion of the circuit into the pump well at the downstream end of the channel. The water and sediment then pass through the pump into the return pipe which includes the venturi meter and heaters, then through the transition section, and back into the

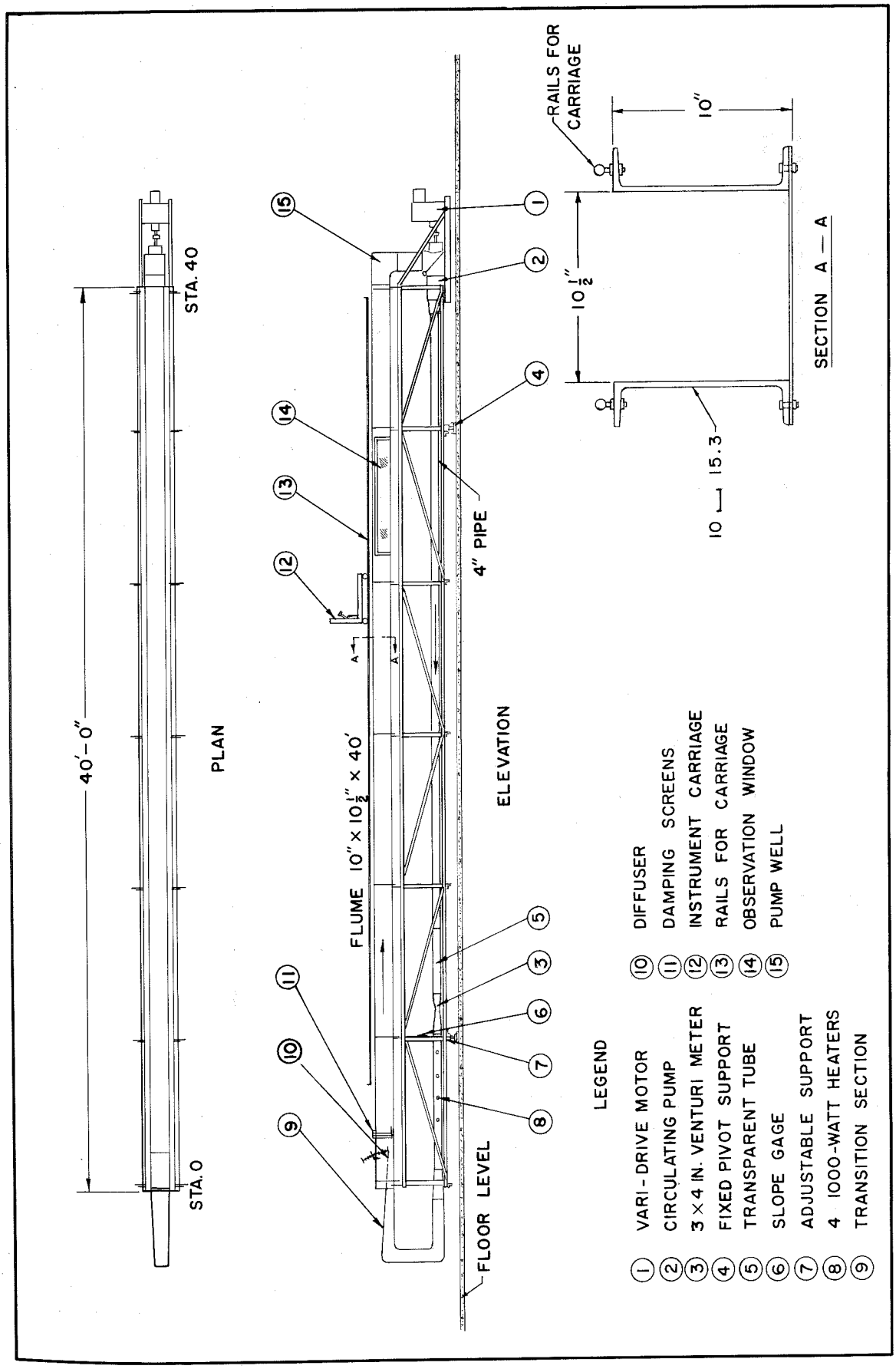

Fig. 3-1. Schematic diagram of 40-foot flume.

flume. The circuit is completely closed so the water and the sediment are continuously recirculated. The depth of flow is regulated by the amount of water in the system and is slightly affected by sediment storage in the pump bowl, transition, and return pipe.

The open channel portion of the circuit consists of two 10-inch structural channels, attached to a bottom plate as shown in section A-A of figure 3-1, giving inside width of $10\text{-}1/2 \pm 1/16$ inches. The inside surfaces of the flume were initially painted with a bitumastic paint which was replaced after the completion of Run Series 5 by an epoxy resin. Both finishes gave a hydrodynamically smooth surface. The channel is supported on a rigid truss which in turn is supported on a pivot near one end and on a jack at the other. This arrangement permits the slope of the flume to be set at any value from -0.001 to 0.032. The value of the slope is read directly to the nearest 0.00001 from a vernier scale attached near the jack.

The water-sediment mixture is circulated by an axial flow pump with a 9-inch diameter impeller. The pump is located at the downstream end of the flume and is driven by an electric motor through a variable-speed drive of the vee-belt type. This arrangement gives a speed range of 120 rpm to 1050 rpm. The maximum possible discharge is about 0.75 cfs.

A transparent lucite tube, 50 inches long with a 4-inch inside diameter, is located just upstream from the venturi meter in the return pipe. This permitted one to determine if sand was being deposited in the return pipe and in general have a better knowledge of the behavior of the lower part of the circuit. For example, in several runs using

the coarse sand, deposition occurred in the return pipe in the form of intermittent dunes about 6 inches long spaced at 3 to 4 feet, which moved downstream with a velocity of about 4 ft/min. In the spaces between the dunes there was no deposition. By observing the passage of the dunes in the transparent section, manometer readings could be taken when no dunes were present in the venturi meter.

Positions along the flume are referred to 1-foot stations marked off on the flume, station zero being 64 inches from the upstream end of the structural channels which form the walls. The window is five feet long and its upstream end is at station 23.

The entrance to the flume used in Runs 4-1 and 5-1 through 5-12 is shown in figure 3-2. The upper elbow of the transition has vanes to minimize secondary currents resulting from the turning. In the flume, a variable angle diffuser, shown in figure 3-1, was used to introduce the flow into the flume. In most runs, one or more 8-mesh screens (8 openings per inch) were placed normal to the flow at the outlet from the diffuser to break the large scale turbulence into smaller eddies which would be damped out in a shorter distance. The number of screens was determined by observing what combination gave the least disturbance to the flow. The effect of such screens in reducing the distance required to establish uniform flow has been discussed by Brooks (20).

In runs with high discharges, it was observed that at the outlet from the diffuser the bed was completely scoured away for a distance of about 6 inches leaving the bottom of the flume uncovered. This scoured section was followed by a section of about the same length

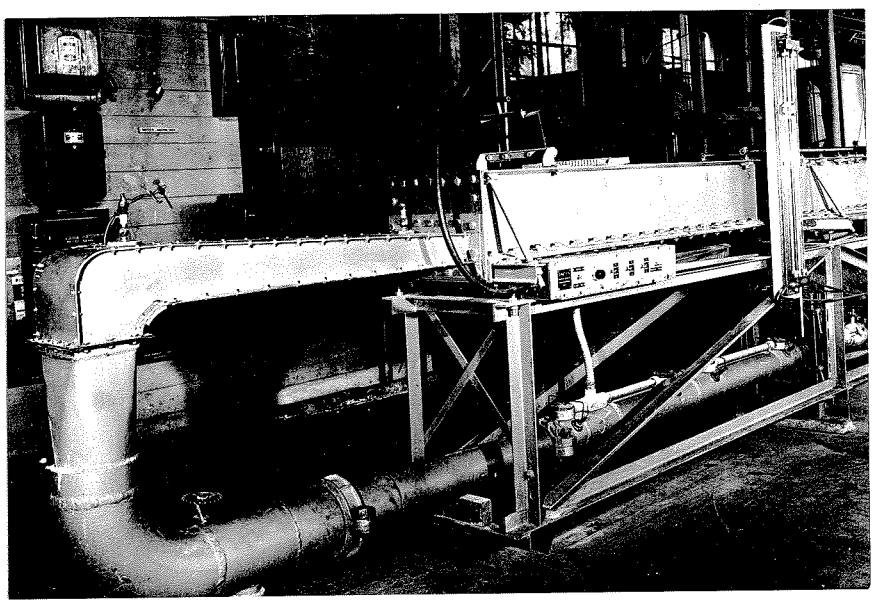

Fig. 3-2. Upstream end of 40-foot flume showing transition and diffuser inlet used in Runs 5-1 through 5-12.

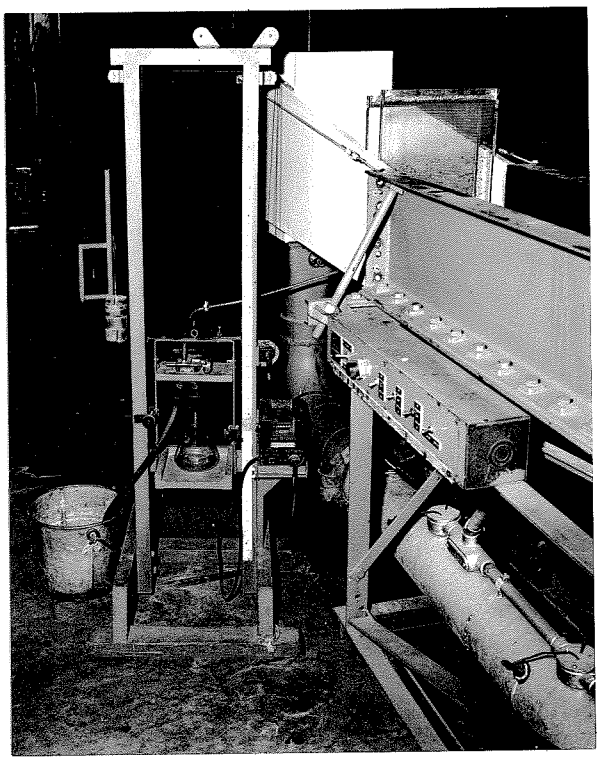

Fig. 3-3. Upstream end of 40-foot flume showing box inlet with sluice gate and screens. The setup for obtaining sediment samples is also shown.

where excessive deposition formed a hump of sand which always gave rise to a stationary surface water wave. In an attempt to eliminate this condition, a sill, 30 inches long and 1-5/8 inches thick was placed below the diffuser outlet in Runs 5-8 through 5-12. This sill was tapered at one end and was placed about 4 inches downstream from the outlet from the diffuser. This was quite effective in reducing the scour condition which existed previously.

Without the stationary wave which always disturbed the flow at the entrance to the channel, it became apparent that the flow configuration was not unique over a wide range of depth and velocity. If the flow was disturbed at the entrance, antidunes formed over the whole length of the channel. If the flow was given no disturbance at the flume entrance, the bed and water surface were flat everywhere. This situation will be described in chapter 4. To eliminate the stationary wave which was caused by the diffuser, the upper part of the transition and the diffuser were replaced by the simple box inlet shown in figure 3-3. In this inlet, the flow emerging from the upstream riser enters the channel behind a sluice gate which can be adjusted to give the desired depth of flow. About two feet downstream from the gate, slots are provided to accomodate up to 3 screens. The unsteady surging upstream of the sluice gate and to a smaller degree below it was greatly reduced by wood boards which floated on the water surface. This inlet arrangement, while not entirely satisfactory, was judged better for high discharge runs than the diffuser inlet.

The outlet from the flume used in Run Series 5 and Run 4-1 is shown in figure 3-4. The pump and electric motor and variable-speed-

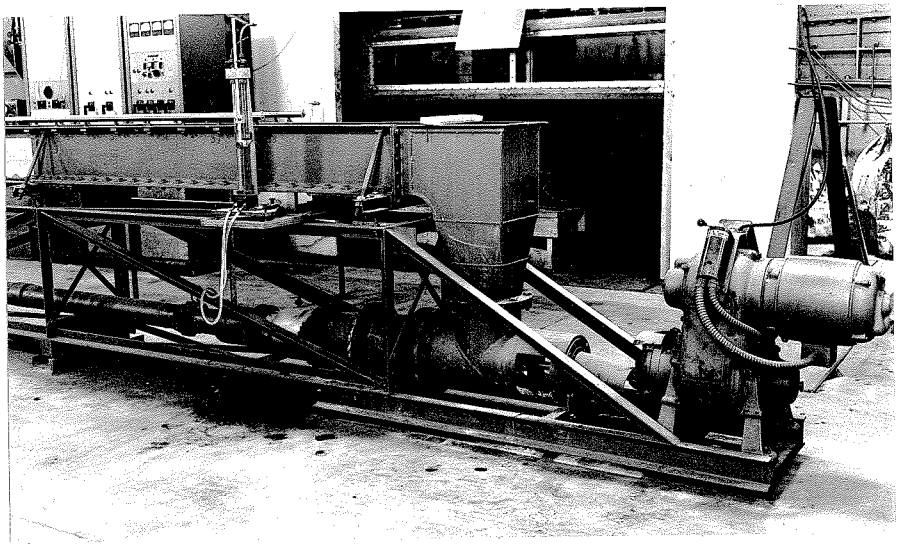

Fig. 3-4. Downstream end of 40-foot flume showing pump well used in Run Series 5.

Fig. 3-5. Downstream end of 40-foot flume showing pump well used in Run Series 4.

drive transmission can also be seen in this figure. The outlet consisted of a simple box which also served as the pump well. One or more 8-mesh screens were usually used just upstream from the outlet to prevent the end of the sand bed from slumping intermittently into the pump well.

During the breaking of the surface waves which formed over antidunes, considerable storage of water occurred in the channel due to the momentary upstream movement of a segment of the flow at each break. This resulted in a lowering of the water level in the pump well and a corresponding temporary drop in the discharge. In the runs with the coarse sand (Run Series 5) the amplitudes of the surges in the pump well were always less than about 6 inches and resulted in discharge surges which could not be detected with the venturi meter. However, the runs with the fine sand (Runs 4-24 to 4-38) exhibited wave breaking which was much more severe and extensive over the length of the flume and resulted in surging which completely drained the pump well, causing severe discharge surges and air entrainment. To reduce this surging to tolerable proportions the larger outlet shown in figure 3-5 was used for Run 4-24 and all subsequent runs in the 40-foot flume. This outlet has a plan area of 6.25 square feet compared to an area of 1.22 square feet for the outlet which it replaced. The surge in the enlarged outlet was always less than 4 inches.

3-2. The 60-foot Recirculating Tilting Flume

Runs 4-3, 4-6, 4-7 and 4-10 through 4-23 were conducted in the 60-foot flume shown in figure 3-6. A detailed description of this flume has been given previously by Vanoni and Brooks (1). The details of the

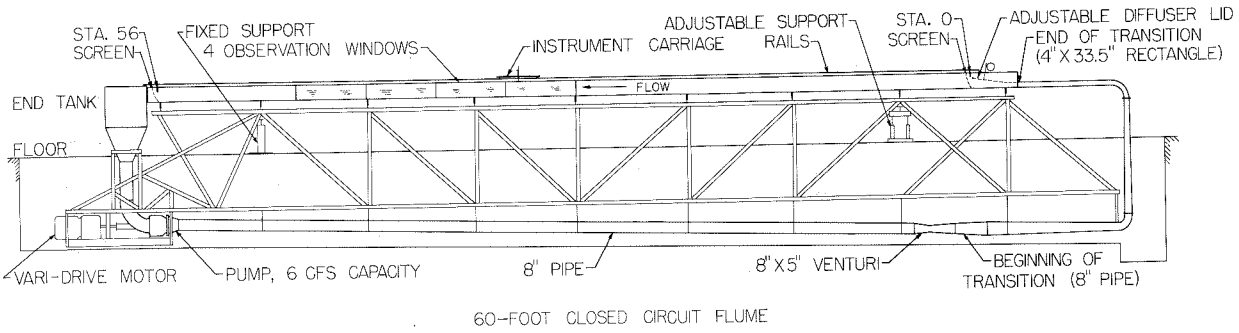

(a) Elevation

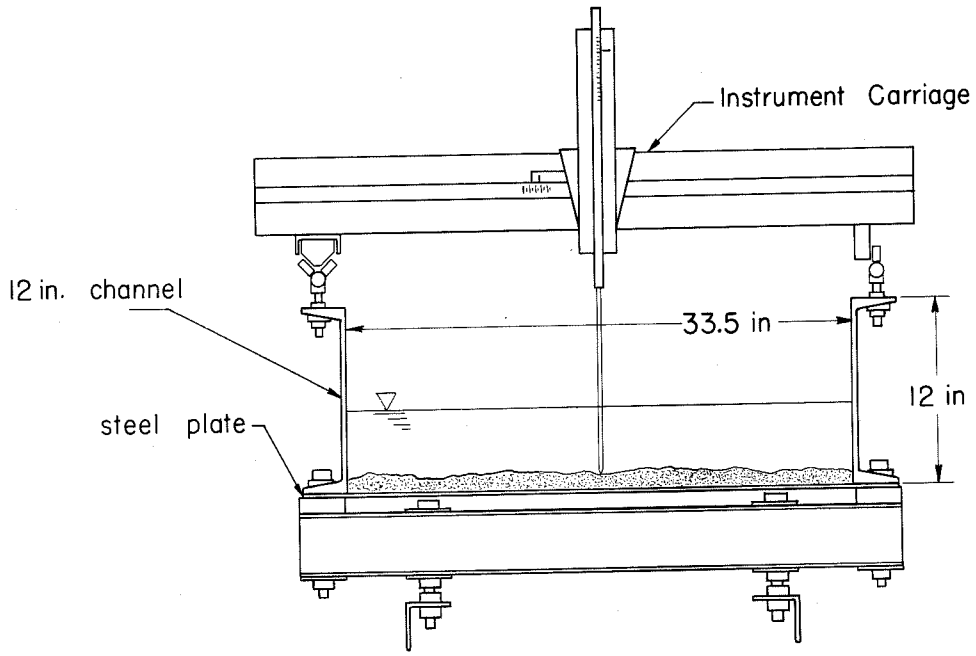

(b) Cross section of flume

Fig. 3-6. Schematic diagram of 60-foot flume.

flume cross section are shown in figure 3-6b. This flume is similar to the 40-foot flume, the water and sediment being continuously recirculated in a closed system. The slope, which could be set at any value from 0 to 0.017, was determined by a micrometer scale which is mounted on one of the jack lead screws. The inside of the channel is painted with an epoxy resin similar to that used in the 40-foot flume, but giving a very slightly rougher surface. However, the surface would still be classed as hydraulically smooth. The discharge range of the pump is 0.50 to 5.75 cfs.

The entrance to the 60-foot flume is through an adjustable diffuser similar to that which was used initially on the 40-foot flume. Figure 3-7 shows the upstream end of the flume, part of the transition, and the diffuser with two 8-mesh screens in place. The objections raised against the diffuser entrance on the 40-foot flume apply to the 60-foot flume also, but it was impractical to change the entrance structure on the latter. Various combinations of one to three 4-mesh and/or 8-mesh screens were placed immediately downstream from the diffuser outlet, the combination selected being that which introduced the flow with the minimum amount of bed and water surface disturbance.

The downstream exit shown in figure 3-8 consists of a tank which also serves as the pump well. The tank is 48 inches by 33.5 inches in plan giving a ratio of flume surface area to outlet surface area of 14.5 compared with 28.7 and 5.60 for the small and large outlets respectively used on the 40-foot flume. Its performance was considered as intermediate between those of the two outlets for the 40-foot flume. With quite radical breaking occurring in the flume, the surge in the outlet

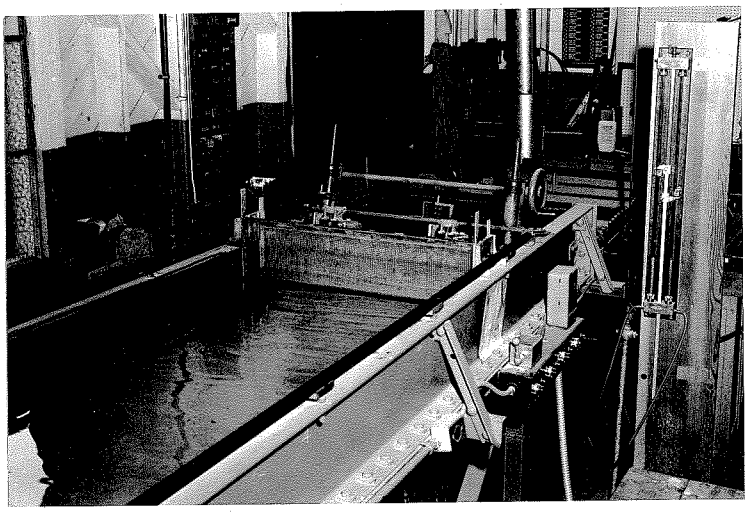

Fig. 3-7. Upstream end of 60-foot flume showing diffuser inlet and screens.

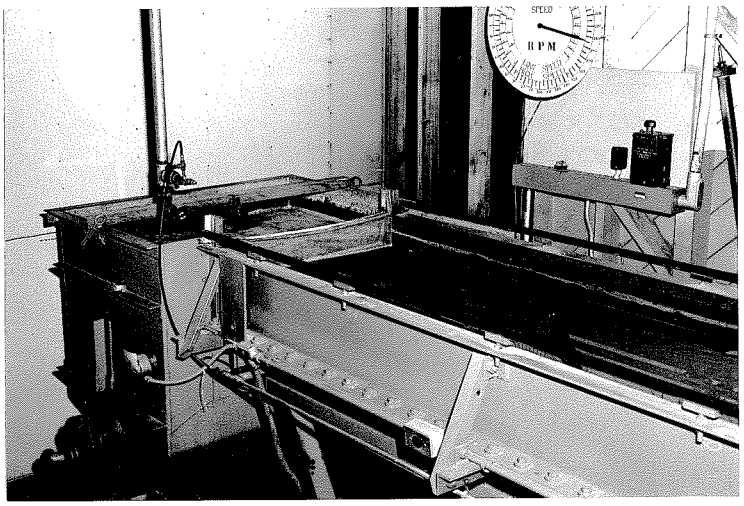

Fig. 3-8. General view of downstream end of 60-foot flume.

was quite small in all runs except 4-6, 4-7 and 4-16 and even in these runs it was less than one foot. Thus it appears that the ratio of flume area to outlet area should be considered in the design of flumes for experiments of this type.

As with the 40-foot flume, one or two 8-mesh screens were placed in the flume at the downstream end to hold the end of the sand bed from slumping into the pump well and, to some extent, to isolate the flume from disturbances in the pump well.

Positions along the flume are referred to one-foot stations which are marked along the flume. Station zero is at the downstream end of the diffuser. The window is 20 feet long with its upstream end at station 27.

3-3. Experimental Procedure

The experimental procedure followed in the conduct of a run will now be described in general to give a broad, overall picture of the laboratory technique. The individual measurements, sampling procedures and other operations will then be fully described.

Initially, the depth and velocity desired for the run were selected, the required discharge was calculated, and the required slope was estimated. With the slope set at zero, the amount of water in the flume was adjusted to give a water surface level which was estimated to yield the desired depth for the discharge required. The flume slope was then set at the estimated value and the pump was started. The pump speed was adjusted until the desired discharge was obtained and then, after a period long enough to allow the flow to reach equilibrium, the water surface slope was determined from the manometer board

which was connected with several piezometer taps placed in the flume. The flume slope was corrected to match the water surface slope, and after another period during which the flow adjusted to the new flume slope, the water surface slope was again determined from the manometer board and the flume slope was again reset as required. This process was continued until the agreement between the flume slope and the water surface slope determined from the manometer board was within a few percent. During this adjustment, the discharge was checked frequently and the pump speed was adjusted to maintain the desired value.

When the flume slope had obtained the final adjustment, the water surface elevation, discharge, water surface slope, temperature, and wave parameters were measured. The pump was then stopped, the flume slope set at zero, and the water level was again determined to check on water losses during the run. The bed was leveled and the bed elevation measured. This completed the first preliminary phase of the run.

The data collected from the preliminary phase were analyzed to determine what the depth had been. On the basis of this analysis the water level in the flume was then adjusted to give the desired depth and another preliminary phase was performed following the same procedure.

When a depth was obtained which was within 0.010 ft of the desired value, the water level in the flume was given a final adjustment and the final phase of the run was conducted. The final phase followed the same procedure as the preliminary phases except that total load sediment samples and still and motion pictures were taken.

In several runs, detailed bed profiles were taken before the bed was leveled.

The techniques used in the various aspects of conducting the laboratory experiments differed very little between the two flumes. The methods and equipment used with the two different flumes will be described and discussed in the following sections.

3-4. Temperature Control

In the 40-foot flume, temperature control was achieved by four 1000-watt immersion heaters which are located in the return pipe near the upstream end of the flume, as shown in figure 3-1. Three of the heaters were wired so that either 110 volts or 220 volts could be impressed across them to give an output of 250 watts or 1000 watts. This arrangement allowed power inputs in 250 watt increments up to 2500 watts and additional inputs of 3000, 3250 and 4000 watts. It was found that due to the large thermal inertia of the system, the desired temperature could be maintained within $\pm 0.5^{\circ}$C by checking the temperature every 30 minutes and raising or lowering the power input as required. A water temperature of 25°C was intended for all runs. However, there was no way to cool the water so the water temperature rose above 25°C in most runs carried out during the summer months.

On the 60-foot flume, no means was provided for temperature control. However, most of the experiments carried out in this flume were done during summer months and the water temperature usually fell slightly above 25°C as mentioned above.

The temperature was measured about every 30 minutes with an immersion thermometer having 0.1°C divisions. The average of the

temperature readings during the time data were being taken was used as the temperature for the run.

3-5. Discharge Measurements

A venturi meter installed in the return pipe of each flume was used to measure the discharge in the circuit. In the 40-foot flume, a 4- by 3-inch venturi meter was installed between the transparent tube and the heater section as shown in figure 3-1 and, in the 60-foot flume, an 8- by 5-inch venturi meter was placed just ahead of the transition section. Both of these meters were calibrated for clear water in the Hydraulic Machinery Laboratory of California Institute of Technology in 1956. The calibration was accurate to 0.1 percent.

In all runs in the 40-foot flume and all but two runs in the 60-foot flume, the differential head across the venturi meter was measured with an air-water differential manometer which could be read to the nearest 0.001 ft. In two runs in the 60-foot flume the differential heads exceeded the height of the water manometer and a mercury-water differential manometer was used which also had a least reading of 0.001 ft. No correction was made for the sand content of the water.

The use of a venturi meter in measuring the discharge of mixtures of water and sediment has been thoroughly discussed by Brooks (20). He concluded that discharge determination made with this apparatus are accurate to within one percent. However, many of the current runs had a discharge surge, which was described in section 3-1, and an accompanying surge in the manometer reading. When this was encountered, the valves in the manometer lines were partially closed to reduce the magnitude of the surge in the manometer. Then

no manometer readings were taken during the surges or afterwards until the manometer had regained its equilibrium position. At least five and usually ten or more such readings were taken during each run. The readings thus obtained differed by less than four percent in even the runs with radical wave breaking, indicating a discharge variation of less than two percent since the discharge varies as the square root of the head. Two percent appears to be a reasonable estimate of the accuracy of the discharge measurements.

3-6. Movable Carriages

Each flume was equipped with a carriage which could be moved on rails along the length of the flume from station 0 to station 34 on the 40-foot flume and from station 0 to station 55 on the 60-foot flume (see figures 3-1 and 3-6). The carriage for the 60-foot flume is shown in figure 3-9 and is very similar to the carriage for the 40-foot flume. The moving mechanism on each carriage has both transverse and vertical motions and both motions have vernier scales so that a point gauge mounted on the carriage can be moved to obtain the location of a point any place within the flume to the nearest 0.001 ft. For convenience, the vertical scales of both carriages were adjusted to read zero ($\pm$ 0.002 ft) when the point gauge was resting on the floor of the flume.

The setting of the flume slope scale and the elevations of the carriage rails were adjusted using a static water surface with the flume horizontal to give an inherent accuracy of the point gauge of $\pm$ 0.001 ft. The details of this procedure have been described by Brooks (20).

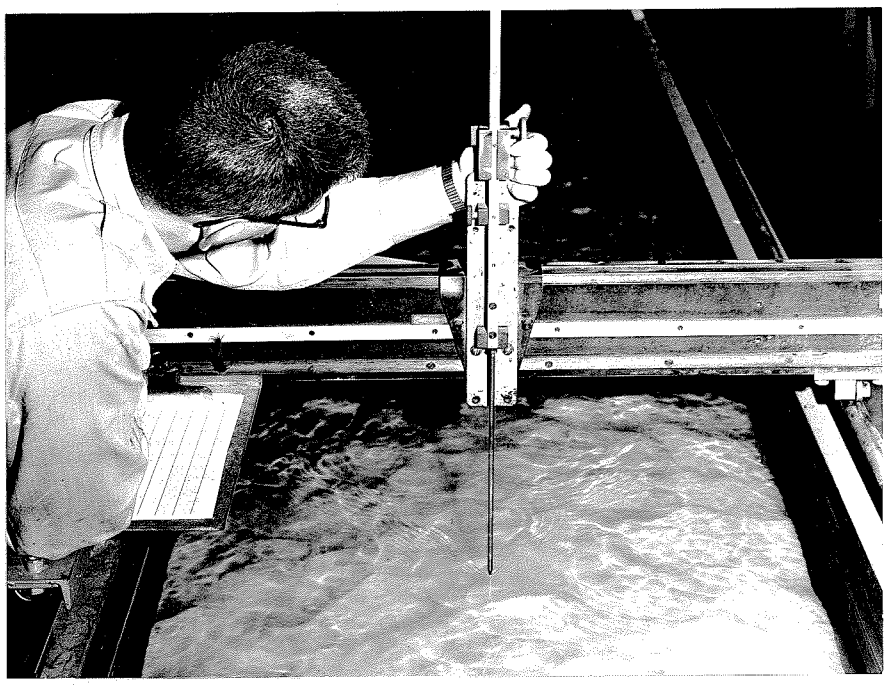

Fig. 3-9. Instrument carriage and point gauge for 60-foot flume.

3-7. Determination of Water Surface Elevation and Water Surface Slope

In order to determine the depth of flow, mean velocity, and elevation of the energy gradient, it was necessary to know the elevation of the water surface relative to the carriage rails. The very unsteady surface waves which formed made this elevation the most difficult quantity to measure. Except for runs in which the bed and water surface were flat, the point gauge could not be used because it was too slow to measure elevations on the unsteady surface waves.

The technique finally adopted for measuring the surface elevation involved the manometer board, shown in figure 3-10, connected to piezometer taps placed in the flume at 5 ft intervals. The maximum and minimum elevations reached by the water surface in each manometer tube were recorded on the glass scale of the manometer board. The average of these values, translated into an elevation on the point gauge scale of the movable carriage, was taken as the elevation of the water surface relative to the carriage rails for the station corresponding to the tube. The manometer board, piezometer taps, and procedure used will now be described.

The manometer board scale is printed on a plate of glass which is mounted in front of the tubes. The scale has 0.01 ft divisions and can be interpolated to 0.001 ft. The tubes have internal diameters of 12 mm which is large enough to eliminate capillary effects. The straightedge shown diagonally across the scale in figure 3-10 is attached to a bevel protractor which in turn is mounted on a bracket that travels vertically on the shaft at the left of the board. With this

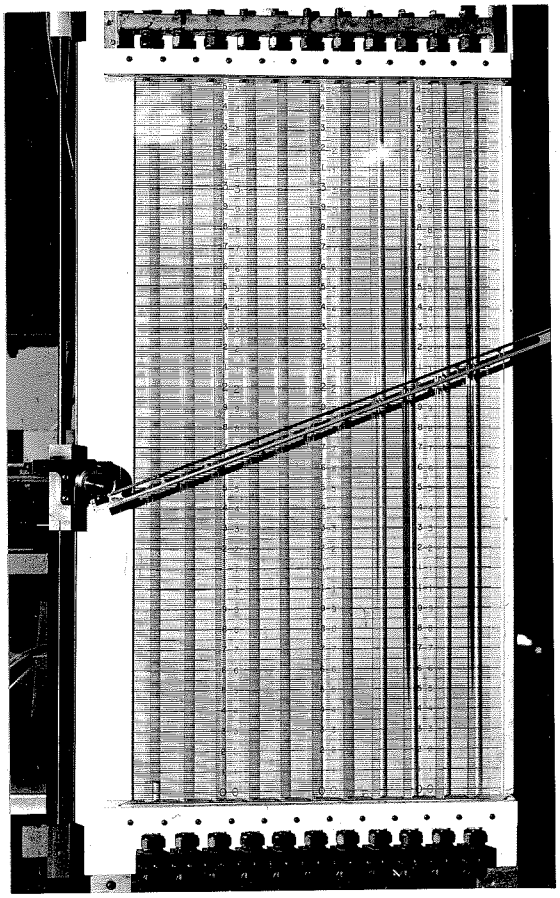

Fig. 3-10. Manometer board.

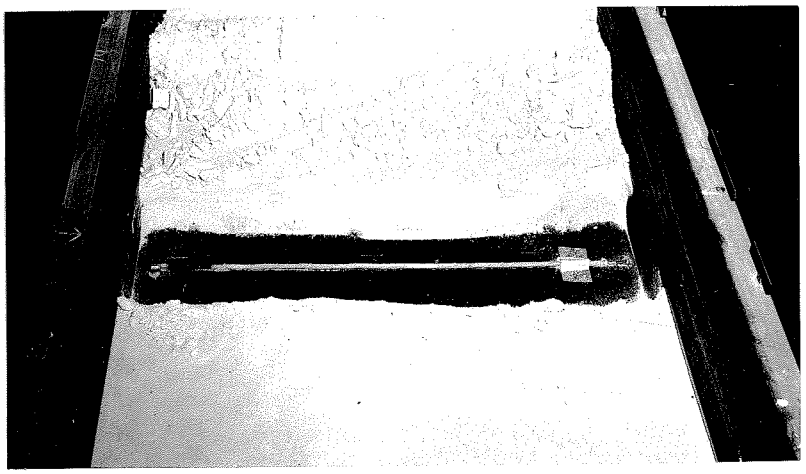

Fig. 3-11. Piezometer tap installed in 60-foot flume. (The sand has been removed to make the tap visible.)

arrangement, the straightedge can be moved to any elevation and aligned with the tops of the water columns in the tubes or reference marks placed on the glass scale. The angle between the straightedge and the horizontal can then be read on the protractor and translated into a slope of the water surface. This feature was extremely useful in adjusting the slope of the flume to that of the water surface during the early stages of a run when equilibrium slope was being sought. It also gave a value of the water surface slope which in some runs with very high Froude numbers was used in deducing the slope of the energy gradient.

A piezometer tap installed in the 60-foot flume is shown in figure 3-11. The same arrangement was used in the 40-foot flume. The taps are made of 3/16-inch copper tubing which extends nearly across the width of the flume. One end is pinched to seal it and the other end is attached to a fitting which leads through the bottom of the flume to plastic tubing running to the manometer board. At two-inch intervals, three holes, about 1/64-inch in diameter, were drilled through the copper tubing at 120^{o} spacings around the tube. To keep sand from entering the lines, the copper tubes are wrapped with three or four layers of cotton cloth which is secured with twine. The stations at which manometer taps were installed are referred to as computation stations.

The manometer tubes on the board are spaced two inches apart while the piezometer taps in both flumes are at intervals of five feet. The tangent of the angle read from the level protractor is thus greater than the slope of the water surface in the flume by a factor of thirty

and even relatively small water surface slopes in the flume have angles on the manometer board which can be read accurately. The bevel protractor is equipped with a vernier which can be read to five minutes of arc. If the water surface slope is 0.01, an error of five minutes in reading the protractor corresponds to an error of less than one percent which is much smaller than the limitation in accuracy brought about by the unsteadiness of the water surface.

It was found desirable to have about the same amount of damping in all lines running from the piezometer taps to the manometer board. The longer plastic tubes leading to the more distant piezometer taps had more inherent damping due to their very length. To compensate for this, pinch clamps were placed on the shorter lines and adjusted so that all lines had about the same attenuating effect on changes of water surface elevation. The adjustment of the pinch clamps depended on the experience of the operator who had to judge which tubes responded too quickly or too slowly, but it was not found difficult to adjust the clamps so that all tubes behaved similarly.

While the run was in progress, the maximum and minimum elevation reached by the water in each manometer tube were marked on the glass scale with a grease pencil. A new mark was made each time the water elevation in a tube rose above the old maximum or fell below the old minimum. This process was continued for several minutes until the water level in each tube traveled only between the levels of the outside marks thus established. These elevations were recorded and averaged for each tube. The slopes of the lines of maximum and minimum elevations were determined with the straightedge and bevel

protractor. These two slopes agreed to within a few percent in practically all cases. In runs for which the fluctuation of elevation was less than about 0.03 ft, a large number of instantaneous elevations and slopes were recorded and averaged.

The glass was then wiped clean and the process was repeated. At least three, and usually five or more such determinations spaced over an interval of about two hours were made for each run. The average of all such surface elevations for each computation station was then translated into a carriage point gauge elevation by a simple computational procedure involving the slope of the flume, the distances between the computation stations and the point at which the flume is pivoted, and the zero correction between the manometer board and point gauge scales. The zero correction was determined before and after each run with the flume level and the water quiescent.

The elevations of the water surface at any computation station given by the individual determinations seldom differed from the average of all elevations for that station by more than 0.012 ft. Usually the agreement was within 0.006 ft and it is believed that the average of all readings for each tube is accurate to $\pm$ 0.004 ft for all runs with maximum wave heights less than half the depth and to $\pm$ 0.006 ft for runs with high waves and active breaking. The individual slopes measured from the manometer board agreed with the average of all determinations to within 5%. Further, this degree of accuracy could be achieved between determinations made by different people and was therefore not subject to personal factors in locating the straightedge.

3-8. Measurement of Bed Elevation

To obtain a bed profile along the length of the flume, it was necessary to stop the pump. With water in the flume, the bed was then leveled with an adjustable scraper in sections which were five feet long and centered on the manometer taps. The scraper for the 60-foot flume is shown in figure 3-12 and is quite similar to the one used in the 40-foot flume. The scraper was passed back and forth over the section, the blade elevation being adjusted as required, until all the sand in this section was redistributed to give a flat surface. The elevation of this surface at the centerline of the flume was then determined with the point gauge. This elevation was taken as the bed elevation. The elevation of the bed could be measured to the nearest 0.001 ft by illuminating the flume from above with a photographic flood light and then lowering the point gauge until it just touched its shadow on the bed.

If antidunes were present on the bed when it was leveled, they usually affected the elevation of each section. Unless an integral number of antidunes happened to be included in a five-foot section, a fractional part of an antidune was included in that section. If this segment happened to be from a crest of an antidune, the measured elevation of the leveled bed section was too high, and conversely if the segment happened to be from a trough of an antidune. To minimize this effect, the pump was stopped when the bed was relatively flat. In runs with much wave activity, it was not always possible to find a time when antidunes didn't exist somewhere along the flume.

Fig. 3-12. Bed-leveler for 60-foot flume.

3-9. Computation of Depth, Mean Velocity and Slope of the Energy Gradient

As was described in sections 3-7 and 3-8 of this chapter, the elevation of the water surface and the bed were both finally obtained as elevations on the carriage point gauge scale. Thus the carriage rails are the datum to which all subsequent elevations are referred. The depth at each station is then the difference between the elevation of the water surface and the elevation of the sand bed at that station. The mean velocity at a station is the discharge divided by the area based on the depth at that station. The elevation of the energy grade line at each station is given by

$$e = y + \alpha \frac{V^2}{2g} \qquad (3\text{-}1)$$

where

e = elevation of the energy gradient on the point gauge scale

y = elevation of water surface on point gauge scale

α = Coriolis coefficient.

The Coriolis coefficient was taken as unity in these experiments since a small error in α has a very small effect on e.

The water surface elevation, bed elevation, depth, velocity, and energy gradient elevation are now known for each computation station and the problem remaining is the determination of the mean depth, mean velocity and slope of the energy grade line for the reach of equilibrium flow. To this end, a graph like that shown in figure 3-13 was made for each preliminary and each final run. In this summary graph the elevation of the sand bed, water surface, energy gradient and the depth are plotted for each computation station. An example of this

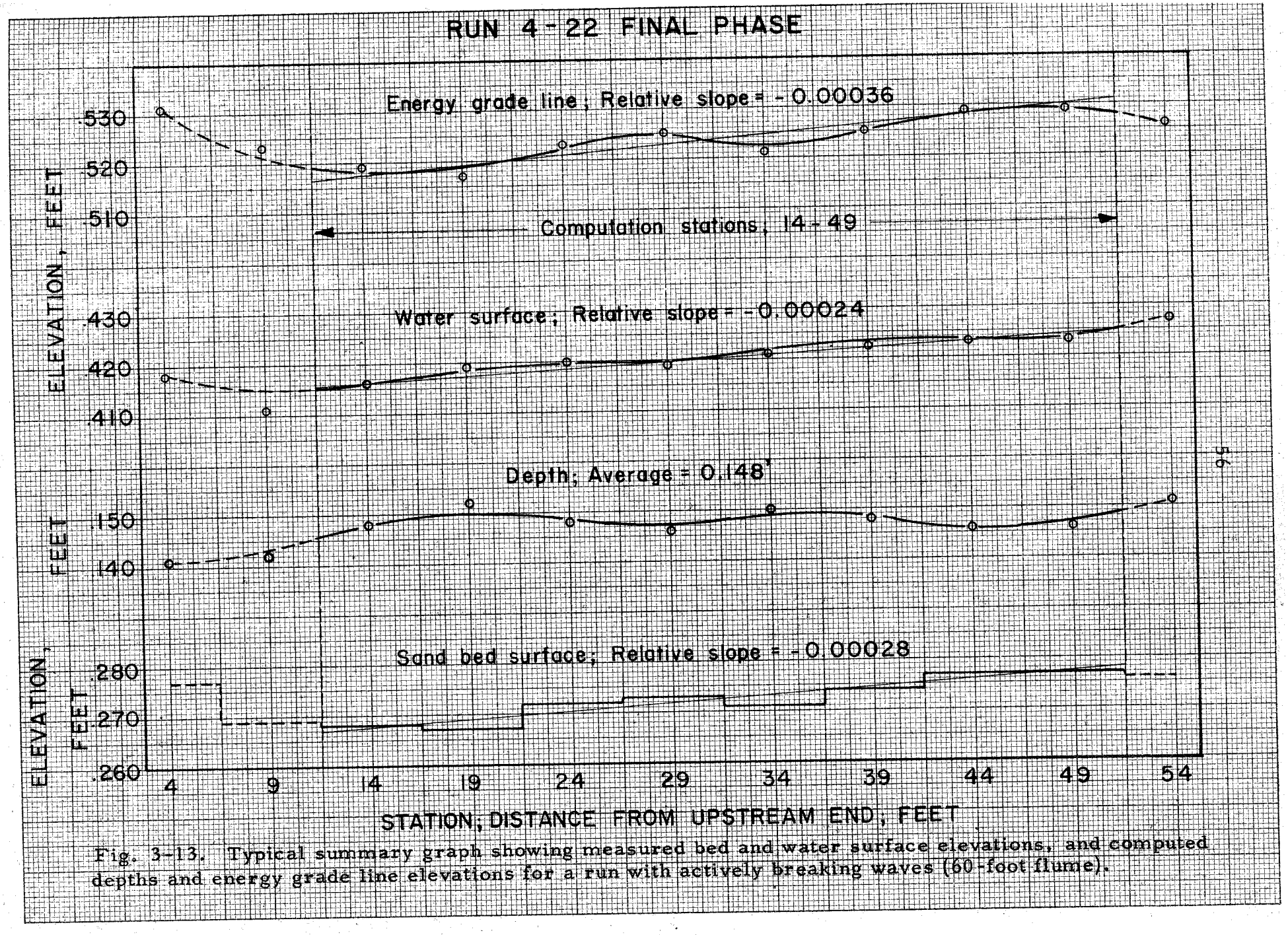

Fig. 3-13. Typical summary graph showing measured bed and water surface elevations, and computed depths and energy grade line elevations for a run with actively breaking waves (60-foot flume).

type of graph is given for Run 4-22. This was a run in the 60-foot flume which had well developed antidunes and frequently breaking stationary waves over the entire length of the flume. The graph shown in figure 3-13 would be described as average with respect to scatter of the points. As the velocity increased and the amplitude of the waves and frequency of wave breaking increased, the scatter of all points, particularly that of the energy gradient points, also increased. This problem will be discussed below.

Inspection of the summary graph first showed which stations were under the influence of the flume entrance or exit and should be excluded in determining the flow parameters. In Run 4-22, the initial drop in the water surface elevation indicates that stations 4 and 9 should not be included. Similarly, the rise of the water surface at station 54 indicates that it is under the influence of the flume exit and it is not included. Thus, for Run 4-22, stations 14 through 49 are selected as those to be used in computing the depth, velocity, and slope. In most runs, the first two stations were not used, and in some high Froude number runs, as many as four stations were excluded. Never more than two stations at the downstream end were excluded and often no stations appeared to be influenced by the exit. The stations remaining constitute the computation section for the run.

The relative slopes (slope with respect to the carriage rails) of the sand bed, water surface, and energy grade line in the computation section were then determined by fitting by eye the straight lines giving the best fits through the respective points. The slopes of each of these quantities should be the same since any nonparallelism between the bed

and water surface will cause local deposition or scour which will tend to make the depth constant along the length of the flume. In Run 4-22, (figure 3-13) the relative slopes of the energy grade line, water surface and sand bed are seen to be -0.00036, -0.00024 and -0.00028 respectively. The flume slope for this run was 0.0070 and thus the three different total slopes are 0.0066, 0.0068 and 0.0067 respectively. The average water surface slope determined from the manometer board for this run was 0.0070. The average of these four slopes, 0.0068, is the slope that was taken as the slope of the energy gradient for this run.

In runs with violent wave activity the scatter of the computed energy gradient points was so large that no attempt was made to fit a straight line through them. The large scatter of the computed energy grade line points can be explained from a relation developed by Brooks (20). He has shown that the slope of the energy gradient can be expressed as

$$S = S_f - (1 - F^2) \frac{dy}{dx} - F^2 \frac{dy_b}{dx} \qquad (3\text{-}2)$$

where

S = slope of energy gradient

S_f = flume slope

y = elevation of the water surface relative to the carriage rails

y_b = elevation of bed relative to the carriage rails

x = distance along flume

F = Froude number = $\dfrac{V}{\sqrt{g(y - y_b)}}$.

Now the bed elevation is based on a single bed profile made at the

conclusion of the run. As was discussed in the preceeding section, an attempt was made to stop the flume when wave activity was at a minimum so that the bed would be as flat as possible and the bed profile would not be influenced by including an extra segment of an antidune trough or crest in a section. But in runs with radical wave activity this became extremely difficult to accomplish since waves reformed as soon as they broke and there was no period during which the bed was flat. Thus the bed profile became more erratic since it was impossible not to include a segment of an extra crest or trough in a section. This situation was made worse by the antidunes becoming longer and higher at higher velocities with the result that a larger volume of sand is included in each one. The net result of these anomalies in the bed profile is to give high local values of $\frac{dy_b}{dx}$ which, when multiplied by the square of the Froude number which was also large in these cases, gives a large irregularity in the computed elevation of the energy gradient. In these runs it was often not possible to fit a straight line to the bed profile either and the slope was based only on the water surface elevation and the slopes determined from the manometer board.

In runs which had very little or no wave activity, the slope of the energy gradient was taken as the slope for the run.

In all runs, the individual slopes used to determine the slope for the run agreed with the average of these slopes to within 7 percent and it is believed that the average value gives the true slope of the energy gradient to within 5 percent.

The depth for the run was taken as the average of the depths in

the computation section. Thus

$$d = \frac{1}{n} \sum_{i=1}^{n} (y - y_b)_i \qquad (3-3)$$

where n is the number of computation stations. This can also be written as

$$d = \frac{1}{n} \sum_{i=1}^{n} y_i - \frac{1}{n} \sum_{i=1}^{n} y_{b_i}. \qquad (3-4)$$

But the last term is the mean bed elevation over the length of computation section. Thus the depth as used here is not subject to the errors due to local irregularities in the bed profile which affected the depths computed for the individual stations. In some of the high Froude number runs, the depths for the individual computation sections differed by as much as 0.010 ft but it is believed that the average depth computed from equation 3-3 is correct to the same accuracy as the water surface elevation, i.e. $\pm$0.004 ft for runs in which the wave height was less than the depth and $\pm$0.006 ft for runs with high waves and active breaking.

The mean velocity, V, for all runs except 5-11, 5-12, 5-13 and 5-18 is simply the discharge, Q, divided by the area, or

$$V = \frac{Q}{bd} \qquad (3-5)$$

where b is the flume width.

Runs 5-11, 5-12, 5-13 and 5-18 were carried out at very low depths ($d < 0.1$ ft) which resulted in velocities in the return pipe which were much lower than those in the flume. Consequently, sand deposited in the return pipe and venturi meter to a depth of about two inches making discharge measurements with the venturi meter

impossible. The velocity in these runs was determined by measuring the time required for a small wooden float, 1/4" x 1/4" x 1/2", to travel between stations 5 and 25 at the centerline of the flume. Five or more determinations of this time were made and these always agreed with the average of all values to within 4 percent. To determine the mean velocity, i.e., Q/bd, it was necessary to know the relation between the centerline surface velocity and the mean velocity. The von Karman universal velocity defect law gives this relation. Thus for these runs

$$V = V_{max} - \frac{U_*}{k} \qquad (3\text{-}6)$$

where

V_{max} = velocity at centerline of surface as determined from measuring float velocities

U_* = shear velocity

k = universal constant.

For water transporting sediment, k varies from 0.2 to 0.4. In computing V from equation 3-6, k was taken as 0.3. This procedure was used only in the four runs mentioned above.

3-10. Measurement of Total Sediment Load

In all runs, except Runs 5-13 and 5-18, the total sediment discharge was determined by withdrawing from the flume representative samples of the water-sediment mixtures. In all runs except 4-1, 4-3, 4-6 and 4-7, twelve or more one-liter samples were withdrawn from the flow, spaced over a period of 30 minutes or longer. In the early runs of Series 4 mentioned above, only eight or nine samples were taken.

The concentration of sediment in these samples was determined by filtering the sample through filter paper, then oven-drying and individually weighing the sediment collected in each sample to the nearest 10 milligrams with an analytic balance. The average of all sample weights for a run was taken as the sediment concentration in grams per liter. It was found that the standard deviation of the weights of the samples was about 10 percent of the average of all samples in a set.

The methods used in withdrawing the samples from the flumes will now be described.

a. 60-foot flume. Samples of the water-sediment mixture were siphoned from the lower part of the pump well through the samplers shown in figure 3-14. The intakes of the sampler were located in the vertical section of pipe just above the pump. The samples were siphoned through the intakes and the vertical tube and then through a section of transparent tubing which discharged into a one-liter bottle. The head on the siphon was adjusted to give the same velocity in the entrances to the sampler intakes as the mean velocity in the cross section from which the samples were withdrawn. A further requirement was that the velocity in the sampler be high enough to prevent internal deposition. For the range of discharge possible in the flume, these requirements necessitated the use of three different samplers. The characteristics of the samplers given by Vanoni and Brooks (1) are summarized in table 3-1.

To compensate for any non-uniformity of concentration across the section from which the samples were withdrawn, the sampler was

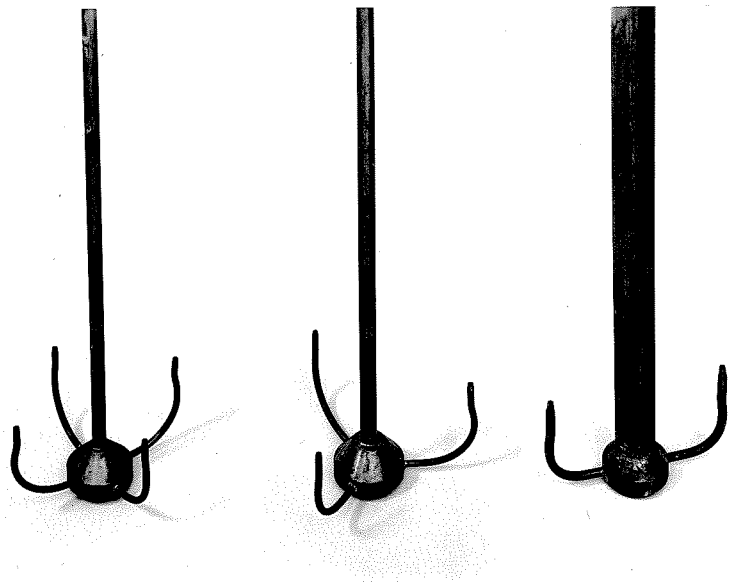

Fig. 3-14. Total load samplers for 60-foot flume.

Table 3-1

Characteristics of Total Load Samplers for 60-foot Flume

Sampler		A	B	C
No. of intakes		4	3	2
Intake opening, in.		0.136	0.129	0.136
Vertical tube I.D., in.		0.305	0.353	0.416
Flume discharge, cfs	min.	0.48	0.98	1.8
	max.	1.04	2.2	4.4
Time required to collect one-liter sample, sec.	max.	99	74	53
	min.	45	33	22

Distance from vertical tube to intakes = 2.7 in. for all samplers.

moved slowly but continuously around in the section during sampling. A liter of clear water was added to the flume after each sample was taken to keep the depth in the flume constant. The siphon was always allowed to run several minutes before samples were collected to allow the sediment flow in the sampler to reach equilibrium. The plastic tubing which ran from the sampler to the collection bottle was held as nearly vertical as possible to prevent deposition in it.

The bottle in which the sample was collected rested on a platform which could be moved vertically in a rack to give the required head on the siphon. This sampler rack and its appurtenances can be seen in figure 3-3. The end of the siphon tube was connected to a two-way swing-spout above the bottle. In one position, the swing-spout directed the flow into the bottle while in the other position, it passed the flow into a bucket. A switch activated by the swing-spout started an electric timer when the flow was diverted into the sample bottle and

stopped the timer when the valve was pushed back. This gave an accurate measure of the time required to withdraw the sample.

b. 40-foot flume. In all runs in the 40-foot flume, except Run 4-1, the samples were withdrawn through a sampler placed in the vertical section of the transition at the upstream end of the flume. This sampler is shown schematically in figure 3-15 and the setup used in sampling from this flume can be seen in figure 3-3. The sampler tube was made of 1/4-inch hard drawn copper tubing. The opening of the sampler had a diameter of 3/16 inches and the wall of the tube was beveled to give a knife edge. The sampler could be moved across practically the full width of the section. Two layers of 4-mesh screen were placed 10 inches below the sampler inlet in an attempt to distribute the sediment evenly across the section and break up concentration gradients resulting from the heavy concentrations near the bottom of the horizontal return pipe being carried into the transition. Although this sampling arrangement was far from ideal, the arrangement of the equipment precluded a better choice.

During the sampling, the head on the tube running from the sampler to the sample bottle was adjusted so that the velocity of the flow entering the sampler was the same as the mean velocity in the riser. Three one-liter samples were taken at each of five sampler positions spaced 1-1/8 inches apart. It was found that a concentration gradient persisted across the riser despite the two screens. The concentration at the center of the section was usually about 10 percent higher than that near the wall corresponding to the bottom of the return pipe and often twice as large as that at the opposite wall. However,

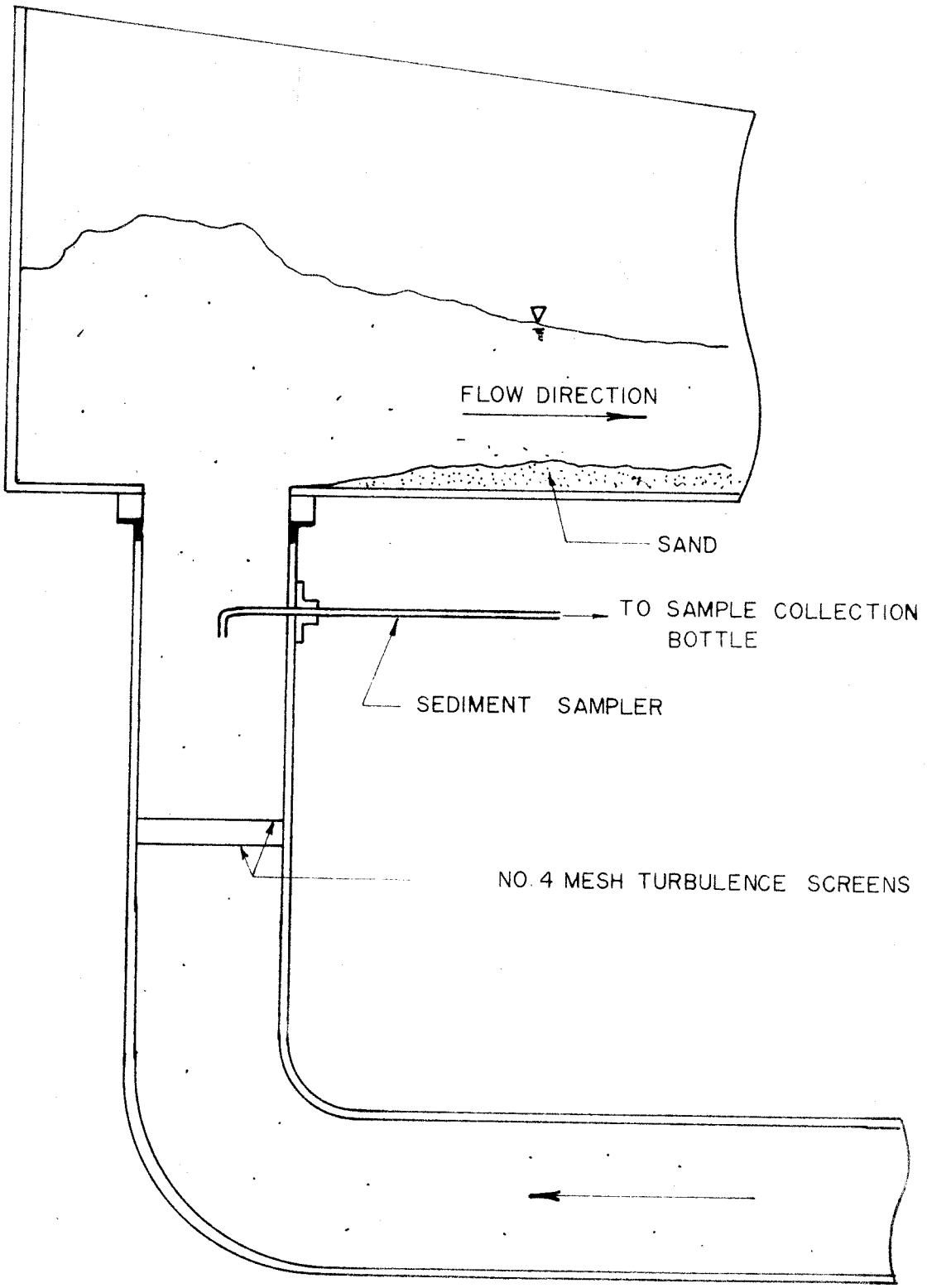

Fig. 3-15. Longitudinal section of 40-foot flume at upstream end showing box inlet and sediment discharge sampler.

the average of all samples gave concentrations which agreed fairly well with samples from equivalent runs in the 60-foot flume and this average was used.

In Run 4-1, a simple bent tube sampler with an inlet diameter of 0.312 inches was used in the pump well of the 40-foot flume. This is the same sample which was used by Brooks (20), Nomicos (21) and Vanoni and Brooks (1) and it has been described and discussed by these authors. It was not used in the later runs in the 40-foot flume because of the surging which occurred in the small pump well. The new large pump well, which was installed after Run Series 5 was completed, reduced the surging but had no straight section which was suitable for sampling.

3-11. Wave Length Measurement

In all runs except 5-1 through 5-12, the wave length of the stationary waves (and thus of the antidunes also, as was discussed in chapter 2) was determined during the run by measuring the length of channel occupied by some integral number of waves at a given instant. This procedure was repeated at least five times and often twenty times or more during each run. Waves in the first 10 feet of the flumes were never included as they were apparently affected by the entrance.

This procedure is not very accurate for several reasons. First, since the waves were rather long and flat, it was difficult to determine the position of a crest or trough to within an interval of less than about one tenth of a wave length. This error is magnified by the fact that the waves often occurred in trains of only seven or eight waves. Since the end waves were not used in the determination, this left only five or

six waves among which the error due to the locations of the first and last waves was divided. A further difficulty arose at higher velocities when the waves would form and break so rapidly that only a few waves could be counted before the pattern would disappear.

The wave length reported was taken as the average of the wave lengths determined by the individual wave counts. It was found that the values corresponding to the individual determinations seldom differed from the average of all values by more than 10 percent. At the lower velocities, the values usually fell within 5 percent of the average. The average value is believed accurate to about 5 percent.

In runs 5-1 through 5-12, no wave counts were made during the run. The wave lengths were later scaled from photographs or determined from detailed bed profiles which were made in some runs before the bed was leveled. It is estimated that the accuracy of these determinations is about the same as that of the measurements made during the run.

3-12. Photographs

Since one of the objectives of the laboratory study was to obtain descriptions of the bed and water surface behavior of the various regimes of flow, extensive use was made of both still and motion photography. For all runs, still and motion pictures of all significant features of the water surface and bed behavior were taken through the windows in the sides of the flumes. For certain runs, still photos were also taken of the bed features after the pump had been stopped. In all photos taken through the window, a steel tape graduated in inches and fractions was placed along the bottom of the window to provide a

reference scale and a coordinate system. Overhead still photographs, looking downstream, were taken in all runs which had pronounced wave activity. Overhead motion pictures were also taken in several runs. Several of the better still photos obtained are shown in chapter 4. The motion pictures were studied in detail during and after the laboratory study to compare the visible effects of flow parameters and sand size on the flow behavior. A motion picture film which shows the formation, growth and breaking of stationary waves has been prepared for Runs 5-14, 5-16, 5-17 and 4-28.

3-13. Calculation of Bed Shear and Friction Factor

In an infinitely wide uniform flow the shear stress exerted on the bed is equal to the component of the weight of the fluid along the bed,

$$\tau_o = \gamma S d \qquad (3\text{-}7)$$

where

τ_o = shear stress on the bed

γ = unit weight of fluid.

When the width of the channel is finite, the shear stress on the walls must also be taken into account. If the cross sectional area of the stream is A, then the component along the channel of the fluid weight is γAS per unit length. This must be resisted by the shear force over the wetted boundary. If the average value of the shear stress over this boundary is $\overline{\tau}_o$, then the resisting force per unit length of channel is $\overline{\tau}_o p$ where p is the wetted perimeter. Equating these two forces, the result is

$$\overline{\tau}_o = \gamma r S \qquad (3\text{-}8)$$

where r is the hydraulic radius, A/p.

The value of the shear stress, τ_o or $\overline{\tau}_o$, must be related to the mean velocity of flow in the section, to be of any value in designing or analyzing fluid systems. The relation between the shear stress and the velocity depends on the shape of the section, the roughness of the walls, and the properties of the fluid. In open-channel flow, this relation is usually expressed by empirical relations such as the Chezy equation

$$V = C\sqrt{rS} \tag{3-9}$$

in which C is a dimensional constant which must be determined experimentally and which depends on the roughness of the walls, geometry of the channel, and properties of the fluid. The relation for C which will be used here is given by the Darcy-Weisbach equation which can be written as

$$V = \sqrt{\frac{8g}{f}}\sqrt{rS}. \tag{3-10}$$

Here the friction factor, f, depends on the same factors as Chezy's C but is dimensionless. If equation 3-8 is substituted into equation 3-10, the average shear stress can be expressed as

$$\overline{\tau}_o = \frac{f}{4}\rho\frac{V^2}{2}. \tag{3-11}$$

This can be put into a more convenient form by introducing the shear velocity, U_*, defined as

$$U_* = \sqrt{\frac{\tau_o}{\rho}} = \sqrt{grS}. \tag{3-12}$$

Then, after some rearranging,

$$f = 8\left(\frac{U_*}{V}\right)^2 . \qquad (3\text{-}13)$$

Equation 3-10 relates the mean velocity to the mean shear stress on the boundary of the flow and in this form can only be applied to cases in which the wall roughness is the same for all surfaces. In the case of flume experiments, the roughness of the flume walls remains constant while the roughness of the sand bed varies over a wide range due to the formation of bed features. Since it is the shear on the bed and the friction factor of the bed that are of interest, these expressions cannot be used in their present form. Rather, some procedure must be used which will separate the wall effects from the bed effects. Such a procedure has been devised by Johnson (22) and modified by Brooks (20). The procedure given by Brooks will be outlined here.

The principal assumption involved is that the cross section can be divided into two areas, In one the flow is resisted only by the bed while in the other it is resisted only by the walls. Associated with each of these areas is a different roughness which is assumed homogeneous for each section. The wall roughness is known and the bed roughness is sought. Further, it is assumed that equation 3-10 can be applied to each section individually, and that the mean velocity and slope of the energy gradient are the same for both sections. Thus

$$A = A_w + A_b \qquad (3\text{-}14)$$

where

A_w = area in which the flow is resisted only by the wall

A_b = area in which the flow is resisted only by the bed.

From equation 3-10,

$$A_b = \frac{p_b f_b V^2}{8 g S} \qquad \text{and} \qquad A_w = \frac{p_w f_w V^2}{8 g S}. \tag{3-15}$$

Here again, the subscripts b and w pertain to the bed and wall respectively. Substituting equation 3-15 into equation 3-14 and substituting for A from equation 3-10, the result is

$$p f = p_b f_b + p_w f_w. \tag{3-16}$$

Since f_b is the only unknown, equation 3-16 can be solved to yield

$$f_b = \frac{p}{p_b} f - \frac{p_w}{p_b} f_w. \tag{3-17}$$

If the channel is rectangular, the relations $p = 2d + b$, $p_w = 2d$, and $p_b = b$ may be substituted and equation 3-17 becomes

$$f_b = f + \frac{2d}{b}(f - f_w). \tag{3-18}$$

The only remaining problem is to determine f_w. To this end, consider the Reynolds numbers for the three sections,

$$R_b = \frac{4 r_b V}{\nu}, \qquad R_w = \frac{4 r_w V}{\nu}, \qquad \text{and} \qquad R = \frac{4 r V}{\nu}, \tag{3-19}$$

where ν is the kinematic viscosity. Since V is the same for all sections, equation 3-19 becomes

$$\frac{R_b}{r_b} = \frac{R_w}{r_w} = \frac{R}{r}. \tag{3-20}$$

If expressions of the form of equation 3-10 for each of the three sections are solved for r_b, r_w, and r and substituted in equation 3-20, the

ratios become

$$\frac{R_b}{f_b} = \frac{R_w}{f_w} = \frac{R}{f} . \qquad (3\text{-}21)$$

Since R and f are known, equation 3-21 can be used to compute R_w/f_w. Then f_w can be obtained from a pipe friction diagram by trial and error if the wall roughness is known. Assuming smooth walls, the graph shown in figure 3-16 has been prepared by Brooks (20) so that f_w can be obtained directly. The value of f_w can now be used in equation 3-18 to get the bed friction factor, f_b. Also equations 3-20 and 3-21 can be solved for r_w and r_b and the bed shear velocity can then be computed as

$$U_{*_b} = \sqrt{g\, r_b S} . \qquad (3\text{-}22)$$

It is realized that the side-wall correction procedure is not entirely applicable to the case in which the flow is both non-uniform and unsteady. Indeed, the division of the shear between bed and walls is quite artificial and open to much question even in the case of steady uniform flow. In the case of flow over antidunes the depth and thus the distribution of shear between bed and walls changes continuously with time and distance and the computed bed shear will represent some sort of an average. However, it is desirable to make the correction to put the results from different flumes on a comparable basis.

3-14. Reproducibility

The reproducibility of the runs was continually checked by comparing the results of the last preliminary phase and the final phase of each run. In practically all cases, the reproducibility was found to be within the limits of the estimated accuracies discussed earlier in this

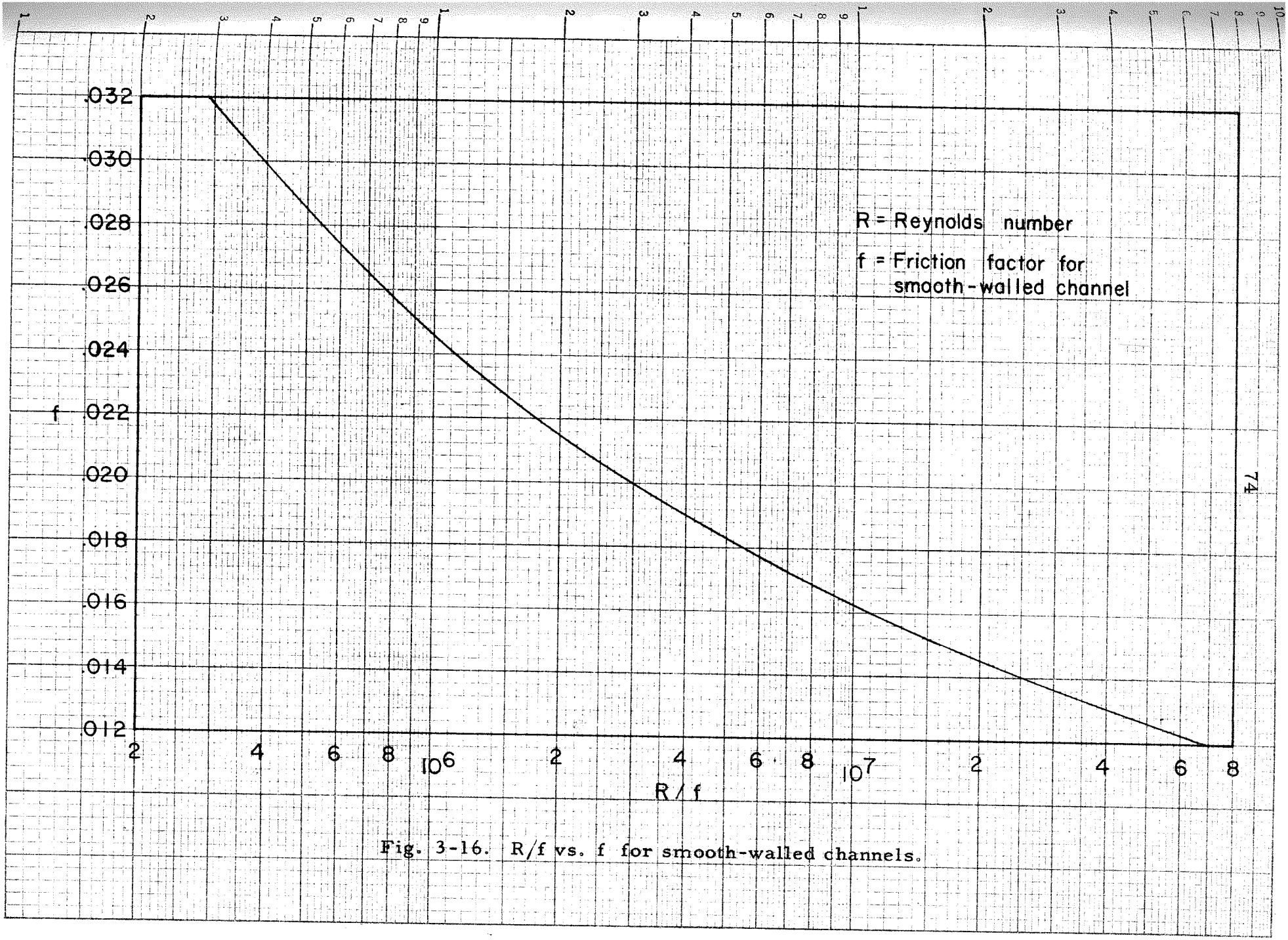

Fig. 3-16. R/f vs. f for smooth-walled channels.

chapter. A typical example is given in table 3-2 which compares the results of a preliminary phase and final phase of Run 4-28, a run in the 40-foot flume. The objectives of this run were $d = 0.150$ ft, $V = 2.52$ ft/sec and $F = 1.15$.

Table 3-2

Example of Reproducibility of Runs
Run 4-28

Phase	Preliminary	Final
Date	9-11-59 A.M.	9-11-59 P.M.
Depth, ft	0.150	0.148
Velocity, ft/sec	2.54	2.55
Flume Slope	0.0065	0.0065
Energy Gradient	0.0065	0.0066
Wave Length, ft	1.27	1.27

3-15. Sand Characteristics

Two different sands were used in this investigation: Sand 1, which had a geometric mean diameter of 0.549 mm, for Run Series 5; and Sand 2, which had a geometric mean diameter of 0.233 mm, for Run Series 4. The sieve analysis procedure and the sand characteristics will be described in this section.

a. Sieve analyses. At intervals during the laboratory investigation, samples of sand were removed from the flumes by forcing a metal cylinder, about two inches in diameter, into the bed until it penetrated to the channel floor. All of the sand contained in the

cylinder was then removed. Samples were taken at three locations in the 40-foot flume and four locations in the 60-foot flume. The samples were then dried and a representative portion of the composite was obtained by splitting the composite into successive halves with a Jones sample splitter until a sample of 50 to 40 grams remained. A sieve analysis of this sample was then made using a $\sqrt[4]{2}$ - series of standard ten-inch Tyler laboratory sieves which were shaken for 15 minutes on a Tyler Rotap Machine. Each sieve fraction (sand contained between successive sieves) was then weighed to the nearest 10 milligrams on an analytic balance.

A similar sieve analysis was performed on the composite of all sediment samples collected during each run.

b. Analyses of sands used in experiments. Both of the sands used in this investigation were predominantly quartz (specific gravity = 2.65). They were obtained from a foundry supply house and given no further processing except washing in the flumes. Sand 1 is a natural sand of the St. Peter formation and is marketed commercially as "Ottawa Sand". Photomicrographs of the sands are shown in figure 3-17. Sand 1 is quite rounded while Sand 2 is much more angular.

The distributions of the sieve sizes of the sands are shown graphically in figure 3-18 plotted on logarithmic-probability paper as suggested by Otto (23). The fact that the distributions plot as straight lines, except for the tails, indicates that the logarithms of the sieve diameters of the sands are distributed according to the normal error law. This distribution is completely defined when the geometric mean, $D_g = D_{50}$, and the geometric standard deviation, σ_g, are given

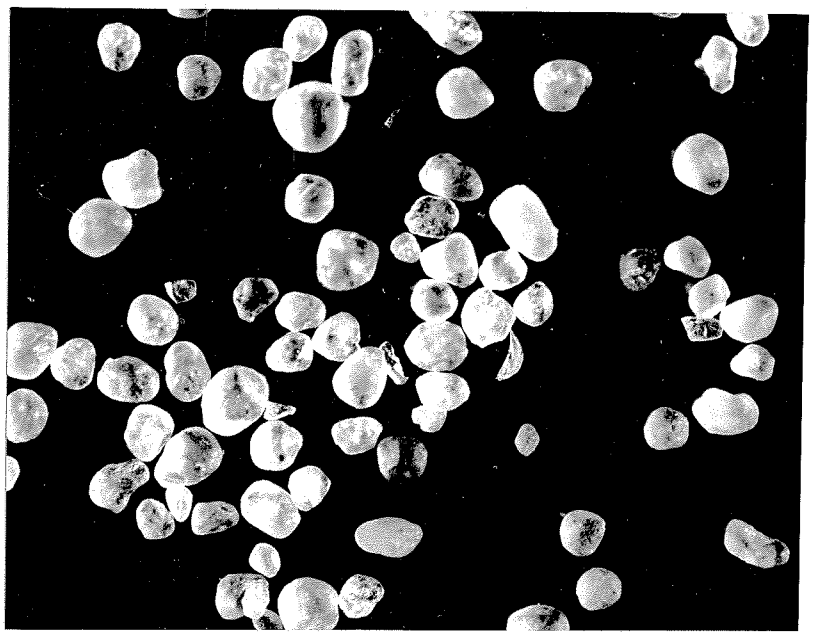

(a) Sand 1 (D_g = 0.549 mm).

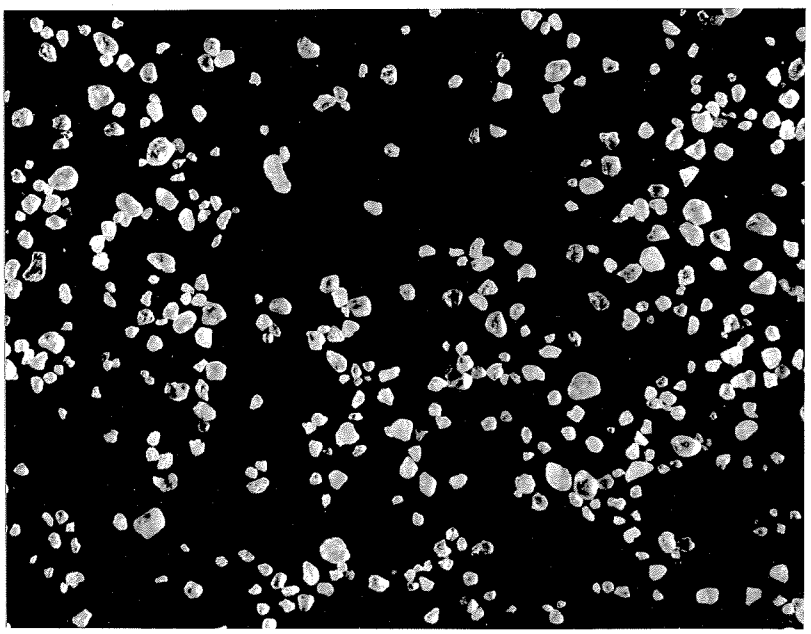

(b) Sand 2 (D_g = 0.233 mm).

Fig. 3-17. Photomicrographs of sands used. (Magnification: 10 times.)

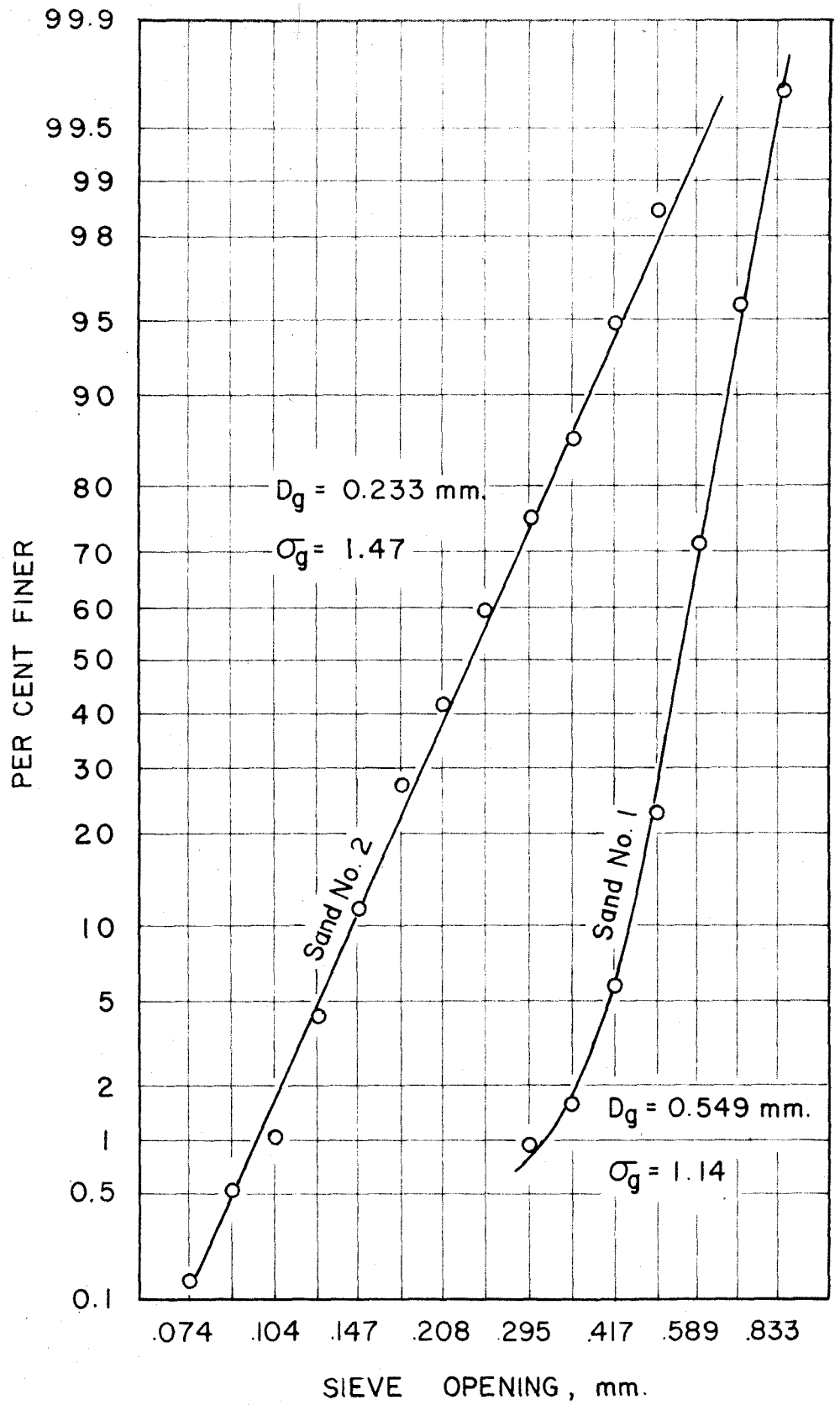

FIG. 3-18. SIEVE ANALYSES OF SANDS USED

The geometric standard deviation is given by

$$\sigma_g = \frac{D_{50}}{D_{15.9}} . \qquad (3\text{-}23)$$

The changes in D_g and σ_g for the sands during the investigation were not significant for either sand.

The properties of the sands used in this investigation are summarized in table 3-3.

Table 3-3

Summary of Sand Properties

	Sand 1	Sand 2
Geometric mean sieve diameter, D_g, mm	0.549	0.233
Geometric standard deviation, σ_g	1.14	1.47
Specific gravity	2.65	2.65
Shape	rounded	subrounded
Used in Run Series	5	4

CHAPTER 4

EXPERIMENTAL RESULTS

In the first section of this chapter the general plan of the experimental program will be explained. The experimental results will then be presented in three interrelated sections. In section 4-2, some general features of high velocity flow over a sand bed will be discussed. This will supplement the general description given in chapter 1. In section 4-3, two systematic sets of runs will be described in some detail and illustrated with photographs. These descriptions will show the succession of bed and surface configurations for a constant depth as velocity is increased. A summary of configurations for all runs and measured wave parameters will also be given. In section 4-4, the roughness and sediment transport characteristics of the laboratory stream will be presented and the roughness will be related qualitatively to the water surface configuration.

4-1. General Outline of Experiments

Each run represented a flow in equilibrium with its sand bed. The measured quantities were obtained using the techniques described in chapter 3. The flume experiments can be divided into three groups:

Group 1. Experiments in the 40-foot flume using Sand 1
(Runs 5-1 through 5-18)

Group 2. Experiments in the 40-foot flume using Sand 2
(Run 4-1 and Runs 4-24 through 4-38)

Group 3. Experiments in the 60-foot flume using Sand 2
(Runs 4-3 through 4-23).

Certain run numbers are missing (e.g. 4-2) so there is not a continuous sequence. The missing numbers represent special experiments which are not reported here.

The main theme of the experimental program was to conduct a set of runs in each group at a constant depth of approximately 0.15 ft. At this depth runs were made with Froude numbers ranging from about 0.75 up to a limiting value imposed by the behavior of the flow or capacity of the equipment (less than 2.0). In addition, to study the effect of depth of flow, several runs were made in each group at depths of 0.25 and 0.35 ft. Several runs were also made in Group 1 at very low depths. Several other runs were made at scattered values of depth and Froude number.

4-2. Some General Features of High Velocity Flow over a Sand Bed

Numerous photographs will be presented in the next two sections to illustrate the different bed and water surface configurations. To show the range of behaviors encountered, most figures will show several photographs of the run being illustrated. The side views through the window will in general show the most uniform flow condition, a condition of well developed waves, and the condition of maximum wave amplitude or wave breaking. Except where noted, the flow is from left to right. In most cases top views will also be given.

a. Formation of stationary waves and antidunes. The first question that naturally arises is why do antidunes and stationary waves ever form. Apparently the chain of events is as follows. Some disturbance gives rise to a stationary surface wave. This disturbance

can arise from a protuberance on the bed, such as a dune, or a direct disturbance of the water surface. At Froude numbers greater than about 1.6, it was impossible (except at very small depths) to avoid such surface disturbances at the inlet and outlet of the flume. If the depth and velocity are above certain limiting values the perturbation velocities accompanying the surface waves affect the local sediment transport capacity of the flow. The material under the wave troughs where the perturbation velocity and flow velocity are in the same direction is entrained by the fluid and deposited under the crests, where the perturbation velocity opposes the flow velocity. Antidunes are the result of this differential deposition. The growth of the antidunes increases the magnitude of the perturbation velocities which in turn cause more differential deposition and further increase of the antidune amplitude. As the antidunes become steeper, the effect of gravity in resisting the sediment movement from the antidune troughs to the crests also increases. Finally a limiting antidune height is reached which depends on the depth of flow, velocity,and transport characteristics of the sand. If the amplitudes of the stationary waves reach the critical value for breaking before the antidunes reach their limiting height, the waves break.

Over a certain range of depth and velocity, it was found that two possible flow conditions exist. If the water and sand were admitted to the flume with a minimum of disturbance, the bed and water surface remained flat. If the water surface was given a persistent disturbance at the upstream end of the flume, stationary waves and antidunes developed over the whole length of the flume. If the disturbance was

then removed, the waves disappeared and the flow again became steady and uniform.

b. Movement of waves and propagation of waves. In the literature (see section 1-2) frequent mention has been made of the upstream movement of the individual stationary waves and antidunes and in section 2-6 it was shown that two-dimensional antidunes would be expected to move upstream. As discussed in the next section, it was found that, depending on the depth of flow, velocity, and sand size, the waves can move upstream, downstream, or not at all. This movement of the individual waves must be clearly distinguished from the propagation of the antidune phenomenon. It was observed that antidunes occurred in trains of 5 to 25 waves and that the whole wave train propagated downstream regardless of the direction of movement of the antidunes.

Consider the train of antidunes at time t_1 shown in figure 4-1a. At the downstream end of the train, the flow coming from the antidune region acts on the bed to form another antidune by scour and deposition. Meanwhile, at the other end of the train, the flow coming from the region where the bed is flat scours away the crest of the upstream antidune and deposits it in the trough, thus leveling the bed. This is the manner in which the wave trains propagate downstream: by forming antidunes at the downstream end of the train and obliterating them at the upstream end. At a time $t_2 > t_1$, the train of antidunes will have propagated downstream to the position shown in figure 4-1b. The mechanism at the downstream end usually works slightly faster so the length of the wave train increases. However, this effect is small.

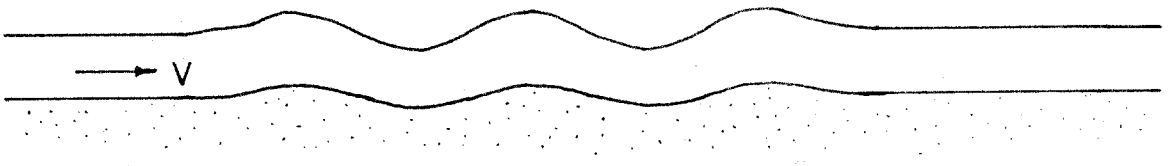

(a) Isolated train of stationary waves and antidunes at time t_1.

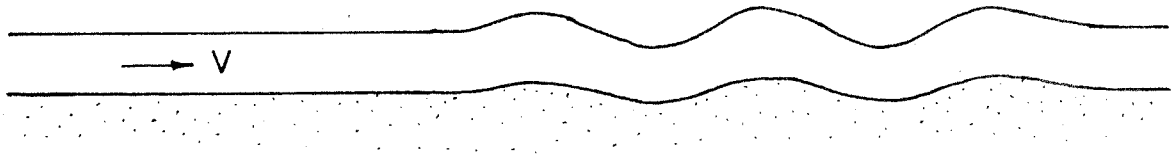

(b) Stationary waves and antidunes of figure (a) at time $t_2 > t_1$. Note downstream propagation.

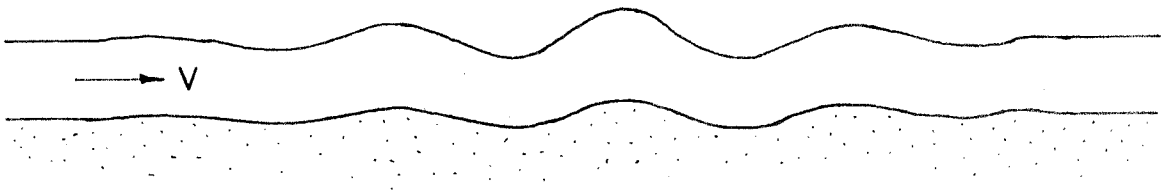

(c) Typical train of stationary waves and antidunes with amplitudes that increase toward the center of the train.

Fig. 4-1. Profiles of stationary waves and antidunes.

This is analogous to the group velocity phenomenon observed in translational waves. If a train of gravity waves propagates in a still medium, it is observed that the leading waves die out and new waves appear at the rear of the train. This is brought about by the rate of energy propagation being slower than the wave celerity. In the case of flow over antidunes, the waves are moving upstream relative to the moving fluid. Thus the leading wave of the train is at the upstream end and this wave disappears. Meanwhile at the rear of the wave train (the downstream end) a new wave appears.

Actually, the wave appearance was observed to be more like that shown in figure 4-1c. The wave amplitude increased from the upstream end of the train, reached a maximum near the center of the train, and then decreased to the downstream end of the train. The end waves were not of vanishingly small amplitude and the wave length was the same for all waves. No explanation is given for the increase in wave amplitude. The oversimplified analysis of section 2-6 indicated that the wave amplitude remains constant as the antidunes move. If this were the case, however, the waves would never attain the critical amplitude for breaking. Wave breaking, if any, occurred near the center of the train where the amplitude was the greatest.

To an observer at a fixed location, the waves usually gave the appearance of increasing, then decreasing in amplitude, as was mentioned several times in section 1-2. This appearance was due to the propagation past the observer of a train of waves with amplitudes that increased toward the center of the train, then decreased to the upstream end of the train.

c. Wave breaking. When the waves and antidunes reached a certain limiting height, one or more of the stationary waves would break. The crest of the wave moved upstream and collapsed into the adjacent wave trough. An example of wave breaking is shown in figure 1-2. During this breaking, there was an actual momentary upstream movement of a segment of the flow and considerable storage of water occurred. The accompanying agitation of the flow obliterated the antidune under the wave and, when the breaking subsided, the bed soon became flat again. At velocities smaller than a critical value that depended on the sand size and flow depth, the breaking of one wave usually did not precipitate the breaking of adjacent waves. This will be called "isolated breaking". At greater depths and velocities, the breaking wave often rushed upstream onto the adjacent wave, thus precipitating its breaking. The water storage occurring in the region of breaking reduced the discharge to the adjacent downstream wave and this often precipitated its breaking. In other instances, several adjacent waves would reach their critical amplitude and break simultaneously. This situation in which two or more waves break at about the same time will be called "multiple breaking". After breaking occurred in a region, the resulting reach of flat bed usually divided the original wave train into two separate trains and propagated downstream between the two new trains.

The waves did not always disappear by breaking or propagating out of the region. Often several adjacent waves or a whole train of waves would spontaneously disappear for no apparent reason. The wave amplitudes rapidly diminished to zero and the bed and water

surface became flat.

d. Three-dimensional stationary waves. In many runs, the stationary waves and antidunes that formed were not of the classical two-dimensional form but were very peaked and three-dimensional. An example of such waves is shown in figure 4-13. These waves were most common in runs of Group 1 (coarser sand). In Groups 2 and 3 (finer sand) they often occurred as small three-dimensional waves superposed on larger two-dimensional waves and were usually not the dominant wave form. These waves are termed "rooster tails" since in appearance they are not unlike the so-called rooster tails which form behind racing hydroplanes. As was discussed in section 2-7, they represent a superposition of a translational wave in the direction of flow and a standing wave normal to the flow. The resultant wave appears stationary since its celerity is just equal to the flow velocity.

The reason that the water-sand system assumes this configuration in preference to two-dimensional waves is not at all clear. A similar phenomenon in the case of standing waves has been reported by Taylor (24). He too was at a loss to explain why the waves assume a three-dimensional form. In flow over antidunes, the rooster tails apparently occurred as a degenerate form of two-dimensional waves. For example, two-dimensional waves generated by the diffuser inlet of the flume would persist for several wave lengths. Then the waves seemed to become unstable and any small disturbance, such as a small shock wave reflected off the flume wall, would cause them to degenerate into rooster tails. This chain of events can be seen in figure 4-2. Rooster tails also emerged whenever a two-dimensional

Fig. 4-2. Top view looking upstream showing growth of rooster tails from two-dimensional waves. Run 4-7, d = 0.195 ft, V = 3.14 ft/sec, F = 1.25, 0.233 mm sand, 60-foot flume.

wave became inclined to the direction of flow. As the antidunes propagated downstream, rooster tails gave rise to successive rooster tails. Apparently a rooster tail is a more stable configuration than a two-dimensional wave or else the two-dimensional waves would not tend to become three-dimensional.

Figures 4-2 and 4-13 give the impression that the walls of the flume are necessary to support the transverse standing wave component of the rooster tails. That such is not the case is clearly seen in figure 4-3 which shows an isolated train of rooster tails in a flume which is eight feet wide. These rooster tails were certainly not influenced by the flume walls. The boundary condition on the sides of these waves is obviously not the same as that at the vertical walls when standing waves occur in a closed basin. It is perhaps more analogous to the boundary condition at the top of an open-ended organ pipe; i.e., the sides of the rooster tails may intersect the mean water surface level at nodes. Rooster tails also occurred in multiple trains which were adjacent or separated. Such trains of waves are shown in figure 4-4. An example of the form of the bed under rooster tails is shown in figure 4-11. The shape of the bed is seen to be three-dimensional in the same general form as the rooster tails.

As their amplitudes increased, the crests of the rooster tails became disturbed and showed signs of breaking. This appearance would often persist for 30 seconds or longer. The downstream rooster tail of figure 4-3 illustrates this effect. It can also be seen in figures 4-10c and 4-13b. In addition, rooster tails often had an oscillation between adjacent upstream and downstream waves. The peaks of the

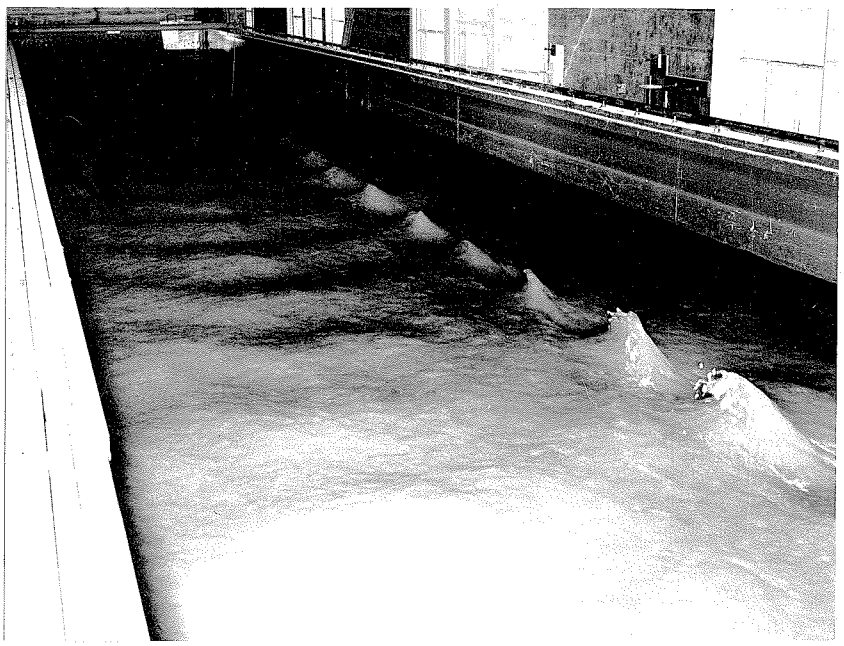

Fig. 4-3. Upstream view of an isolated train of rooster tails in an 8-ft wide flume. d = 0.279 ft, V = 2.50 ft/sec, F = 0.82, λ = 1.59 ft, D_g = 0.546 mm. (Photograph courtesy of Colorado State University.)

Fig. 4-4. Downstream view showing multiple trains of rooster tails. Run 4-11, d = 0.148 ft, V = 2.74 ft/sec, F = 1.26, G = 16.6 lb/ft-min, f_b = 0.0397, λ = 1.45 ft, 0.233 mm sand, 60-foot flume.

waves would bob up and down, adjacent waves being 180° out of phase. This too was more common as the waves became higher. For lack of a better word, the term skittish is applied to these occasional erratic types of behavior.

e. A limiting flow condition. Above a certain critical velocity which apparently depended on the depth and sand size, the antidune type of flow gave way to the torrential type of flow shown in figure 4-5. The flow pattern consisted of reaches of subcritical flow on top of sand mounds, chutes, and hydraulic jumps repeated in a semi-regular sequence. The whole configuration moved upstream at a rate of several feet per minute and the shape and spacing of the large sand mounds changed rapidly during this movement. The flow pattern was predominantly two-dimensional. The flow was so complex that every imaginable open channel phenomenon could be observed in the flume!

In this flow, the sediment transport rate was so high that no orderly pattern of differential deposition could occur. The flow accelerated as it descended a sand chute and its sediment transport capacity became so high that it scoured the bed completely away and exposed the steel bottom (see figure 4-5b). When the flow reached another sand mound, it rapidly decelerated and deposited much of its sediment load on the upstream face of the mound. On the top of the mound the flow was subcritical. On reaching the downstream end of a mound, the flow again accelerated and eroded away the downstream face. When a jump occurred at the base of a sand chute, a small sand mound like the one shown in figure 4-5a resulted.

The run shown in figure 4-5 (Run 4-6) used the 0.233 mm sand.

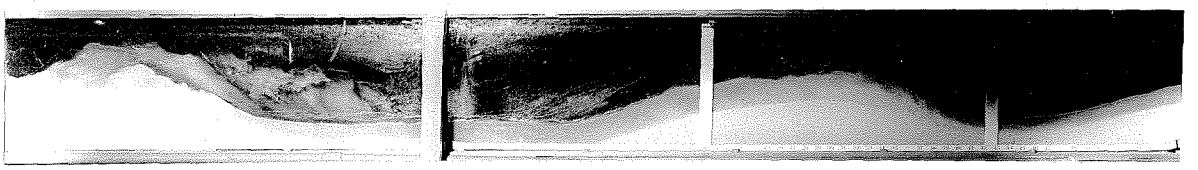

(a) Side view showing isolated sand mound. Flow from right to left.

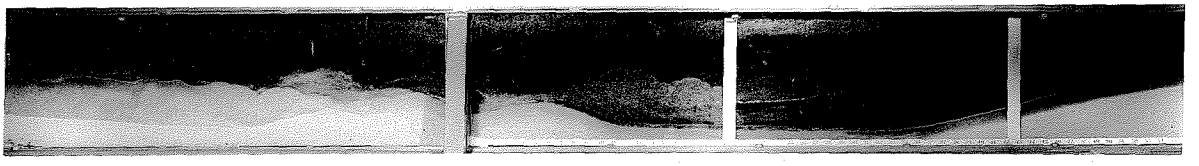

(b) Side view showing end of sand chute and extreme bed scour. Flow from right to left.

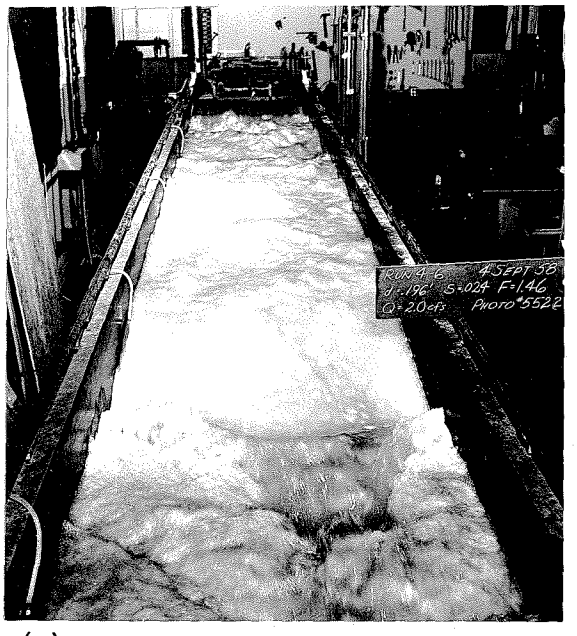

(c) Top view looking upstream.

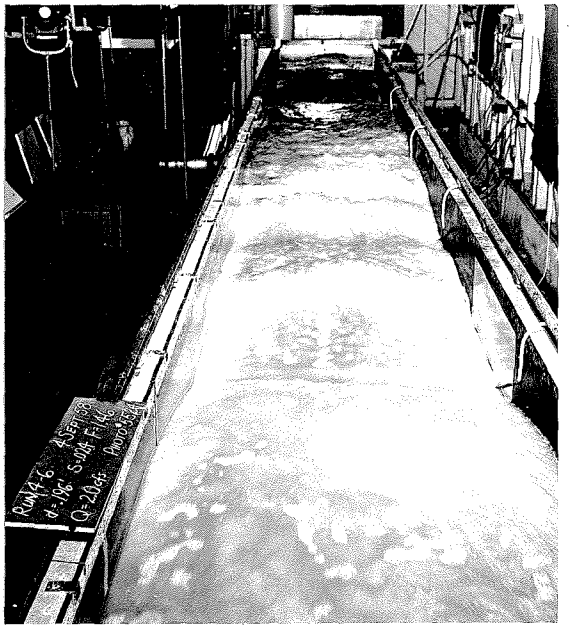

(d) Top view looking downstream.

Fig. 4-5. Top and side views showing torrential type of flow. Run 4-6. d = 0.218 ft, V = 3.29 ft/sec, F = 1.24, G = 156 lb/ft-min, f_b = 0.115, 0.233 mm sand, 60-foot flume. (Note: Data given in figures c and d are not correct.)

A run which had a larger velocity, depth and Froude number but used the 0.549 mm sand (Run 5-5) had a much lower transport rate and very moderate wave activity and surface waves which broke only occasionally. This illustrates the profound effect the size and transportability of the sand can have on the behavior of the flow.

Only one run with the torrential type of flow was carried out. When this flow condition was encountered with other runs they were discontinued. No systematic set of experiments was made at very high Froude numbers to delineate the depth and velocity combination at which this condition occurs.

4-3. Observations of Bed and Water Surface Configurations

Practically every run had some bed and water surface features which were peculiar to that run. To describe every run completely would be somewhat tedious and of questionable value. On the other hand, classifying the runs into fixed categories would disregard many features which are essential to the understanding of the laboratory stream. To avoid the difficulties and still retain the best features of each of these approaches, a compromise will be made. First, a systematic set of runs from Groups 1 and 2 will be discussed in detail and illustrated with photographs to give the reader a definite concept of the different configurations. Then, several categories of behavior will be defined and a summary of the configuration for all runs will be presented in terms of these categories. The measured wave lengths and wave amplitudes at breaking will also be presented and the ranges of depth and velocity over which the different configurations occurred will be discussed. At the end of the section, a summary of

observations and conclusions relative to the flow configuration will be presented.

a. Examples of bed and water surface configurations of experiments from Group 1. The general outline followed in this discussion and the discussion of runs from Group 2 will be the same as that of the experimental program. For a depth of about 0.15 ft, the flow behavior will be described as the Froude number increases from about 0.75 to 2.0 for the coarse sand and 1.5 for the fine sand. In addition, comparisons will be made with runs of other depths to illustrate the effect of depth variation. The runs discussed in examples 1 through 6 used Sand 1 (D_g = 0.549 mm).

Example 1. Run 5-2. d = 0.148 ft, V = 1.65 ft/sec, F = 0.757, f_b = 0.0703, G = 1.54 lb/ft-min, λ = 0.58 ft*. See figure 4-6. The bed features were sharp crested, each had a separation eddy on its lee side, and they moved downstream quite rapidly (3 to 6 in/min). These features would be classified as dunes. The water surface was usually randomly choppy. At other times small, very narrow rooster tails formed and moved downstream in groups of 15 to 20. The waves never broke. They either diminished spontaneously or moved to the downstream end of the flume. The coupling between the bed and water surface was weak since the bed features and surface waves usually existed independently of each other.

Example 2. Run 5-1. d = 0.346 ft, V = 2.58 ft/sec, F = 0.773,

* Note: d = depth of flow, ft; V = mean velocity, ft/sec; F = Froude number; f_b = bed friction factor; G = sediment transport rate, lb/ft-min; λ = wave length, ft.

f_b = 0.0746, G = 7.25 lb/ft-min, λ = 1.25 ft. See figure 4-7. A comparison of this run and Run 5-2 (example 1) shows the effect of increasing the depth while keeping the Froude number constant. The bed features were larger and more rounded than the dunes of example 1 and moved downstream faster (at about 1 ft/min). The increased sediment transport rate made possible the formation of these larger bed features. The surface waves were also larger and more nearly two-dimensional, and isolated breaking was frequently observed (see figure 4-7c). When a wave broke the agitation accompanying it would persist for 10 or 15 seconds, and the bed features in the vicinity of the breaking reverted to sharp crested dunes. The bed features and the water surface were strongly coupled since each bed feature was accompanied by a stationary wave. The bed features, unlike those of example 1, were definitely antidunes under the definition given in chapter 1. It was found to be generally true that for a constant Froude number, the amount of wave activity increased with depth.

In this run (and also Run 5-2, example 1) the factors (whatever they may be) that govern the form of the bed were such that dunes formed. Due to the rather high Froude number, the disturbances caused by the dunes resulted in the formation of surface waves. The perturbation velocities accompanying these waves acted on the dunes and caused them to become larger and more rounded and sinuous as shown in figure 4-7c. (In example 1, the perturbation velocities were not strong enough at the level of the bed to have much effect on the dunes.) Thus the disturbances which caused the waves,which in turn acted on the dunes to give them a sinuous form,originated at the bed.

At higher velocities, the disturbances originated at the surface (see example 4).

Example 3. Run 5-10. $d = 0.150$, $V = 2.19$ ft/sec, $F = 1.00$, $f_b = 0.0580$, $G = 4.68$ lb/ft-min, $\lambda = 0.85$ ft. See figure 4-8. The irregular form of the bed shown in figures 4-8a, b indicates that this is another case in which the disturbances originated from dune-type features on the bed. The bed features moved downstream with a velocity of less than 2 in/min. The surface waves were usually rooster tails that were quite skittish and had occasional isolated breaking. The bed features were usually accompanied by surface waves which occasionally acted on the bed to form rounded antidunes as shown in figure 4-8c. The coupling between the bed and water surface would be described as moderate.

In Run 5-7 ($F = 1.19$, $d = 0.147$ ft, not shown) the irregular dune-type features were barely perceptible. In Run 5-4 ($F = 1.25$, $d = 0.150$ ft, not shown) they no longer could be seen. This implies that without the complication of surface waves the bed form would change from dunes to flat at about $F = 1.2$ when the depth is approximately 0.15 ft. Without the dunes present to initiate surface disturbances, it was found that two distinct flow configurations were possible for each velocity and depth. This is the non-uniqueness which was mentioned in section 4-2a. Runs 5-16 and 5-17 will be used to illustrate this phenomenon. The upper limit of depth and velocity above which only one flow configuration is again possible will be discussed in part d of this section.

Example 4. Run 5-16. $d = 0.154$ ft, $V = 3.45$ ft/sec, $F = 1.55$

f_b = 0.0383, G = 22.5 lb/ft-min. See figure 4-9. Run 5-17. d = 0.146 ft, V = 3.56 ft/sec, F = 1.64, f_b = 0.0396, G = 20.6 lb/ft-min, λ = 1.67 ft. See figures 4-10 and 4-11.

If the sluice gate of the box inlet was adjusted to admit the flow to the flume with very little disturbance (see figure 4-12a), the bed and water surface remained flat over the entire flume length. This condition is shown in figure 4-9.

When one or more 8-mesh screens were placed downstream from the sluice gate, the water surface was given a small disturbance as it emerged from the screen as shown in figure 4-12b. This disturbance caused the formation of an antidune and accompanying two-dimensional surface wave from which antidunes and stationary waves propagated downstream in the manner described in section 4-2. At six to eight wave lengths downstream from the screen, the two-dimensional waves degenerated into rooster tails and the resulting flow is shown in figure 4-10. When the screens were removed, the waves propagated downstream out of the flume and the flow again became uniform.

In figure 4-10d, the lighting is such that the intricate flow pattern over rooster tails can be seen. The flow alternately converged toward the peaks of the rooster tails and then diverged away from the flume centerline at the troughs. This alternately converging and diverging flow caused the bed to assume the three-dimensional configuration shown in figure 4-11. The small pools of water shown in figure 4-11 give an indication of the contours of the antidunes. The bed had the same general three-dimensional form as the surface waves, but

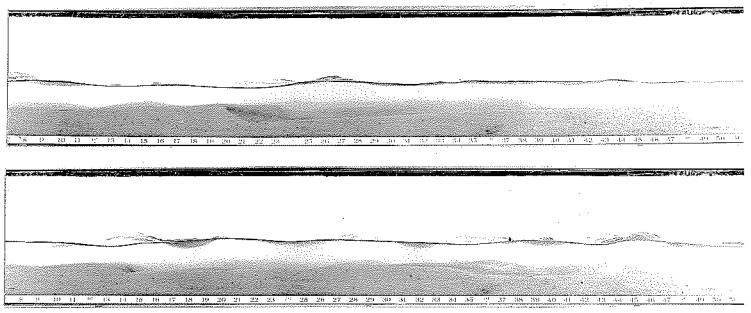

Fig. 4-6. Side views of flow configuration for Run 5-2 (text example 1). d = 0.148 ft, V = 1.65 ft/sec, F = 0.75, G = 1.54 lb/ft-min, f_b = 0.0703, λ = 0.58 ft.

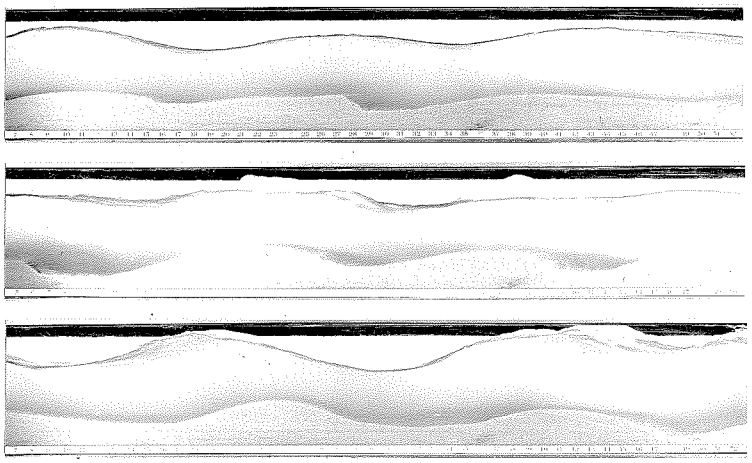

Fig. 4-7. Side views of flow configuration for Run 5-1 (text example 2). d = 0.346 ft, V = 2.58 ft/sec, F = 0.77, G = 7.25 lb/ft-min, f_b = 0.0746, λ = 1.25 ft.

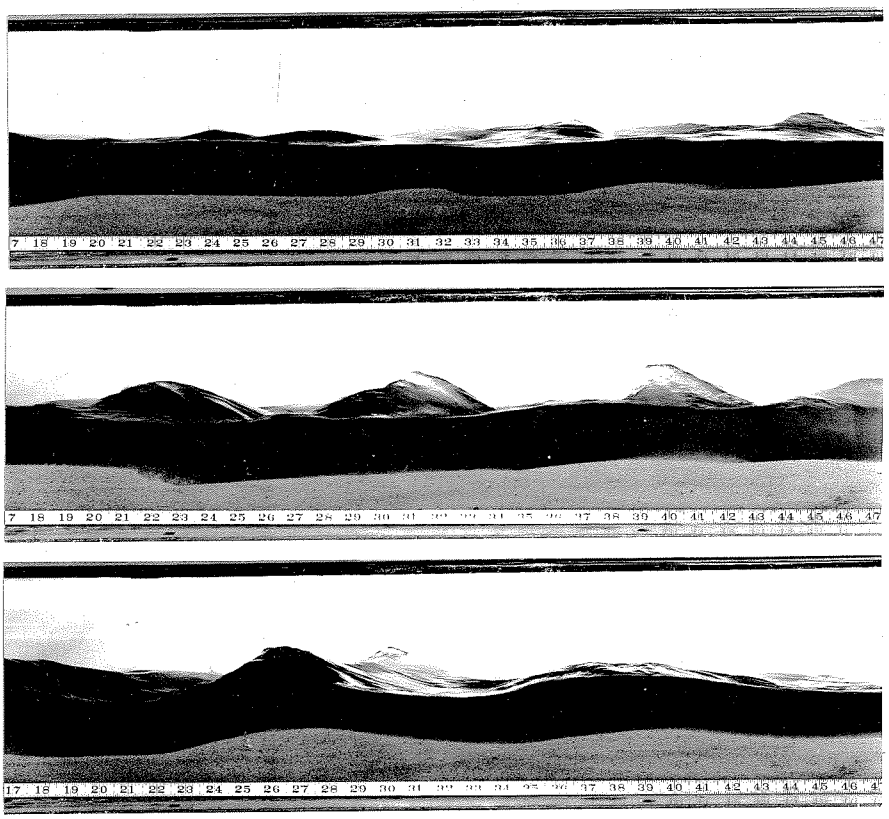

(a, b, c) Side views.

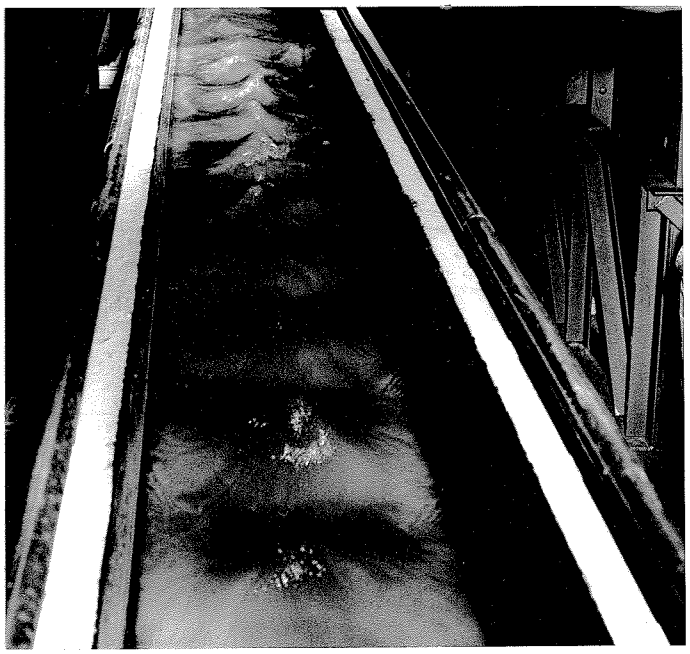

(d) Top view looking downstream.

Fig. 4-8. Side views and top view of flow configuration for Run 5-10 (text example 3). d = 0.150 ft, V = 2.19 ft/sec, F = 1.00, G = 4.68 lb/ft-min, f_b = 0.0580, λ = 0.85 ft.

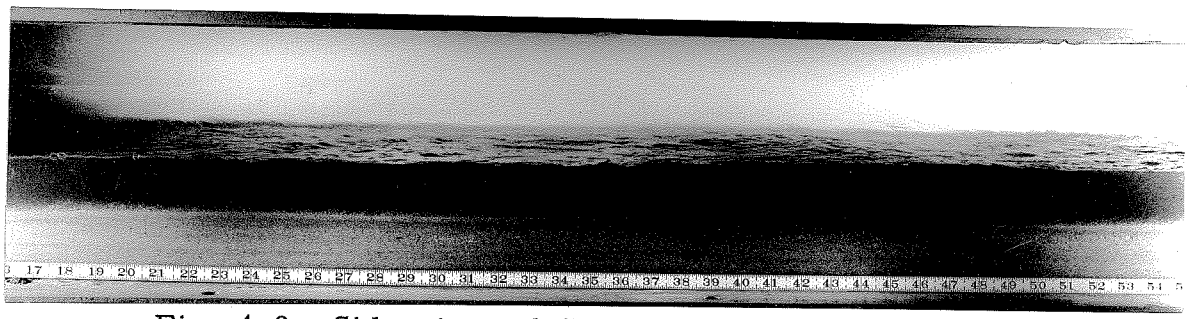

Fig. 4-9. Side view of flow configuration for Run 5-16 (text example 4). d = 0.154 ft, V = 3.45 ft/sec, F = 1.55, G = 22.5 lb/ft-min, f_b = 0.0383. Compare with Run 5-17 (figure 4-10) which had induced stationary waves and anti-dunes.

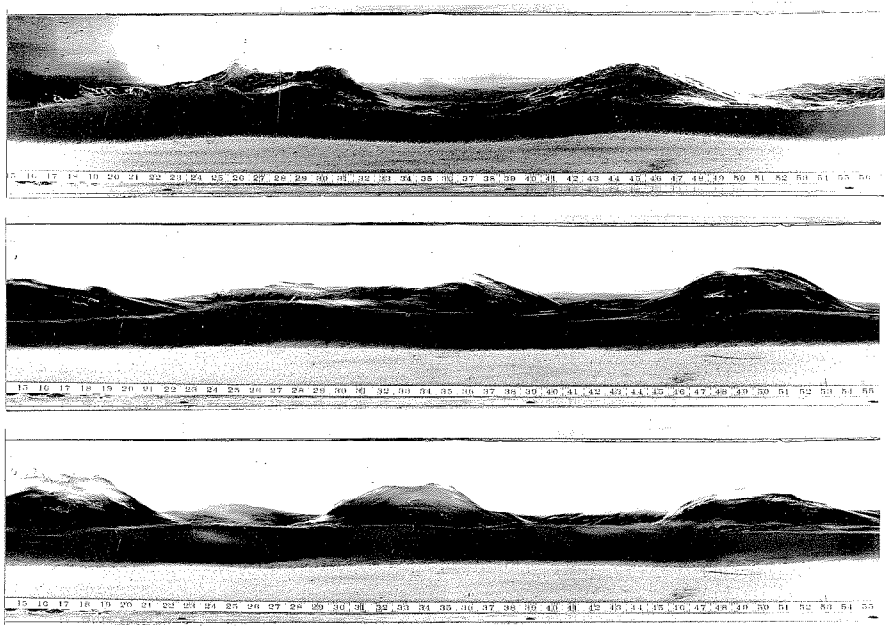

(a, b, c) Side views.

(d) Top view looking downstream.

Fig. 4-10. Side views and top view of flow configuration for Run 5-17 (text example 4). d = 0.146 ft, V = 3.56 ft/sec, F = 1.64, G = 20.6 lb/ft-min, f_b = 0.0396, λ = 1.67 ft.

Compare with Run 5-16 (figure 4-9) which did not have induced stationary waves and antidunes. See figure 4-11 for view of bed configuration.

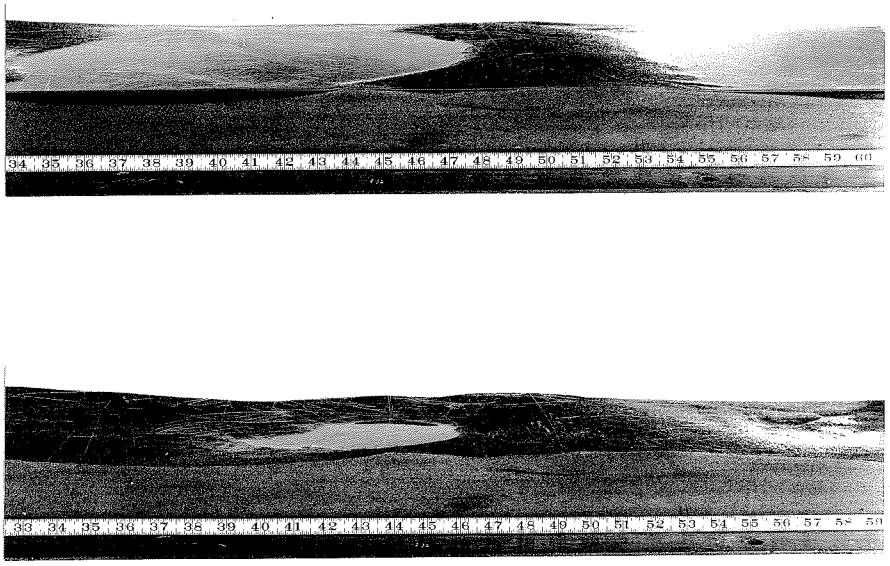

(a)

(b)

Fig. 4-11. Side views of bed configuration under rooster tails of Run 5-17 (see figure 4-10, text example 4). The flume has been leveled and partially drained.

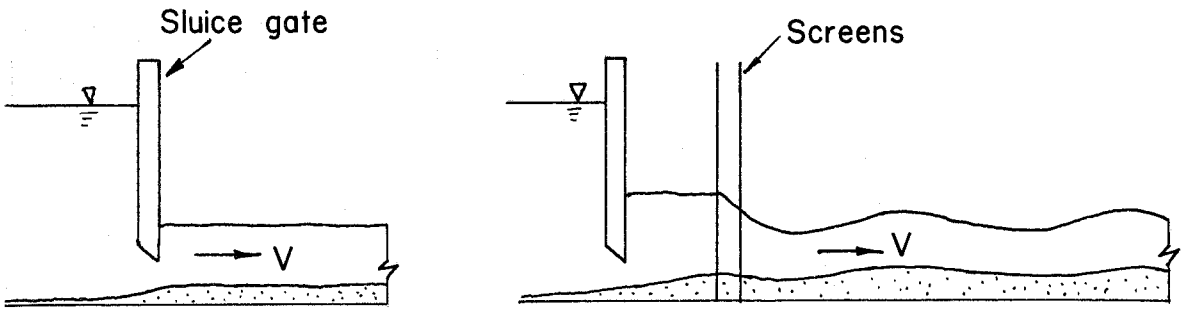

(a) Channel entrance with sluice gate adjusted to admit the flow with minimal disturbance.

(b) Channel entrance with screens downstream from sluice gate to generate an initial stationary wave and antidune.

Fig. 4-12. Effect of flow disturbance at the flume entrance on bed and water surface configurations.

the antidunes were not as high and their peaks were not as sharp.

Figure 4-10c shows an interesting demonstration that rooster tails are a superposition of waves in two different directions. At the centerline of the flume, the amplitudes of the two waves add to give the high, peaked rooster tails and deep troughs. At the walls of the flume, the amplitudes are of opposite sign and the surface profile is nearly flat.

In Run 5-17, the waves never broke and had no noticeable movement. However, they were extremely skittish (see figure 4-10b,c). At random intervals, two or three waves would fail to make the transformation from two-dimensional waves to rooster tails and instead, diminished and disappeared. Then, below about station ten the waves propagated past a given point in trains of five to ten waves separated by short reaches of uniform flow.

Example 5. Run 5-8. $d = 0.147$ ft, $V = 4.27$ ft/sec, $F = 1.96$,

f_b = 0.0330, G = 43.4 lb/ft min, λ = 2.15 ft. See figure 4-13. The water surface had trains of very large rooster tails separated by reaches in which the bed and water surface were flat. The individual waves and antidunes moved very slowly upstream. The waves were very skittish and isolated breaking frequently occurred (see figure 4-13c). At this depth and velocity, it was found impossible to prevent large disturbances at the diffuser inlet and the uniqueness of the flow configuration could not be investigated. However, at this high transport rate, even very small disturbances resulted in significant differential deposition and therefore antidunes and stationary waves were probably the only possible configuration for this flow.

No complete runs were made at this depth (approximately 0.15 ft) with higher Froude numbers. A reconnaissance with this depth at higher velocities indicated that the flow became torrential (see section 4-2e) at about F = 2.25.

Example 6. Run 5-14. d = 0.123 ft, V = 4.65 ft/sec, F = 2.34, f_b = 0.0349, G = 76.8 lb/ft-min, λ = 2.65 ft. See figures 4-14 and 1-2. This run had the highest Froude number investigated. It is included in this discussion since it is the only run in Group 1 with a Froude number greater than unity for which the waves were predominantly two-dimensional.

The antidunes and waves moved upstream at about 1.7 ft/min. Violent wave breaking occurred frequently, but the breaking of one wave seldom precipitated the breaking of another. Apparently the waves were too far apart for one wave to be affected by the breaking of an adjacent wave. An antidune was completely obliterated when the wave above it broke and the resulting flat bed propogated downstream between adjacent

trains of waves.

Although the waves were predominantly two-dimensional, there was some peaking at the centerline of the flume (see figure 4-14b) which indicated the presence of a relatively small transverse wave. These rooster tail effects were quite small compared to the two-dimensional waves.

b. Examples of bed and water surface configurations of runs from Group 2. As in the preceding discussion, the descriptions will recount the bed and water surface behavior of a series of runs with a depth of about 0.15 ft as the Froude number increases from F = 0.70. The runs in the following examples used sand 2 (D_g = 0.233 mm).

Example 7. Run 4-25. d = 0.157 ft, V = 1.57 ft/sec, F = 0.700, f_b = 0.0448, G = 0.68 lb/ft-min, λ = 0.60 ft. See figure 4-15. This run had nearly the same depth and velocity as Run 5-2 (example 1). The dunes which formed on the bed were not as high or as well defined as those of Run 5-2, but they moved downstream faster. Occasionally the surface waves were predominantly two-dimensional, as shown in figure 4-15c, but rooster tails or a randomly choppy pattern were more common. Otherwise, the bed and water surface configurations of this run were very similar to those of Run 5-2 (example 1). It is interesting that Run 5-2 had the higher transport rate even though it used a coarser sand.

Example 8. Run 4-24. d = 0.147 ft, V = 2.26 ft/sec, F = 1.04, f_b = 0.0292, G = 2.52 lb/ft-min, λ = 0.91 ft. See figure 4-16. Upstream from station 28, the bed and water surface were always flat. Below station 28, small rooster tails and antidunes formed periodically.

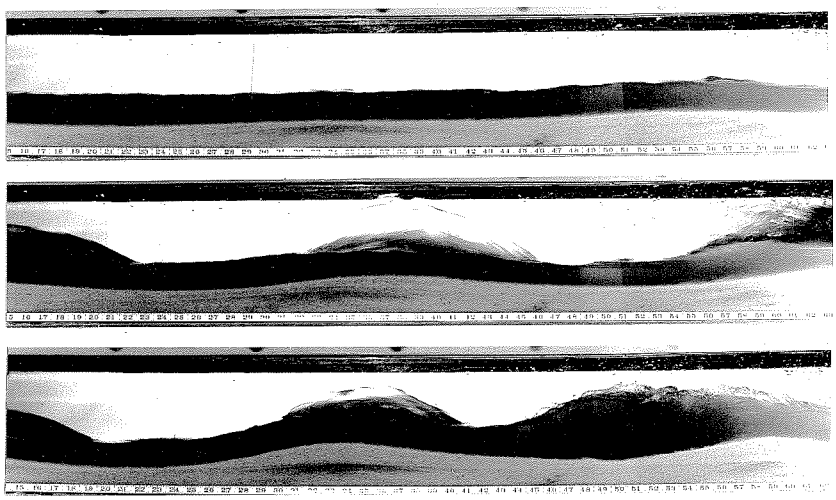

(a)

(b)

(c)

(a, b, c) Side views.

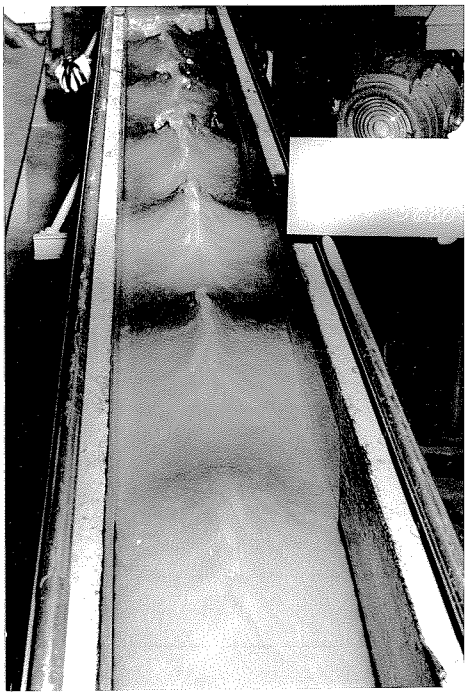

(d) Top view looking downstream.

Fig. 4-13. Side views and top view of flow configuration for Run 5-8 (text example 5). d = 0.147 ft, V = 4.27 ft/sec, F = 1.96, G = 43.4 lb/ft-min, f_b = 0.0330, λ = 2.15 ft.

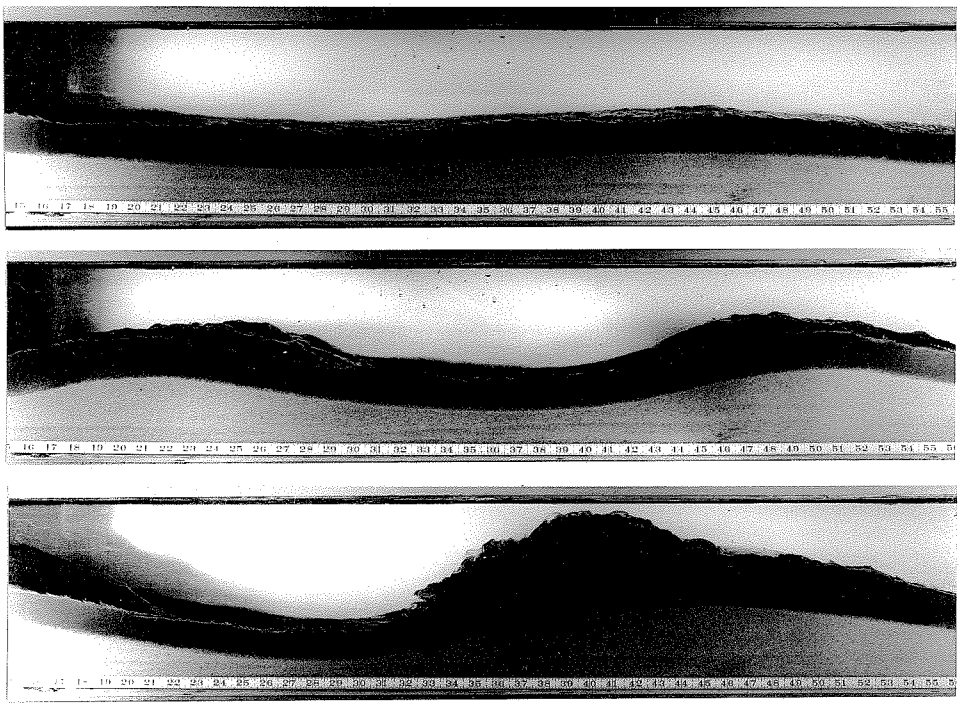

(a)

(b)

(c)

Fig. 4-14. Side views of Run 5-14 (text example 6). d = 0.123 ft, V = 4.65 ft/sec, F = 2.34, G = 76.8 lb/ft-min, f_b = 0.0349, λ = 2.65 ft. (See figure 1-2 also.)

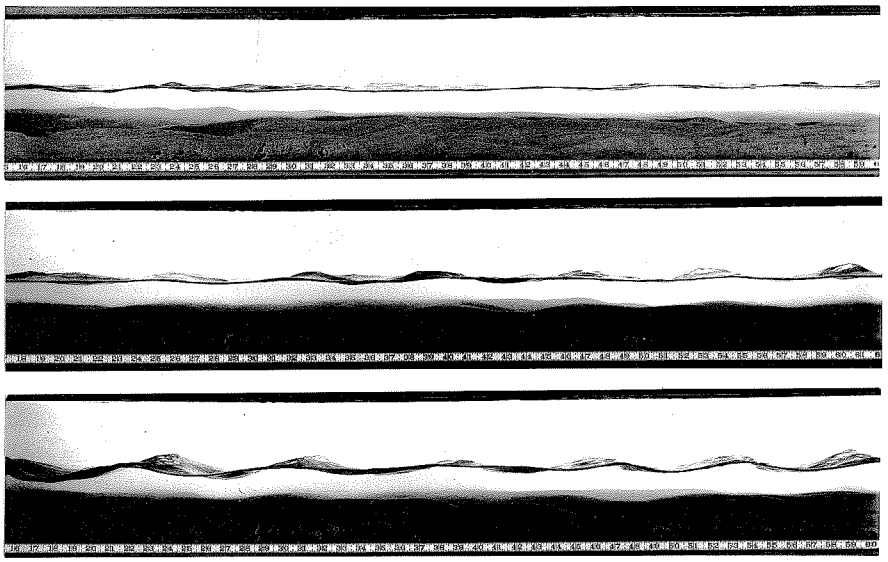

(a)

(b)

(c)

(a, b, c) Side views. Flow from right to left.

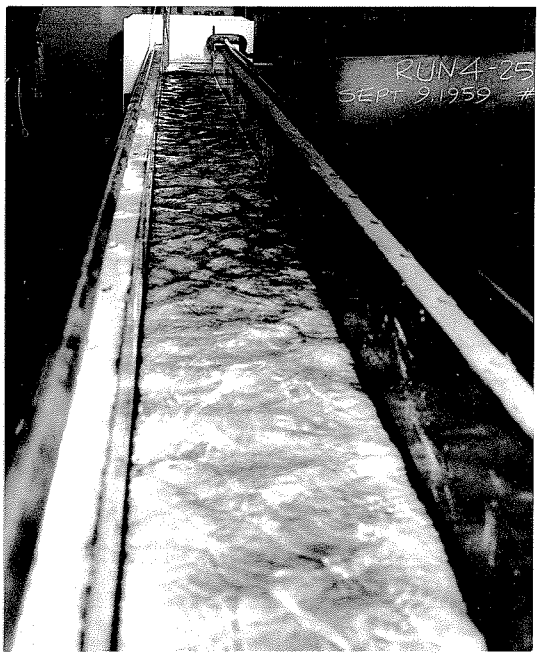

(d) Top view looking downstream.

Fig. 4-15. Side views and top view of flow configuration for Run 4-25 (text example 7). d = 0.157 ft, V = 1.57 ft/sec, F = 0.70, G = 0.68 lb/ft-min, f_b = 0.0448, λ = 0.60 ft.

(a)

(b)

(a, b) Side views. Flow from right to left.

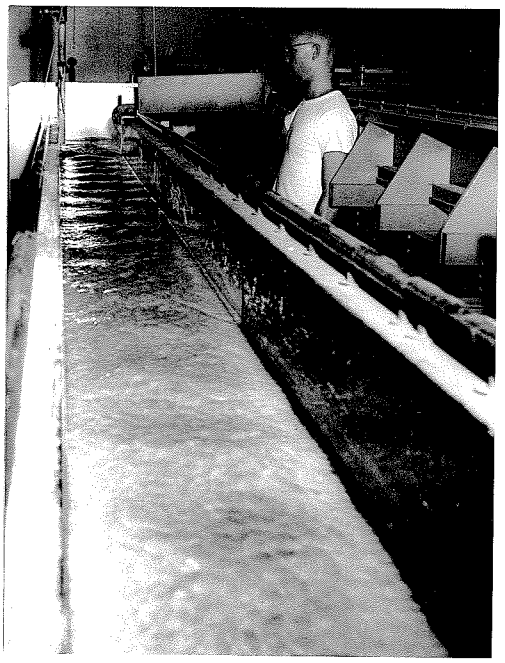

(c) Top view looking downstream.

Fig. 4-16. Side views and top view of flow configuration for Run 4-24 (text example 8). d = 0.147 ft, V = 2.26 ft/sec, f = 1.04, G = 2.52 lb/ft-min, f_b = 0.0291, λ = 0.91 ft.

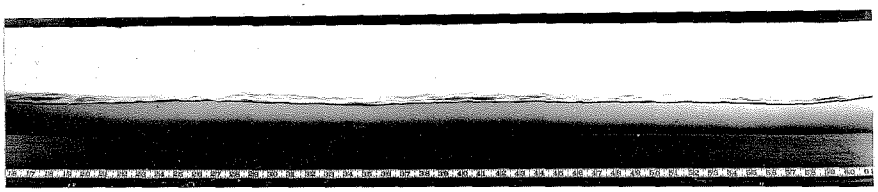

(a) Side view. Flow from right to left.

(b) Top view looking downstream.

Fig. 4-17. Side view and top view of flow configuration for a flow with the same depth of flow and velocity as Run 4-29 (see figure 4-18 and text example 9). The flow shown here had no induced waves at the upstream end of the flume.

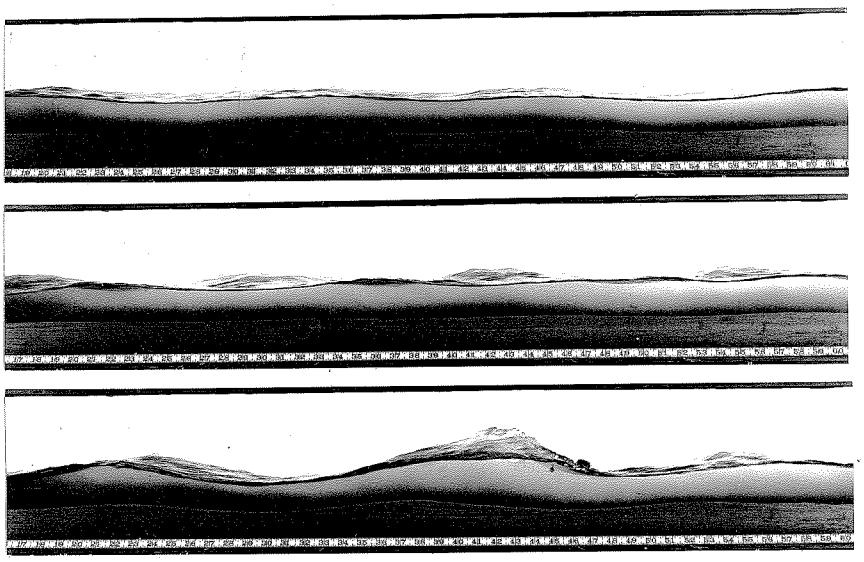

(a, b, c) Side views. Flow from right to left.

(d) Top view looking downstream.

Fig. 4-18. Side views and top view of flow configuration for Run 4-29 (text example 9). d = 0.154 ft, V = 2.46 ft/sec, F = 1.10, G = 10.5 lb/ft-min, f_b = 0.0410, λ = 1.19 ft.

Compare with flow shown in figure 4-17 which had the same depth and velocity as Run 4-29 but no induced waves.

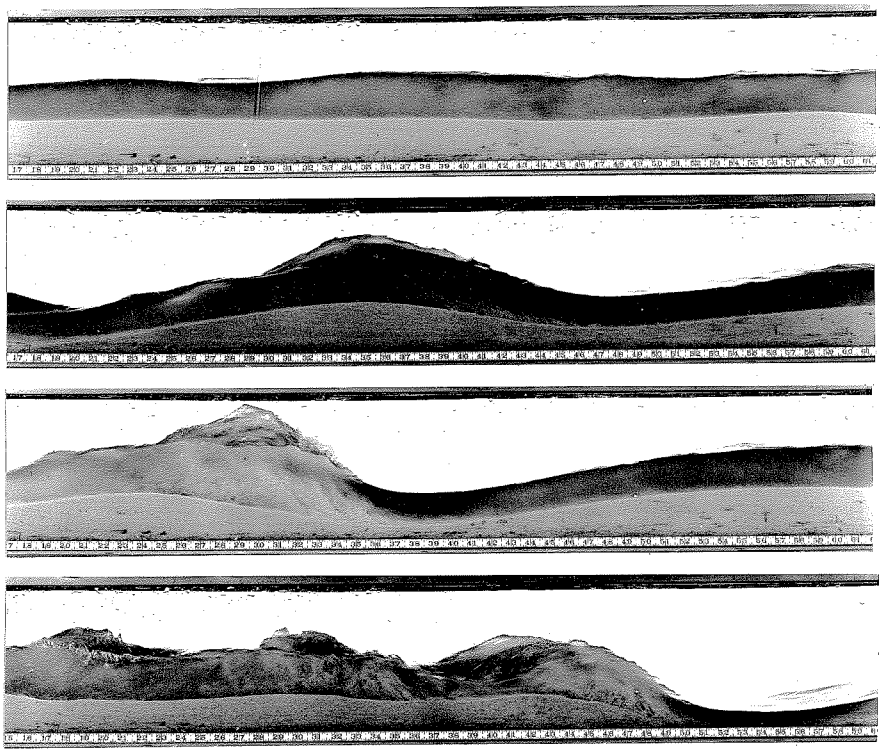

(a)

(b)

(c)

(d)

(a, b, c, d) Side views. Flow from right to left.

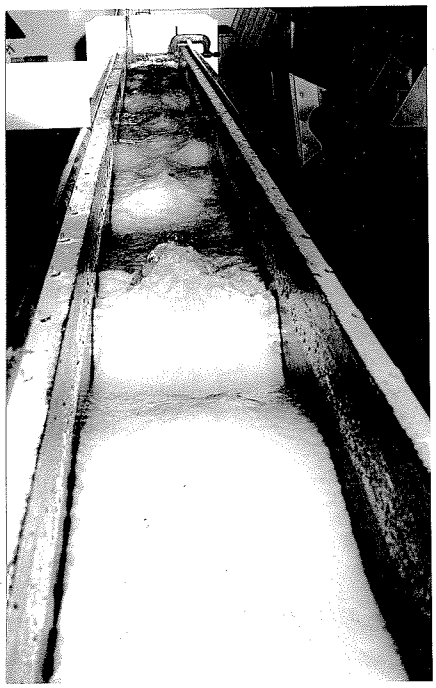

(e) Top view looking downstream.

Fig. 4-19. Side views and top view of flow configuration for Run 4-27 (text example 10). d = 0.152 ft, V = 3.29 ft/sec, F = 1.49, G = 65.2 lb/ft-min, f_b = 0.0512, λ = 2.28 ft.

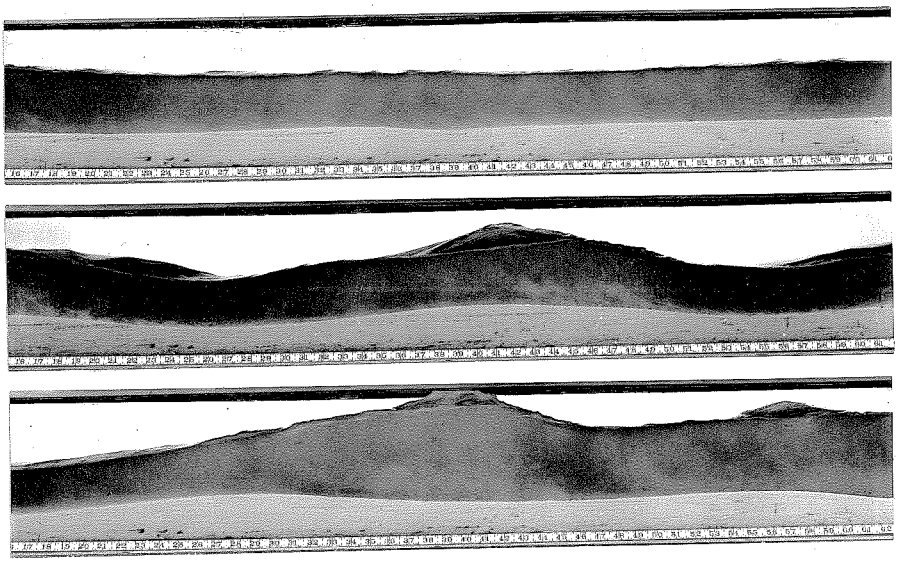

(a)

(b)

(c)

(a, b, c) Side views. Flow from right to left.

(d) Top view looking downstream.

Fig. 4-20. Side views and top view of flow configuration for Run 4-33 (text example 11). d = 0.248 ft, V = 3.30 ft/sec, F = 1.17, G = 30.0 lb/ft-min, f_b = 0.0288, λ = 1.97 ft. Compare with Run 4-27 (figure 4-19, text example 10) which had the same velocity but a smaller depth of flow.

These moved upstream very slowly and never broke. The origin of the surface waves was not clear in this case. It appears that the disturbance at the downstream end of the flume (one 8-mesh screen was used at the outlet) caused a train of waves to form. The amplitude of these waves decreased in the upstream direction and the waves could never be seen upstream from station 28. These waves caused the formation of antidunes and the resulting stationary waves and antidunes then propagated downstream and the bed and water surface became flat again. The process was repeated with a period of three to four minutes. This run apparently represented a situation in which the exciting disturbance was downstream from the antidune reach. In Runs 4-28 and 4-10 waves generated in this way became high enough to break. The bed friction factor, f_b, for this run was much lower than that of Run 4-25 (example 7). This decrease was due to the disappearance of the dunes.

A comparison of this run and the equivalent run from Group 1 (Run 5-10, example 3, figure 4-8) shows very little similarity. The coarser sand of Run 5-10 formed dunes which created disturbances all along the flume.

Example 9. Run 4-29. $d = 0.154$ ft, $V = 2.46$ ft/sec, $F = 1.10$, $f_b = 0.0410$, $G = 10.5$ lb/ft-min, $\lambda = 1.19$ ft. See figures 4-17 and 4-18. This flow was in the regime where two very different types of flow are possible. A similar situation from the Group 1 experiments was described in example 4. If no screens were used at the upstream end of the flume to generate a persistent surface disturbance, the bed and water surface remained essentially flat over the length of the flume.

This configuration is shown in figure 4-17. Very small two-dimensional waves formed periodically (see figure 4-17b) but these were too weak to form antidunes. When one or more screens were placed at the upstream end of the flume to give a persistent disturbance, stationary waves and antidunes propagated downstream and the flow configuration became that shown in figure 4-18. Run 4-29 was carried out with the screens in place to give antidunes and stationary waves.

The two-dimensional waves generated at the screen became rooster tails in three or four wave lengths and these usually underwent multiple breaking between stations 15 and 20. Two-dimensional stationary waves and antidunes were generated downstream from the region of breaking and prevailed to the end of the flume (figure 4-18d). These waves showed frequent multiple breaking and small superposed rooster tails. The stationary waves and antidunes moved slowly upstream.

For Run 4-24 (example 8), $f_b = 0.0292$ compared to $f_b = 0.0410$ for Run 4-29 of this example. This increase in friction factor was probably due to the energy dissipation in wave breaking in Run 4-29.

Example 10. Run 4-27. $d = 0.152$, $V = 3.29$ ft/sec, $F = 1.49$, $f_b = 0.0512$, $G = 65.2$ lb/ft-min, $\lambda = 2.28$ ft. See figure 4-19. This run bordered on the torrential flow condition. Radical multiple breaking occurred over the whole flume regardless of the entrance condition. The wave breaking, such as that shown in figure 4-19c, scoured out long, deep gouges in the bed. These gouges often persisted for 30 seconds or longer and resulted in the situation shown in

figure 4-19d (far right). The bed features and waves moved upstream at a rate of 0.5 to 1.0 ft/min. The further increase in f_b over that of Run 4-29 (example 9) was apparently due to the increased rate of energy dissipation in wave breaking. The radical increase in the sediment transport rate over that of Run 4-29 (example 9) was due, at least in part, to the violent wave breaking of Run 4-27 which was very effective in entraining the bed material.

Example 11. Run 4-33. $d = 0.248$, $V = 3.30$ ft/sec, $F = 1.17$, $f_b = 0.0288$, $G = 30.0$ lb/ft-min, $\lambda = 1.97$ ft. See figure 4-20. Examples 1 and 2 showed the effect of varying the depth while keeping the Froude number constant. A comparison of this example and example 10 (Run 4-27) shows the effect of keeping the velocity constant and increasing the depth (and thus decreasing the Froude number). The waves of Run 4-33 were not as active as those of Run 4-27. The multiple breaking was not as frequent or as violent and the bed features did not move upstream as fast. The reduced wave activity was reflected in f_b and G which were somewhat smaller for Run 4-33 than for Run 4-27. It was found to be generally true that, for a given velocity, the wave activity decreased as the depth increased.

c. Summary of bed and water surface configurations for all runs. Data on the bed and water surface configurations, wave lengths, and critical wave amplitudes are summarized in table 4-1. Within each group, the data are generally tabulated in the order of increasing depth except where several runs had nearly the same depth. For these depths, the runs are tabulated in the order of increasing velocity. To simplify the description of the configurations, several categories

have been established and each run is classified into one of them. These categories and the symbols assigned to them will be discussed below. The quantities in each column of the table are as follows:

Column 1. d = average depth in feet in the reach of equilibrium flow. This was determined from the bed and surface profiles as described in section 3-9.

Column 2. $V = \frac{Q}{bd}$ = mean velocity, ft/sec (cf. section 3-9).

Column 3. $F = \frac{V}{\sqrt{gd}}$ = Froude number.

Column 4. λ = average wave length in feet measured as discussed in section 3-11.

Column 5. $\frac{2A_c}{\lambda}$ = critical wave steepness at breaking. This is the ratio of wave height at breaking to wave length (cf. section 2-6 for discussion of theory). The values of $2A_c$ were scaled from photographs. No values are given for runs which had predominantly three-dimensional waves (rooster tails) or runs for which no good photographs of incipient wave breaking were obtained.

Column 6. The various categories of water surface configurations and the symbols used to represent them are as follows:

f = flat water surface.

Where a numeral appears followed by a letter, the numeral refers to the type of wave and the letter describes the wave breaking as follows:

2 = predominantly two-dimensional waves

3 = predominantly three-dimensional waves (rooster tails).

The following symbols are always used in conjunction with "2" and "3" above:

b = isolated breaking

B = multiple breaking

o = no breaking.

Where numbers appear in parentheses, they give the station at which a change of water surface configuration occurred.

Example: Run 4-28. "f(15)2b" signifies that the water surface was flat upstream from station 15, and that downstream from that station, two-dimensional waves occurred which broke singly. The fact that the surface was flat in the upstream part of the flume and the waves broke singly indicates that the breaking in the downstream part of the flume was not very violent.

Column 7. The various categories of bed configurations and their symbols are as follows: The first letter denotes the form of the bed.

f = flat bed

w = dunes weakly coupled with the water surface

m = dunes moderately coupled with the water surface

s = dunes strongly coupled with the water surface

i = bed form was image of water surface; i.e., if the water surface was flat, the bed was flat; if the water surface was wavy, the bed had antidunes.

The second letter denotes the direction and rate of movement of the bed features:

d = bed features moved downstream slowly

D = bed features moved downstream rapidly

u = bed features moved upstream slowly

U = bed features moved upstream rapidly

o = features did not move

N = direction of movement was not observed.

The division between slow and rapid movement was taken as about 0.3 ft/min.

Example: Run 4-28. The water surface was flat upstream from station 15 and had two-dimensional waves downstream from station 15. The symbol "iu" indicates that the bed was flat upstream from station 15 and had two-dimensional antidunes downstream from station 15, and that the antidunes moved upstream at a rate of less than 0.3 ft/min.

Column 8. Uniqueness refers to the possibility of more than one flow condition existing for a given depth and velocity (cf. examples 3 and 9, section 4-3).

I = only one flow condition was possible

II = two flow conditions were possible. Bed and water surface remained flat if flow was undisturbed; stationary waves and antidunes formed otherwise.

N = failed to determine uniqueness.

The condition under which the run was carried out can be determined from the water surface description.

Column 9. Upstream condition. In sections 3-1 and 4-3 (examples 4 and 9) the effect of using screens at the flume inlet was described. This column gives the number of screens used and their mesh, as well as any other special features of the entrance. The word "Gate" refers to the sluice gate of the box inlet.

Example: Run 5-17: "Gate, 2-8" signifies that the sluice gate was placed just upstream from two screens which had eight opening per inch.

TABLE 4-1

SUMMARY OF BED AND WATER SURFACE CONFIGURATIONS

Run No.	1 d Depth ft	2 V Velocity ft/sec	3 F Froude No.	4 λ Wave Length ft	5 $\frac{2A_c}{\lambda}$ Critical Wave Steepness	6 Water Surface Config.	7 Bed Config.	8 Uniqueness	9 Upstream Condition	10 Flume Inlet and Outlet	11 Shown in Figure	12 Remarks	Run No.
Group 1: Sand 1 (D_g = 0.549 mm) in 40-foot Flume													
5-11	0.074	3.09	2.00	- -	- -	f	f	II	2-8, sill	x	- - -	1	5-11
5-12	0.084	3.35	2.04	- -	- -	f	f	N	3-8, sill	x	- - -	1	5-12
5-13	0.092	3.20	1.86	- -	- -	f	f	II	3-8, sill	y	- - -	1	5-13
5-18	0.093	3.15	1.82	- -	- -	3o(20)f	iN	II	6-8, sill	y	- - -	2	5-18
5-14	0.123	4.65	2.34	2.65	0.13	2b	iU	I	Gate	y	4-14, 1-2	-	5-14
5-2	0.148	1.65	0.75	0.58	- -	3o	wD	I	3-8	x	4-6	-	5-2
5-10	0.150	2.19	1.00	0.85	- -	3b	md	I	3-8	x	4-8	-	5-10
5-7	0.147	2.60	1.19	1.00	- -	3o	md	I	1-8	x	- - -	-	5-7
5-4	0.150	2.74	1.25	1.33	- -	3o	id	N	- - -	x	- - -	-	5-4
5-9	0.159	3.33	1.47	1.60	- -	3b	io	N	4-8, sill	x	- - -	1	5-9
5-16	0.154	3.45	1.55	- -	- -	f	f	II	Gate	y	4-9	-	5-16
5-17	0.146	3.56	1.64	1.67	- -	3o	io	II	Gate, 2-8	y	4-10, 4-11	-	5-17
5-8	0.147	4.27	1.96	2.15	- -	3b	iu	N	3-8, sill	x	4-13	1	5-8
5-3	0.245	2.18	0.77	1.00	0.14	2b	mD	I	- - -	x	1-1	-	5-3
5-5	0.239	3.55	1.28	2.00	- -	3b	id	N	1-8	x	- - -	-	5-5
5-1	0.346	2.58	0.77	1.25	0.14	2b	sD	I	- - -	x	4-7	-	5-1
Group 2: Sand 2 (D_g = 0.233 mm) in 40-foot Flume													
4-25	0.157	1.57	0.70	0.60	- -	3o	wD	I	- - -	z	4-15	-	4-25
4-37	0.151	2.01	0.91	0.85	- -	2o(18)f	iN	II	2-8	z	- - -	-	4-37
4-24	0.147	2.26	1.04	0.91	- -	f(28)3o	iu	II	- - -	z	4-16	-	4-24
4-29	0.154	2.46	1.10	1.19	0.16	3B(20)2B	iu	II	2-8	z	4-17, 4-18	-	4-29
4-28	0.148	2.55	1.17	1.77	0.16	f(15)2b	iu	II	- - -	z	- - -	-	4-28
4-26	0.153	2.68	1.21	1.58	0.14	2B	iu	I	- - -	z	- - -	-	4-26
4-27	0.152	3.29	1.49	2.28	0.14	2B	iU	I	- - -	z	4-19	-	4-27
4-1	0.236	2.10	0.76	- -	- -	f	f	N	- - -	x	- - -	-	4-1
4-30	0.251	2.13	0.75	- -	- -	f	f	I	- - -	z	- - -	-	4-30
4-31	0.256	2.77	0.96	- -	- -	f	f	II	- - -	z	- - -	-	4-31
4-36	0.247	2.88	1.02	1.50	0.16	2b	iu	II	2-8	z	- - -	-	4-36
4-33	0.248	3.30	1.17	1.97	0.14	2B	iU	N	1-8	z	4-20	-	4-33
4-32	0.259	3.42	1.18	2.18	0.15	2B	iU	I	1-8	z	- - -	-	4-32
4-38	0.346	2.55	0.76	- -	- -	f	f	I	- - -	z	- - -	-	4-38
Group 3: Sand 2 (D_g = 0.233 mm) 60-foot Flume													
4-12	0.145	1.69	0.78	0.60	- -	2o	wN	I	1-8	-	- - -	-	4-12
4-10	0.154	2.09	0.94	0.90	- -	f(36)2b	iN	N	2-8	-	- - -	-	4-10
4-22	0.148	2.63	1.18	1.49	- -	2b(22)2B	iu	II	1-8	-	- - -	-	4-22
4-11	0.148	2.74	1.26	1.45	0.13	2b	iu	I	1-8	-	4-4	3	4-11
4-7	0.195	3.14	1.25	N	- -	2B(20)3B	iU	I	- - -	-	4-2	-	4-7
4-6	0.218	3.29	1.24	N	- -	2B	iU	I	- - -	-	4-5	4	4-6
4-3	0.228	1.35	0.50	- -	- -	f	wd	I	1-8, 1-4	-	- - -	5	4-3
4-19	0.252	2.13	0.75	- -	- -	f	f	I	1-8	-	- - -	-	4-19
4-17	0.253	2.77	0.97	1.67	- -	2b	iN	II	1-8	-	- - -	-	4-17
4-16	0.257	3.45	1.20	2.20	0.14	2B	iU	I	1-8	-	- - -	-	4-16
4-13	0.335	2.62	0.89	1.41	- -	2o	iN	N	1-8	-	- - -	-	4-13
4-23	0.356	2.48	0.73	- -	- -	f	f	N	1-8	-	- - -	-	4-23
4-14	0.348	3.42	1.02	2.12	- -	2b	iN	N	1-8	-	- - -	-	4-14

Table 4-1A

Remarks Pertaining to Table 4-1

Numbers correspond to those tabulated in last column of Table 4-1.

1) A wooden sill, 30 inches long and 1-5/8 inches high was placed on the floor of the flume just downstream from the flume inlet. The upstream end of the sill was beveled. The screens were placed just upstream from the sill.

2) Run 5-18 has essentially the same depth and velocity as Run 5-13. In Run 5-13, no screens were placed at the downstream end of the sill and the bed and water surface were flat over the whole length of the flume. In Run 5-18, three additional screens were placed at the downstream end of the sill. Rooster tails then formed from the sill to station 20 and the flat bed and water surface persisted from station 20 to the end of the flume. (The sill used is described under Remark No. 1.)

3) Many well-defined rooster tails were superposed on the two-dimensional waves (cf. figure 5-4).

4) This run had the torrential flow shown in figure 5-5. The depth was calculated from volumetric considerations of the amount of sand and water in the open channel part of the flume.

5) The dunes of this run had very little effect, if any, on the free surface.

Column 10. Flume entrance and pump well. On the 40-foot flume two different entrances and two different exits were used. The entrance and exit combinations are denoted by the following symbols:

x = diffuser entrance and small pump well (cf. figures 3-2 and 3-4)

y = box inlet (cf. figure 3-3) and small pump well

z = box inlet and large pump well (cf. figure 3-5).

The same entrance and pump well were used for all runs with the 60-foot flume (cf. figures 3-7 and 3-8).

Column 11. If a photograph of the run appears, its figure number is given in this column.

Column 12. Remarks. The numbers refer to the remarks listed in table 4-1A, page 121.

Where entries are missing in table 4-1, either the item does not apply or the quantities were not obtained. Additional quantitative data for the laboratory experiments are given in table 4-2, section 4-4a.

d. Relation between Froude number and bed and water surface configuration. The configuration data given in table 4-1 are plotted against depth and velocity in figures 4-21, 4-22 and 4-23. Lines of constant Froude number are shown on the graphs.

In the depth range investigated, the following conclusion about the experiments in the 40-foot flume using the 0.549 mm sand can be drawn from figure 4-21:

(1) For a given depth and velocity, two flow conditions are possible in the Froude number range $1.3 < F < 2.0$. In this range, the flow is steady and uniform if there is no persistent disturbance which causes stationary surface waves to form. If such a disturbance

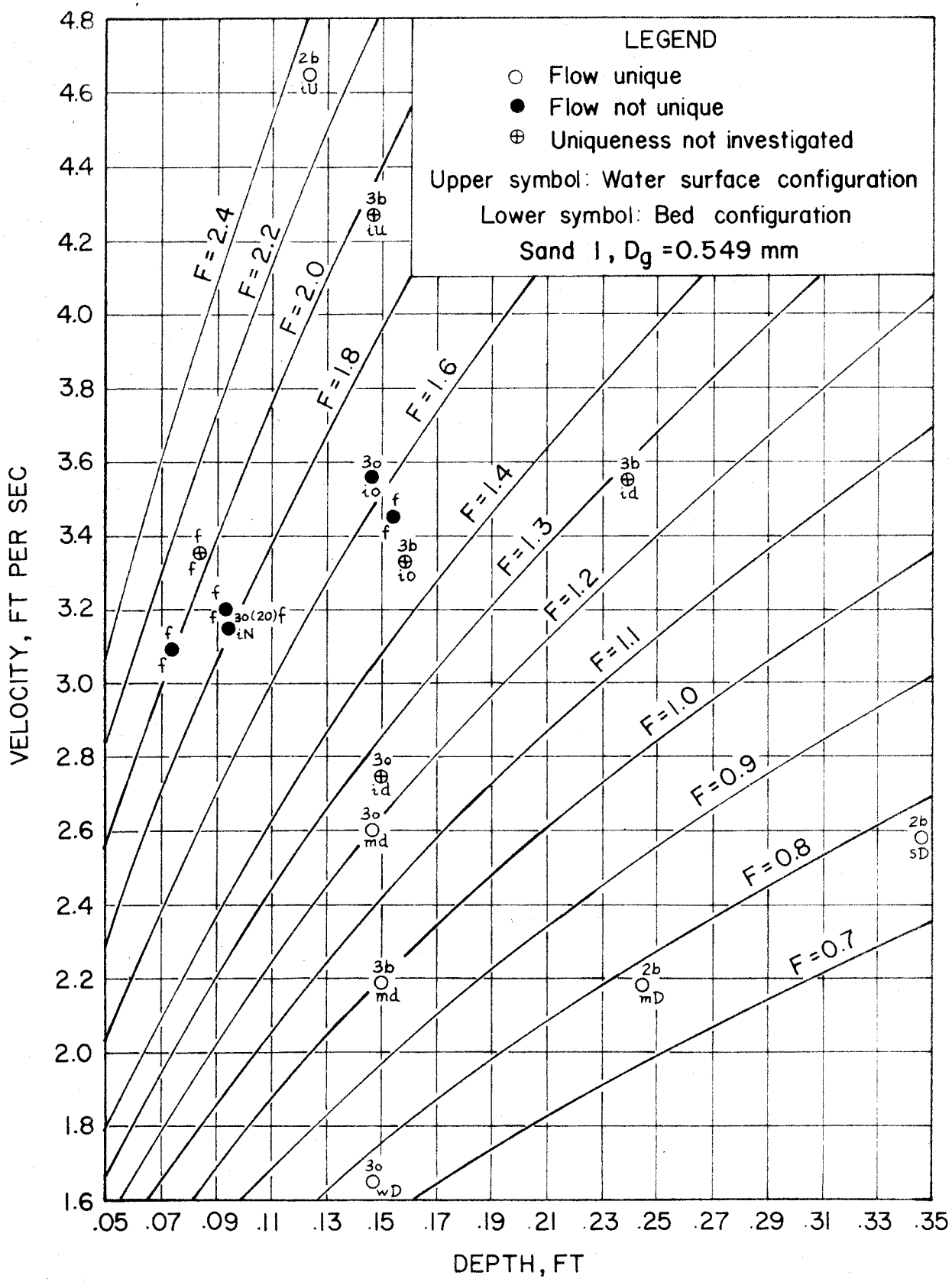

Fig. 4-21. Bed and water surface configurations vs. depth and velocity for runs of Group 1. (See pp. 117-119 for definitions of symbols.)

exists, antidunes and stationary waves form. In the depth range investigated, the lower limit on the Froude number, $F = 1.3$, corresponds approximately to the upper end of the regime in which dunes form on the bed. At lower Froude numbers, the dunes initiate the surface waves.

(2) Waves usually break one at a time, i.e. the breaking of a wave seldom precipitates the breaking of adjacent waves.

(3) If waves form, the amount of wave activity increases with depth for a constant Froude number.

(4) If waves form, the amount of wave activity increases with increasing velocity for a constant depth.

(5) In the ranges of depth and velocity investigated, rooster tails are overwhelmingly the predominant wave form.

(6) The bed configurations move downstream if the Froude number is less than 1.3, upstream if the Froude number is greater than 1.8, and do not move if $1.3 < F < 1.8$.

(7) At very low depths ($d < 0.1$ ft) the bed and water surface are flat for even very high Froude numbers ($F > 1.75$). Runs 5-11, 5-12 and 5-13 had this type of flow. If the entrance was disturbed to induce antidunes and stationary waves they persisted for 15 to 20 wave lengths and the bed and water surface again became flat (see Run 5-18).

The following conclusions are drawn from figures 4-22 and 4-23 and apply to experiment Groups 2 and 3 (Sand 2, $D_g = 0.233$ mm) for the values $0.145 < d < 0.348$ ft and $1.57 < V < 3.45$ ft/sec:

(1) For a given depth and velocity, two flow conditions are possible in the Froude number range $0.8 < F < 1.2$. At smaller Froude

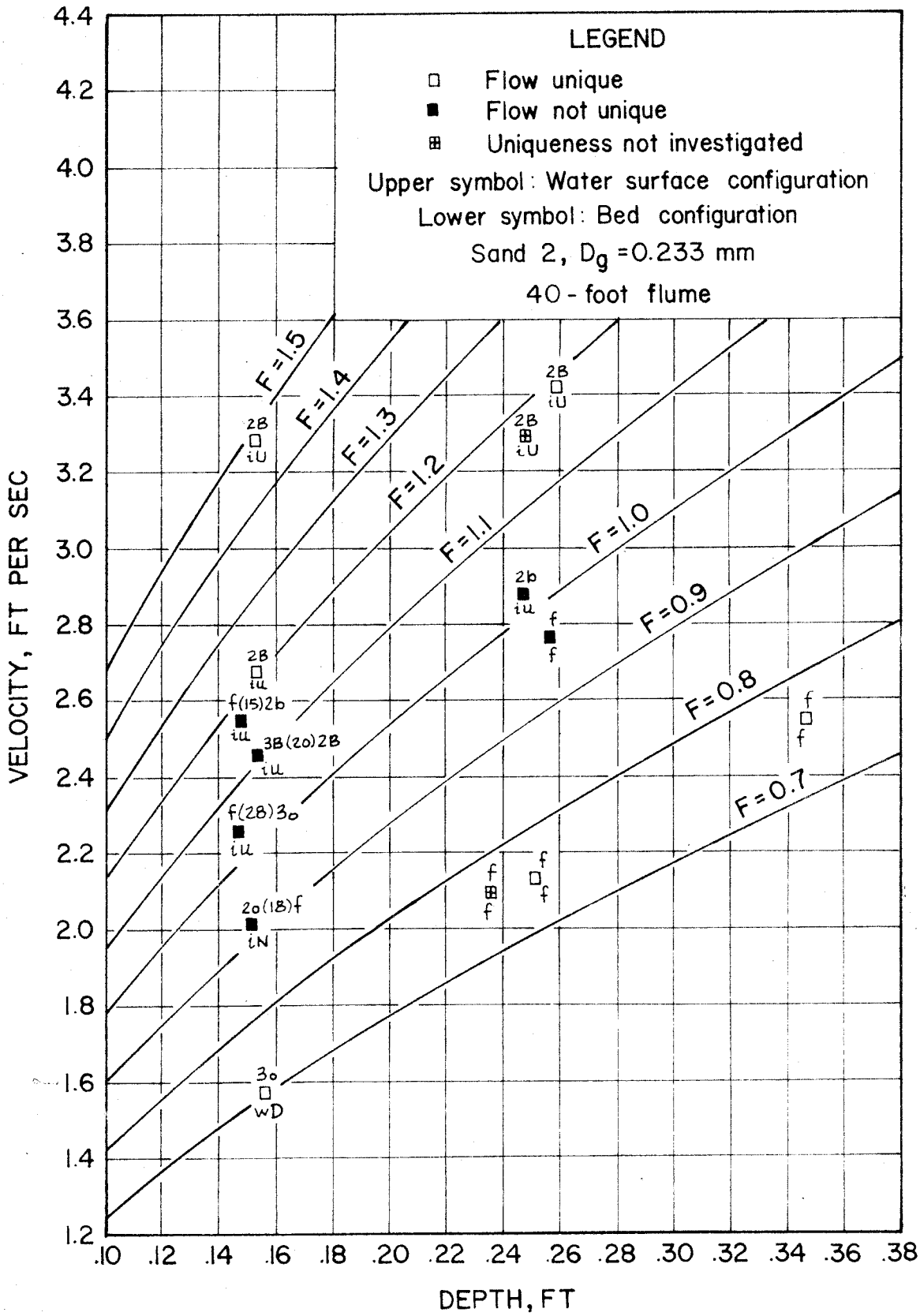

Fig. 4-22. Bed and water surface configurations vs. depth and velocity for runs of Group 2. (See pp. 117-119 for definitions of symbols.)

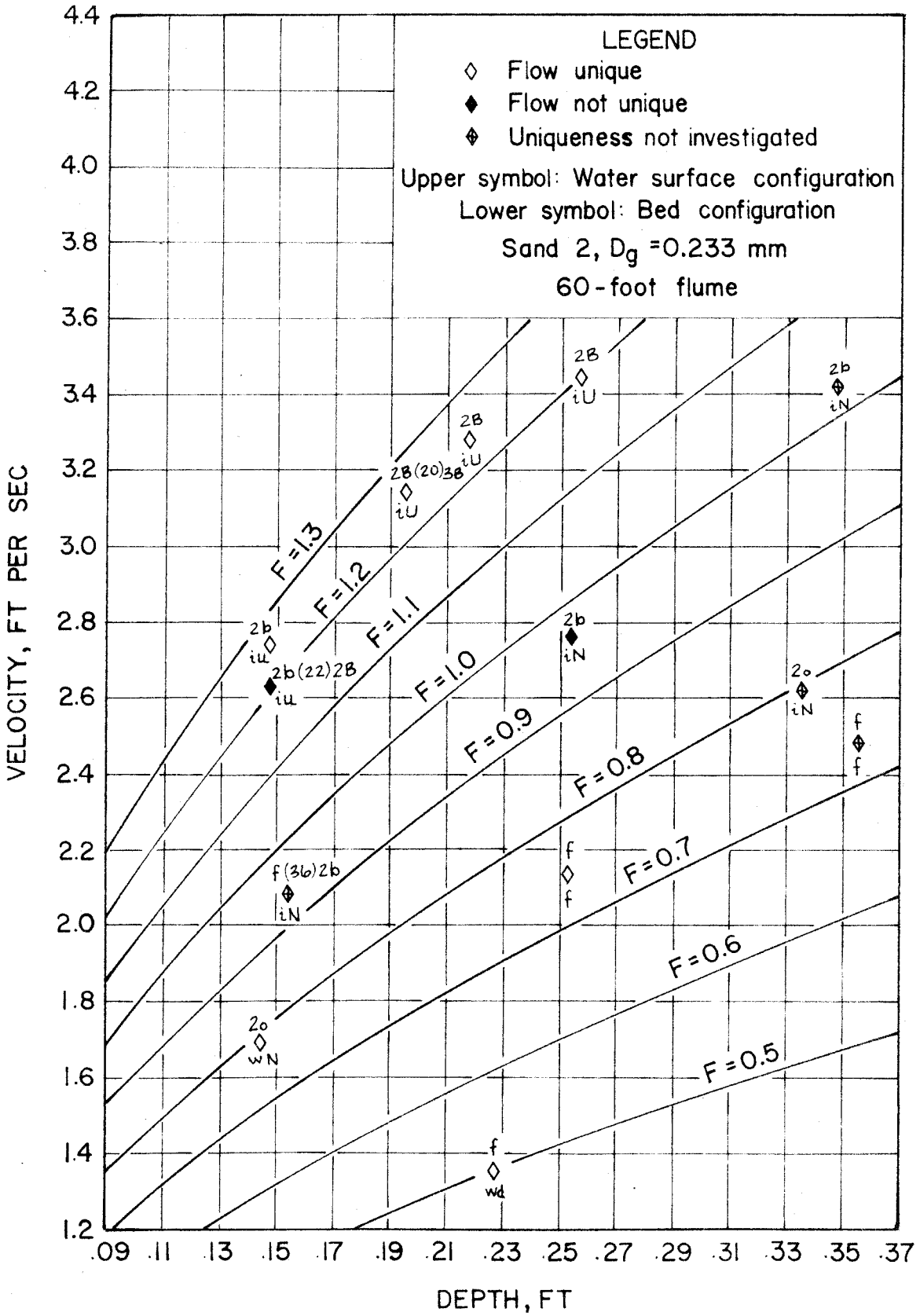

Fig. 4-23. Bed and water surface configurations vs. depth and velocity for runs of Group 3. (See pp. 117-119 for definitions of symbols.)

numbers there exists a regime in which the bed and water surface are flat and waves cannot be induced.

(2) If stationary waves form, they usually break. The breaking is usually isolated if $F < 1.1$ and multiple breaking predominates at higher Froude numbers.

(3) If waves form, the amount of wave activity increases with flow depth for a constant Froude number.

(4) If waves form, the amount of wave activity increases with increasing Froude number.

(5) For $F > 1.1$, there is no apparent difference in the configurations between equivalent runs in the two different flumes. At smaller Froude numbers, the differences, if any, are masked by the differences in the flume inlets.

(6) In the ranges of depth and velocity investigated, two-dimensional waves are the dominant water surface configuration.

(7) The bed features move upstream if the Froude number is greater than unity.

These conclusions apply only to the laboratory flumes and only to the depth and velocity ranges investigated. The question of their general applicability remains a subject for further research, although there is no apparent reason to believe that they are not generally valid for these depths. However, since the behavior of antidunes and stationary waves is intimately related to the sediment transport and differential deposition phenomena, the validity of these conclusions cannot be assured at larger depths until these phenomena are better understood, and their variation with depth can be predicted.

e. Summary. For flow in the laboratory flumes in the depth range investigated, the most important characteristics of the bed and water surface configurations may be summarized as follows:

(1) There exists a range of Froude numbers over which the flow is uniform if surface waves are not induced. If the surface is disturbed, stationary waves and antidunes form and propogate downstream.

(2) With the 0.549 mm sand, flows at very low depths ($d < 0.1$ ft) can have a flat bed at even very high Froude numbers ($F > 1.75$).

(3) If waves form, the amount of wave activity increases with depth for a constant Froude number, and with velocity for a constant depth.

(4) Two-dimensional, sinusoidal-form antidunes move upstream. Sharp-crested dunes always move downstream.

(5) For two flows with the same depth and velocity but different sands, the flow which has the finer, more easily transported sand will have more wave activity.

4-4. Hydraulic and Sediment Transport Characteristics of the Laboratory Streams

a. Summary of data. The most important measured and calculated quantities for each flow are tabulated in table 4-2. Each run represented a flow in equilibrium with its sand bed. The procedures used in obtaining the different quantities and the properties of the sands were presented in chapter 3. The bed and water surface configurations were discussed in section 4-3 and summarized in table 4-1. In table 4-2, the runs are tabulated in the same order as in table 4-1. Each group of runs is presented separately. Within each group, the runs are tabulated in order of increasing depth except where several runs had

nearly the same depth. For these depths, the runs are tabulated in the order of increasing velocity. The quantities tabulated in each column of the table are as follows:

Column 1. d = average depth in feet in the reach of equilibrium flow. The depth was determined from the bed and water surface profiles (cf. section 3-9).

Column 2. $V = \frac{Q}{bd}$ = mean velocity in ft/sec in the reach of equilibrium flow (cf. section 3-9). b is the flume width (b = 2.79 ft for the 60-foot flume; b = 0.875 ft for the 40-foot flume).

Column 3. q = Vd = discharge per unit width, cfs/ft.

Column 4. $F = \frac{V}{\sqrt{gd}}$ = Froude number.

Column 5. $r = \frac{bd}{b+2d}$ = hydraulic radius, ft.

Column 6. S = slope of energy grade line determined as discussed in section 3-9.

Column 7. $U_* = \sqrt{grS}$ = shear velocity for the composite channel section (sand bed and vertical walls), ft/sec.

Column 8. $f = 8\left(\frac{U_*}{V}\right)^2$ = Darcy-Weisbach friction factor for the composite channel section.

Column 9. $r_b = r\frac{f_b}{f}$ = hydraulic radius for bed section of channel, ft. See section 3-13 for discussion.

Column 10. $U_{*_b} = \sqrt{gr_bS}$ = shear velocity for the bed section, ft/sec. See section 3-13.

Column 11. $f_b = 8\left(\frac{U_{*_b}}{V}\right)^2$ = Darcy-Weisbach friction factor for bed section only, calculated from side-wall correction procedure described in section 3-13.

TABLE 4-2

SUMMARY OF HYDRAULIC AND SEDIMENT TRANSPORT DATA FROM LABORATORY EXPERIMENTS

Run No.	1 d Depth ft	2 V Mean Velocity ft/sec	3 q Unit Discharge cfs/ft	4 F Froude No.	5 r Hydr. Radius ft	6 S Slope	7 U_* Shear Velocity ft/sec	8 f Friction Factor	9 r_b Bed Hydr. Radius ft	10 U_{*_b} Bed Shear Velocity ft/sec	11 f_b Bed Friction Factor	12 $\frac{f_b}{f}$ Friction Factor Ratio	13 T Water Temp. °C	14 $\overline{C}$ Disch. Conc. gr/ℓ	15 G Sed. Disch. Rate lb/ft-min	16 17 Analysis of Sediment Load D_g mm	σ_g	Run No.
Group 1: Sand 1 (D_g = 0.549 mm) in 40-foot flume																		
5-11	0.074	3.09	0.229	2.00	0.0632	0.0208	0.206	0.0356	0.0676	0.213	0.0381	1.12	26.3	15.3	13.2	0.580	1.14	5-11
5-12	0.084	3.35	0.281	2.04	0.0705	0.0214	0.221	0.0348	0.0762	0.229	0.0376	1.14	25.7	16.2	17.2	0.571	1.16	5-12
5-13	0.092	3.20	0.294	1.86	0.0762	0.0185	0.213	0.0354	0.0833	0.223	0.0387	1.22	26.8	- -	- -	- -	- -	5-13
5-18	0.093	3.15	0.293	1.82	0.0765	0.0182	0.212	0.0362	0.0840	0.222	0.0397	1.26	28.0	- -	- -	- -	- -	5-18
5-14	0.123	4.65	0.572	2.34	0.0960	0.0272	0.292	0.0315	0.108	0.307	0.0349	1.18	27.0	35.9	76.8	0.549	1.14	5-14
5-2	0.148	1.65	0.244	0.75	0.110	0.0056	0.141	0.0585	0.133	0.155	0.0703	2.48	24.5	1.68	1.54	0.548	1.15	5-2
5-10	0.150	2.19	0.328	1.00	0.112	0.0081	0.171	0.0486	0.133	0.186	0.0580	2.07	24.8	3.81	4.68	0.552	1.15	5-10
5-7	0.147	2.60	0.382	1.19	0.110	0.0109	0.196	0.0456	0.132	0.215	0.0540	1.94	25.2	7.04	10.0	0.549	1.14	5-7
5-4	0.150	2.74	0.411	1.25	0.111	0.0125	0.211	0.0474	0.133	0.231	0.0566	2.03	24.3	8.79	13.4	0.569	1.15	5-4
5-9	0.159	3.33	0.529	1.47	0.116	0.0140	0.229	0.0378	0.138	0.249	0.0448	1.65	25.3	10.4	20.6	0.575	1.15	5-9
5-16	0.154	3.45	0.531	1.55	0.114	0.0134	0.222	0.0331	0.132	0.239	0.0383	1.39	24.7	11.3	22.5	0.600	1.15	5-16
5-17	0.146	3.56	0.520	1.64	0.110	0.0154	0.233	0.0343	0.126	0.250	0.0396	1.41	24.6	10.6	20.6	0.590	1.16	5-17
5-8	0.147	4.27	0.628	1.96	0.110	0.0187	0.257	0.0291	0.125	0.274	0.0330	1.19	24.9	18.5	43.4	0.590	1.14	5-8
5-3	0.245	2.18	0.534	0.77	0.157	0.0055	0.167	0.0470	0.208	0.192	0.0622	2.48	25.0	1.86	3.73	0.561	1.15	5-3
5-5	0.239	3.55	0.848	1.28	0.155	0.0110	0.234	0.0348	0.197	0.264	0.0443	1.77	25.2	7.11	22.7	- -	- -	5-5
5-1	0.346	2.58	0.893	0.77	0.193	0.0067	0.204	0.0500	0.288	0.249	0.0746	3.26	25.0	2.17	7.25	0.547	1.16	5-1
Group 2: Sand 2 (D_g = 0.233 mm) in 40-foot flume																		
4-25	0.157	1.57	0.246	0.70	0.115	0.0032	0.109	0.0386	0.134	0.117	0.0448	1.88	27.2	0.73	0.68	0.170	1.45	4-25
4-37	0.151	2.01	0.303	0.91	0.112	0.0038	0.117	0.0272	0.123	0.123	0.0299	1.26	25.0	2.35	2.68	0.215	1.45	4-37
4-24	0.147	2.26	0.332	1.04	0.110	0.0048	0.130	0.0266	0.121	0.136	0.0291	1.23	25.6	2.03	2.52	0.202	1.48	4-24
4-29	0.154	2.46	0.379	1.10	0.114	0.0073	0.164	0.0354	0.132	0.176	0.0410	1.78	25.7	7.40	10.5	0.209	1.51	4-29
4-28	0.148	2.55	0.377	1.17	0.111	0.0066	0.152	0.0289	0.124	0.162	0.0324	1.41	28.5	6.30	8.90	0.229	1.48	4-28
4-26	0.153	2.68	0.410	1.21	0.113	0.0095	0.186	0.0386	0.133	0.200	0.0453	1.99	27.0	11.0	13.1	0.216	1.52	4-26
4-27	0.152	3.29	0.500	1.49	0.113	0.0160	0.241	0.0429	0.134	0.263	0.0512	2.28	28.0	34.7	65.2	0.181	1.43	4-27
4-1	0.236	2.10	0.496	0.76	0.153	0.0026	0.113	0.0233	0.173	0.121	0.0264	1.22	30.1	2.44	4.53	0.193	1.54	4-1
4-30	0.251	2.13	0.535	0.75	0.160	0.0026	0.115	0.0235	0.182	0.123	0.0268	1.24	25.4	1.52	3.04	0.185	1.46	4-30
4-31	0.256	2.77	0.709	0.96	0.162	0.0042	0.148	0.0227	0.186	0.158	0.0261	1.24	24.7	4.03	10.4	0.221	1.55	4-31
4-36	0.247	2.88	0.711	1.02	0.158	0.0045	0.151	0.0221	0.180	0.161	0.0251	1.19	25.1	4.70	12.5	0.215	1.60	4-36
4-33	0.248	3.30	0.818	1.17	0.158	0.0065	0.182	0.0244	0.187	0.198	0.0288	1.37	25.2	9.82	30.0	0.187	1.56	4-33
4-32	0.259	3.42	0.886	1.18	0.163	0.0094	0.222	0.0337	0.210	0.254	0.0434	2.14	24.5	20.2	67.1	0.181	1.50	4-32
4-38	0.346	2.55	0.882	0.76	0.193	0.0026	0.127	0.0199	0.223	0.136	0.0229	1.12	26.5	1.87	6.18	0.187	1.59	4-38
Group 3: Sand 2 (D_g = 0.233 mm) in 60-foot flume																		
4-12	0.145	1.69	0.245	0.78	0.131	0.0034	0.120	0.0401	0.137	0.123	0.0421	1.80	24.5	0.49	0.45	- -	- -	4-12
4-10	0.154	2.09	0.322	0.94	0.139	0.0042	0.137	0.0346	0.146	0.141	0.0363	1.60	25.1	2.07	2.50	- -	- -	4-10
4-22	0.148	2.63	0.389	1.18	0.134	0.0068	0.171	0.0338	0.140	0.166	0.0354	1.56	27.3	9.27	13.2	0.213	1.52	4-22
4-11	0.148	2.74	0.405	1.26	0.134	0.0082	0.188	0.0377	0.141	0.193	0.0397	1.76	24.4	10.9	16.6	0.186	1.53	4-11
4-7	0.195	3.14	0.612	1.25	0.171	0.0088	0.220	0.0393	0.184	0.228	0.0423	2.02	23.6	15.4	35.2	0.172	1.51	4-7
4-6	0.218	3.29	0.717	1.24	0.188	0.0229	0.372	0.102	0.212	0.395	0.115	5.68	24.5	58.5	156.	0.177	1.47	4-6
4-3	0.228	1.35	0.308	0.50	0.196	0.0026	0.128	0.0709	0.218	0.136	0.0788	3.70	26.0	0.55	0.63	0.134	1.73	4-3
4-19	0.252	2.13	0.537	0.75	0.214	0.0021	0.120	0.0255	0.227	0.124	0.0268	1.31	24.2	1.17	2.36	0.150	1.48	4-19
4-17	0.253	2.77	0.701	0.97	0.214	0.0034	0.152	0.0242	0.228	0.157	0.0258	1.28	26.6	3.57	9.35	0.171	1.67	4-17
4-16	0.257	3.45	0.887	1.20	0.217	0.0071	0.223	0.0335	0.237	0.233	0.0366	1.85	24.5	15.0	50.0	0.162	1.52	4-16
4-13	0.335	2.62	0.878	0.89	0.270	0.0025	0.148	0.0254	0.295	0.154	0.0277	1.46	23.0	1.62	5.34	0.177	1.61	4-13
4-23	0.356	2.48	0.883	0.73	0.284	0.0017	0.124	0.0202	0.302	0.129	0.0215	1.13	25.4	1.70	5.62	0.158	1.49	4-23
4-14	0.348	3.42	1.19	1.02	0.279	0.0032	0.170	0.0197	0.298	0.176	0.0210	1.12	24.6	5.15	22.9	0.165	1.62	4-14

Column 12. f_b/f'_b = friction factor ratio. This is the ratio of bed friction factor to the theoretical friction factor of a bed with roughness elements of the same size as the mean size of the bed material. The bed hydraulic radius is used as the characteristic length. f'_b is determined from a pipe-friction diagram. See Part b of this section for further discussion.

Column 13. T = average water temperature during run, ^{o} C.

Column 14. $\overline{C}$ = average sediment discharge concentration, g/ℓ. Note that this concentration includes both bed load and suspended load.

Column 15. G = total sediment transport rate, or total sediment discharge, lb/ft-min.

Column 16. D_g = geometric mean sieve size of sediment load, mm. This was determined from a sieve analysis as discussed in section 3-15.

Column 17. σ_g = geometric standard deviation of sieve diameters of sediment load. See section 3-15 for discussion.

The omissions in table 4-2 represent quantities which were not obtained during the experiment. Tables 4-1 and 4-2 when used together give a complete description of every run. Indeed, many of the changes of the hydraulic characteristics given in table 4-2 can be properly interpreted only in light of the bed and water surface configurations given in table 4-1.

b. General comments on alluvial channel roughness. Some general comments on the roughness of alluvial channels will be helpful in understanding the remaining parts of this section. Water flowing over

a movable sand bed encounters two types of roughness on the bed: grain roughness and form roughness such as dunes. The resistance of the latter is often the largest and is subject to wide variations as the bed form changes.

The presence of sediment in suspension further complicates the roughness problem. It has been shown by Vanoni (16) and Vanoni and Nomicos (19) that suspended sediment reduces the friction factor of the flow by modifying the turbulence pattern. As the sediment concentration increases, this mechanism acts to decrease the friction factor.

Equations such as the Darcy-Weisbach formula (equation 3-10) relate friction factor to flow velocity and channel geometry. Interpreted another way, the Darcy-Weisbach formula may be written as

$$S = \frac{fV^2}{8gr}, \qquad (3\text{-}10)$$

where the slope, S, is the average amount of energy dissipated by a unit weight of fluid as it travels a unit distance along the channel. Now in the case of flow over antidunes the wave breaking gives another mechanism for energy dissipation and thus the friction factor, f, depends on three different factors: grain resistance, form drag, and wave breaking. In the design and analysis of alluvial channels it is the last two factors that cause the difficulty since there is no way to predict their contribution to f and their effect on the grain resistance.

In interpreting experimental results it is expedient to relate the bed friction factor, f_b, to the theoretical friction factor for the same flow over a <u>flat</u> bed of the same sand, f'_b. A friction factor ratio such

as f_b/f'_b then gives a measure of the effect of bed features and wave breaking on the friction factor. It should be approximately unity for flow over a flat bed.*

The remaining problem is to evaluate f'_b. It has been found that friction factor for flow over a flat bed can be determined with fair accuracy from a pipe-friction diagram if the bed hydraulic radius, r_b, is used as the characteristic length and the geometric mean size of the bed material, D_g, is used as the size of the roughness elements. This is the procedure which was used in this investigation for estimating f'_b.

c. Roughness of runs using Sand 1 (D_g = 0.549 mm). In figure 4-24 the values of f_b/f'_b are plotted against Froude number for all runs of Group 1. The water surface configuration and flow depth from table 4-1 are noted by each point. There is no reason to expect that f_b/f'_b is uniquely related to F, and in general it is not. However, this plot is a convenient means to illustrate several points. In describing the bed and water surface configuration of the runs of Group 1 (cf. section 4-3, part a) it was noted that at Froude numbers less than about 1.2 or 1.3 in the depth range investigated, sharp-crested dunes formed. These were often accompanied by a leeside separation eddy and therefore had appreciable form drag. At Froude numbers in the range $1.3 < F < 2.0$ the bed was flat or had antidunes depending on whether or not the water surface was given a persistent disturbance. At Froude numbers greater than approximately two, stationary waves

---

* The use of the quantity f_b/f'_b was suggested by Prof. N. H. Brooks and R. Hugh Taylor of California Institute of Technology.

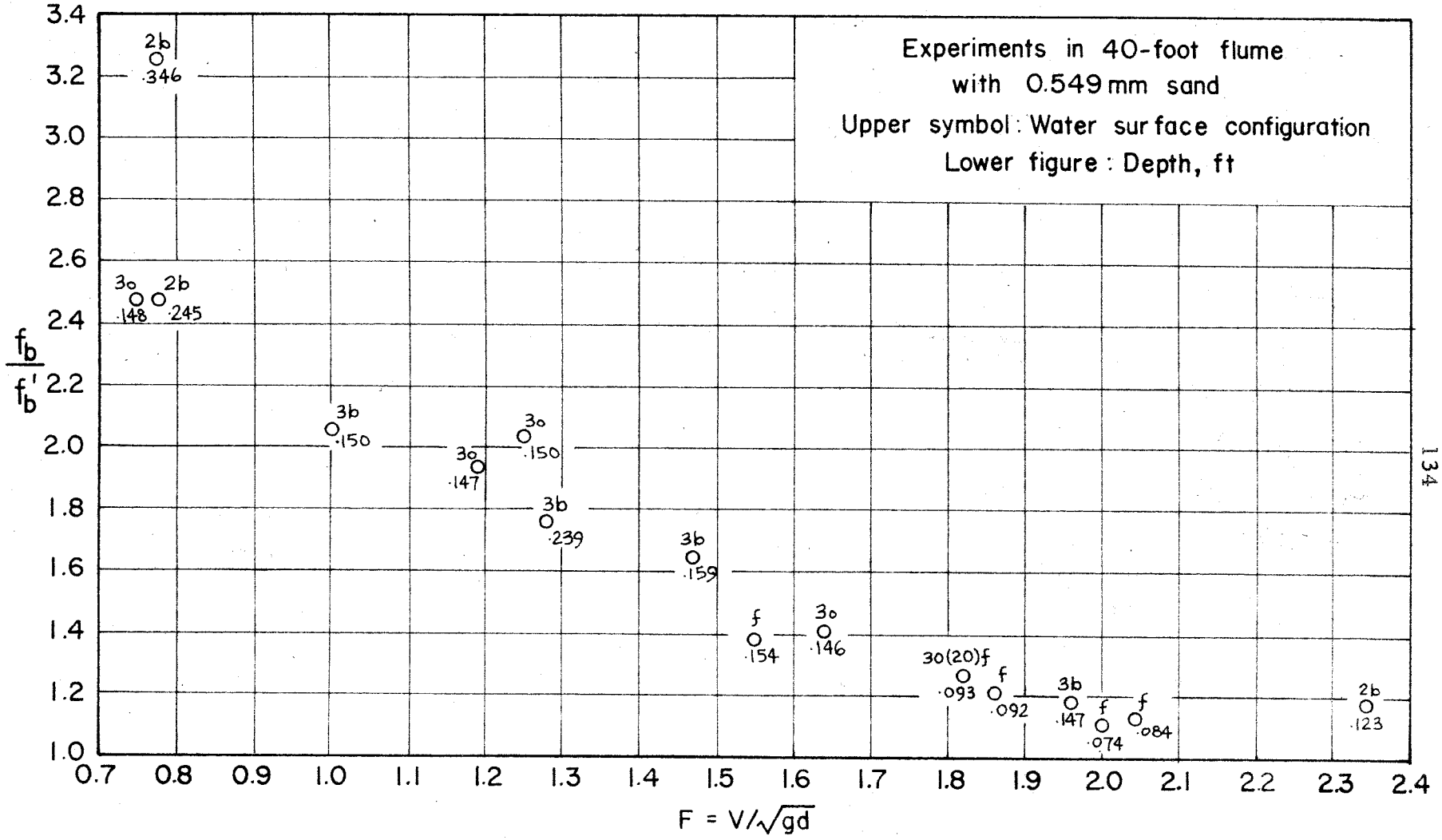

Fig. 4-24. Relation of friction factor ratio to Froude number for 0.549 mm sand.

and antidunes always formed. None of the flows showed multiple breaking and in all runs except Runs 5-14 and 5-1 the breaking was quite weak and accompanied by very little agitation.

Figure 4-24 reflects the effects of this succession of configurations on the friction factor.* The ratio f_b/f'_b is largest at the lower Froude numbers and generally decreases with increasing Froude number. The decrease in the range $0.75 < F < 1.3$ is due mainly to the dunes becoming more rounded under the influence of the surface waves and also becoming longer. The decrease beyond this point is probably due to the increase in sediment discharge concentration. At the higher Froude numbers, f_b/f'_b approaches unity.

A comparison of Runs 5-16 and 5-17 (see example 4 of section 4-3 and figures 4-10 and 4-11) shows that nonbreaking stationary waves have very little effect on the friction factor. These runs had very nearly the same depth and velocity. Run 5-16 had a flat bed and water surface while Run 5-17 had induced stationary waves and antidunes. Even though the behavior of the runs was quite different they had very nearly the same friction factor: $f_b = 0.383$ for Run 5-16 and $f_b = 0.0396$ for Run 5-17. A similar comparison of Runs 5-13 and 5-18 also illustrates this point.

The roughness ratio f_b/f'_b of Run 5-14 (see example 6, section 4-3 and figures 1-2 and 4-14) has no significant increase even though the wave breaking was quite violent. Apparently the energy dissipated in wave breaking was small compared to the energy dissipation due to

---

* In the discussions of particular runs that follow, the reader will often have to refer to tables 4-1 and 4-2 to determine the characteristics of the runs.

grain resistance at this high velocity. Consequently wave breaking had little effect on f_b/f'_b in this run or any of the runs of Group 1 (Sand 1, D_g = 0.549 mm).

d. Roughness of runs using Sand 2 (D_g = 0.233 mm). Figure 4-25 shows the values of f_b/f'_b plotted against Froude number for runs of Groups 2 and 3. The water surface configuration and depth of flow are noted by each point. The friction factor ratio of these runs generally increases with increasing Froude number. Exactly the opposite trend was observed with runs using Sand 1 (D_g = 0.549 mm) shown in figure 4-24. This trend can be explained in terms of the succession of bed and water surface configurations accompanying increasing Froude numbers. With the exception of Runs 4-13, 4-12 and 4-25 which had dunes, the runs at lower Froude numbers had flat beds or small antidunes. These configurations had low friction factors. With increasing Froude number, larger antidunes formed which were accompanied by active wave breaking. The rate of energy dissipation in wave breaking increased with Froude number faster than the energy dissipation due to grain resistance which was relatively low for this fine sand. Consequently, f_b/f'_b also increased. At higher Froude numbers, f_b/f'_b exceeded two indicating that the wave breaking caused the rate of energy dissipation to be more than twice what it would have been for a flow with the same depth and velocity over a flat bed of the same sand.

For the runs of Groups 2 and 3 the friction factor ratio was often multi-valued for a given Froude number and depth. This reflects the significant role played by the wave activity in determining the friction

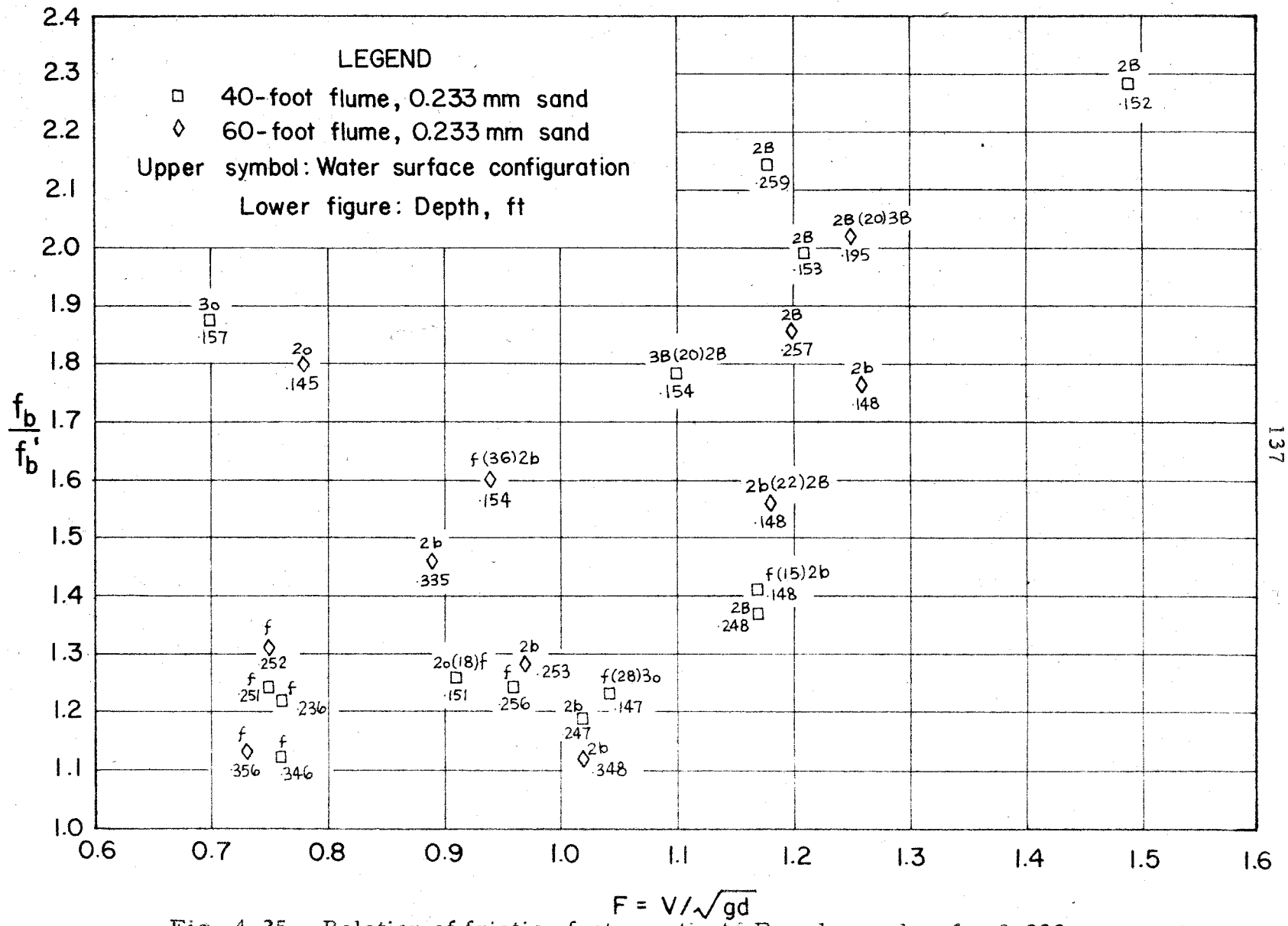

Fig. 4-25. Relation of friction factor ratio to Froude number for 0.233 mm sand.

factor. For a given Froude number the amount of wave activity depended on the depth and to a certain extent on the flume inlet condition. For these Froude numbers, f_b/f'_b increased as the depth increased or as the inlet condition was changed to produce more wave activity.

A comparison of Run 4-32 (F = 1.18) and Run 4-33 (F = 1.17, see example 11 and figure 4-20) illustrates this point. These runs had nearly the same Froude number but Run 4-32 had a depth of 0.259 ft compared to a depth of 0.248 ft for Run 4-33. Run 4-32 had waves that were much more active and broke more frequently and violently than those of Run 4-33. Accordingly, Runs 4-32 and 4-33 had friction factor ratios of 2.14 and 1.37 respectively.

A similar comparison of Run 4-28 of Group 2 and 4-22 of Group 3 illustrates the effect of the flume inlet. These runs had nearly the same depth and velocity, but Run 4-22 had more wave activity due to the screen placed at the entrance to the flume. The waves which did form in Run 4-28 broke quite weakly if at all. For Run 4-28, $f_b/f'_b = 1.41$ and for Run 4-11, $f_b/f'_b = 1.76$.

Several other examples can be drawn from the runs of Groups 2 and 3. These all conform to the principle outlined above. For a given Froude number in the regime where antidunes can form, f_b/f'_b increased as the amount of wave activity increased with Froude number and with depth for a fixed Froude number, and over a certain range of Froude numbers (cf. part d, section 5-3) the amount of wave activity was influenced by the inlet condition.

The runs of Group 1 did not have this multiplicity of friction

factor ratio. This was a result of the fact that the friction factors of flows over the coarser sand were unaffected by the presence of antidunes and stationary waves.

At high Froude numbers, the friction factors were in some cases smaller for flows over Sand 1 (D_g = 0.549 mm) than for comparable flows over Sand 2 (D_g = 0.233 mm). For example, Runs 5-9 (Sand 1) and 4-27 (Sand 2) had nearly the same depth and velocity, but the f_b-values were 0.0448 and 0.0512 respectively. The waves of Run 5-9 never broke while the waves of Run 4-27 had frequent, violent breaking. As is discussed in chapter 5, the increased wave activity with the finer sand was due to the fact that this sand was more easily transported and the perturbation velocities could rapidly form antidunes with breaking stationary waves. With the coarse sand (Run 5-9) the limiting height of the antidunes was not large enough to cause the waves to break. The energy dissipated in wave breaking accounted for the larger friction factor of Run 4-27.

e. Sediment transport characteristics. The sediment discharge rates are plotted against mean velocity in figure 4-26. The total transport rate for each sand can be approximated by an exponential relation of the form used in section 2-6 in analyzing the movement of antidunes. Thus, very roughly,

$$G = 0.31\,V^{3.4} \qquad (4\text{-}1)$$

for Sand 1 (D_g = 0.549 mm) and

$$G = 0.028\,V^{6.2} \qquad (4\text{-}2)$$

for Sand 2 (D_g = 0.233 mm). Depth had little effect on the transport rate in the range investigated ($0.074 < d < 0.356$ ft) but these relations

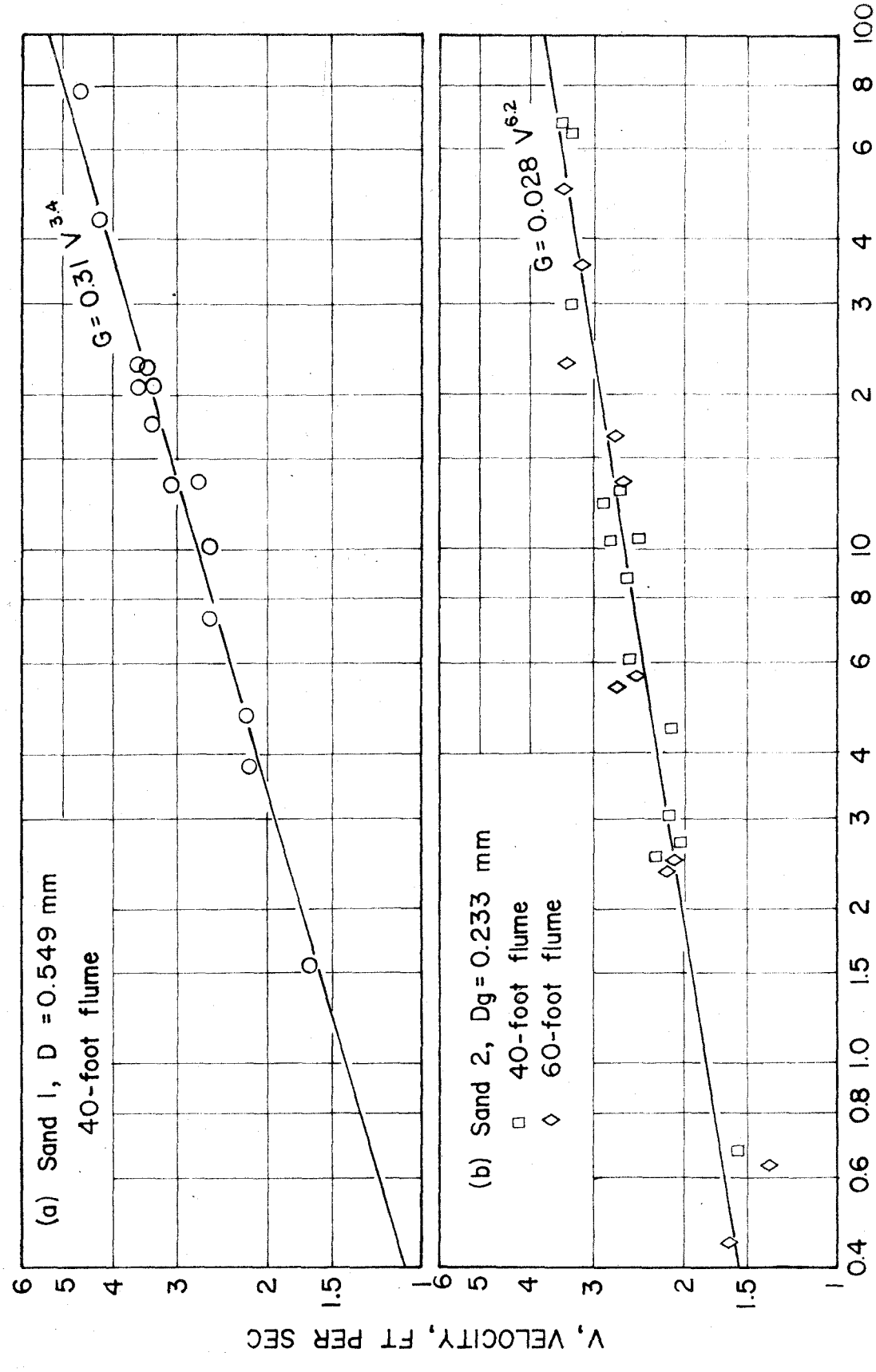

Fig. 4-26. Variation of sediment discharge rate with mean velocity.

are definitely not valid over a wide range of depth. The effects of waves and wave breaking are discussed in section 5-4.

In runs of Group 1 (coarse sand), the geometric mean diameter of the transported material was equal to or greater than the geometric mean size of the bed material in all but two cases (Runs 5-1 and 5-2). No explanation for this curious effect is offered here.

f. Summary. The conclusions regarding the friction factor and sediment transport characteristics of flows in the laboratory flumes may be summarized as follows:

(1) Flows using Sand 1 (D_g = 0.549 mm) have a single-valued friction factor for each depth and velocity. The friction factor is practically unaffected by the presence of antidunes and stationary waves. As the Froude number is increased, the friction factor generally decreases and approaches the value that would be expected for a flat bed and water surface.

(2) For flows over a bed composed of Sand 2 (D_g = 0.233 mm), the friction factor generally increases as the Froude number is increased. At depths and velocities for which the flow configuration is not unique the friction factor is not unique either. In these cases, the friction factor increases as the amount of wave activity increases.

(3) In the depth range investigated, the rate of sediment transport generally increases with velocity and can be very roughly expressed as

$$G = m V^n \qquad (2\text{-}32)$$

where m and n are constants which depend on the sand characteristics.

The validity of the conclusions can be assured only in the depth

range investigated. However, there is no reason to believe that the principles are not qualitatively accurate in general.

CHAPTER 5

DISCUSSION OF RESULTS

This chapter will extend the discussion given in chapter 4 in connection with the presentation of experimental results. In section 5-1, the measured wave lengths will be compared with the values given by the velocity-wave length relation derived in chapter 2. Then the mechanism of antidune formation and growth will be described in detail, and this description used to deduce the quantities involved in the criteria for the formation of antidunes and the occurrence of breaking waves. The work of previous investigators in this field will also be briefly considered. The effect of waves on the sediment transport rate will be discussed and the problem of stationary waves of finite amplitude of the waves will be posed. Finally, the limited data available on antidunes in natural streams will be presented and compared with the results of this investigation.

5-1. Velocity - Wave Length Relation

The measured wave lengths and corresponding mean velocities reported in table 4-1 are plotted in figure 5-1. The straight line represents the theoretical velocity-wave length relation for two-dimensional waves which was derived from the minimum energy hypothesis in section 2-4 (equation 2-23). The curved line represents the velocity-wave length relation derived in section 2-7 for three-dimensional waves (rooster tails),

$$V^2 = \frac{g\lambda}{2\pi}\sqrt{1 + \left(\frac{\lambda}{b}\right)^2}. \qquad (2\text{-}37)$$

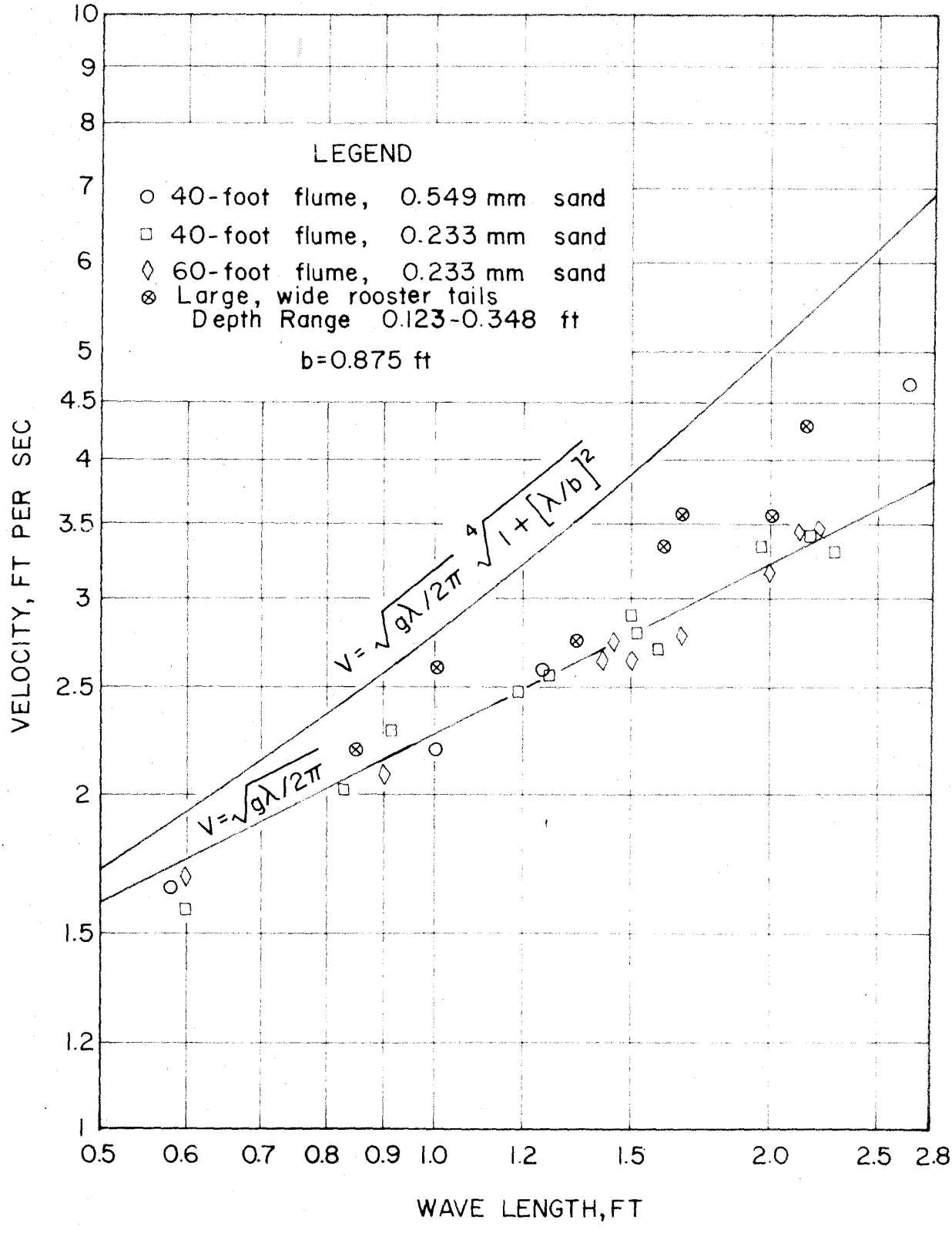

Fig. 5-1. Measured and computed values of wave length as a function of velocity for laboratory data.

In plotting figure 5-1, the wave length in the transverse direction, b, has been taken as the width of the 40-foot flume (b = 0.875 ft).

The agreement between the experimental points and the theoretical two-dimensional relation is well within the limits of experimental accuracy with the exceptions of Run 5-14 and those runs in the 40-foot flume which had large, wide rooster tails. For a given velocity, the wave length of the large rooster tails was smaller than the wave length of a two-dimensional wave. This agrees qualitatively with the theoretical three-dimensional solution (equation 2-37). This solution cannot be expected to be more than qualitatively accurate since the transverse wave length of the rooster tails, b, is not necessarily equal to the flume width. Further, as was discussed in section 4-2d, the boundary condition along the sides of rooster tails is quite nebulous and probably not the same as that used in obtaining the three-dimensional solution.

The effect of the shape of the waves on the velocity-wave length relation is illustrated by Run 5-3 (d = 0.245 ft, V = 2.18 ft/sec, λ = 1.00 ft, see figure 1-1) and Run 5-7 (d = 0.147, V = 2.60 ft/sec, λ = 1.00 ft). Both of these runs had the same wave length, but the waves of Run 5-3 were two-dimensional while Run 5-7 had large, wide rooster tails. Accordingly, the velocity-wave length relations conform quite well to the two-dimensional and three-dimensional solutions respectively.

Although the waves of Run 5-14 gave the impression of being predominately two-dimensional, their wave length did not agree with the two-dimensional solution. Close inspection of the waves (see figure 4-14) shows that the waves actually were slightly three-dimensional.

This relatively small transverse oscillation was probably responsible for the discrepancy.

5-2. Discussion of the Mechanism of Antidune Formation and Growth

a. Magnitude of the horizontal perturbation velocity at the level of the bed. For the discussion of this section, it will be convenient to have an expression for the horizontal perturbation velocity. The velocity potential of the perturbation velocities, $\overline{\phi}$, is the second term on the right of equation 2-13,

$$\overline{\phi} = \frac{A V}{\sinh k H} \cosh k (y+H) \cos k x. \qquad (5-1)$$

In the case of flow over antidunes, $H = \infty$ (see section 2-4) and

$$\overline{\phi} = A V e^{ky} \cos k x. \qquad (5-2)$$

The horizontal perturbation velocity is

$$\overline{\phi}_x = - A k V e^{ky} \sin k x. \qquad (5-3)$$

For flow over antidunes it was shown in section 2-4 that

$$V^2 = \frac{g \lambda}{2\pi} \qquad (2-23)$$

or

$$k = \frac{g}{V^2}. \qquad (5-4)$$

Substituting equation 5-4 into equation 5-3 yields

$$\overline{\phi}_x = - \frac{A g}{V} e^{gy/V^2} \sin k x. \qquad (5-5)$$

At the level of the bed ($y = - d$) the horizontal perturbation velocity,

u, is

$$u = -\frac{Ag}{V} e^{-1/F^2} \sin kx. \qquad (5\text{-}6)$$

The wave height, 2A, can have any value between zero and 0.142λ (see section 2-5). Thus when the ratio of wave height to the critical height for breaking is at a given value, the height is proportional to the wave length. Stated another way, when the waves of two different flows are at equivalent stages of development, the wave heights, 2A, are proportional to the respective wave lengths. Substituting $A = C_1\lambda$ and equation 2-23 into equation 5-6, gives

$$u = -2\pi C_1 V e^{-1/F^2} \sin kx. \qquad (5\text{-}7)$$

Equation 5-7 can be used to compare the magnitudes of u for different flows in which the wave heights are a given proportion of the critical value for breaking. The magnitude of u is seen to increase with velocity and Froude number.

b. The role of the perturbation velocities. Stationary waves in open channels can occur over a wide range of Froude numbers. If they do not arise spontaneously they can often be induced. The perturbation velocities which accompany these waves are responsible for the formation of antidunes. Under the wave troughs, the horizontal perturbation velocity and the flow velocity are in the same direction so the total horizontal velocity is greater than its mean value and local scour results. Conversely, under the wave crests the perturbation velocity opposes the flow velocity and local deposition results. This pattern of scour and deposition is called differential deposition. Differential deposition which occurs on a flat bed forms antidunes. Since

most of the sediment transport occurs near the level of the bed, it is the horizontal perturbation velocity in this vicinity which is important in causing differential deposition.

If the depth of flow, velocity, and sand size are such that dunes are present when stationary waves occur, the form of the dunes will be modified by the perturbation velocities if they are sufficiently large in the vicinity of the bed. The perturbation velocities cause the dunes to become periodically larger and more rounded than dunes which are not coupled with the free surface. Such dunes which are strongly coupled with the water surface are, by definition, also antidunes (see section 1-1 for definition). Text examples 1 and 2 (figures 4-6 and 4-7) of section 4-3 illustrate this type of flow. In this case, differential deposition does not actually form the antidunes, but it does modify their shape and size. No instances of this phenomenon occurring in natural streams have been reported and dunes strongly coupled with the water surface may be a laboratory curiosity. This type of antidune will not be considered further in this discussion.

In the more common situation in which antidunes form from a flat bed, as the amplitude of the antidunes increases due to differential deposition, the amplitude of the surface waves also increases. This increase in wave amplitude causes an increase in the magnitude of the perturbation velocity (see equation 5-6) which tends to increase the rate of differential deposition. However, as the antidunes become higher and steeper, the gravity force resisting the movement of sediment from antidune troughs to crests also increases. When the effects of gravity and the perturbation velocity balance each other, the antidunes

do not grow further. This limiting height of the antidunes depends on the depth of flow, mean velocity, and transport characteristics of the sand. If the wave steepness corresponding to this limiting height exceeds the critical value, the waves will break.

Even though the antidunes have reached their limiting height, they can move upstream since scour still occurs on the downstream slopes and sediment is deposited on the upstream slopes. However, no further deposition occurs at the peaks of the antidunes and no further scour occurs at the bottoms of the troughs. Thus, at the limiting height, differential deposition causes the antidunes to move upstream but does not increase their height. A more complete discussion of antidune movement is given in section 2-6.

c. Importance of the transport capacity of a stream for its bed material. In section 4-4 it was shown that the measured sediment transport rates were roughly proportional to a power of the mean velocity. This power, n, was 3.4 for Sand 1 (D_g = 0.549 mm) and 6.2 for Sand 2 (D_g = 0.233 mm). Other investigators have also found that the transport rate can be expressed as a power (usually greater than three) of the mean velocity if the sediment is transported primarily as bed load. It therefore seems not unreasonable to expect that the local transport rate is proportional to a power of the local total horizontal velocity.* If this is the case, the small relative changes in the total local velocity due to the perturbation velocity can result in a large relative change in the local transport capacity. Thus the perturbation

* This is one of the assumptions which was made in investigating the movement of antidunes. See section 2-6.

velocities which are quite small, and could not themselves transport enough sediment from crests to troughs to form antidunes, can affect the local transport of the stream and cause the differential deposition which forms antidunes.

Since the local transport rate is proportional to a power greater than unity of the local velocity (by assumption), the rate of differential deposition caused by a perturbation velocity of a given magnitude will depend on the flow velocity and thus the gross transport rate. Thus, if the transport rate is low, even relatively large perturbation velocities can cause very little differential deposition and the antidunes which form (if any) are of vanishingly small amplitude. At the other extreme, no antidunes will form, regardless of how high the transport rate is, unless the horizontal perturbation velocity in the vicinity of the bed is large enough to affect the local transport capacity and cause differential deposition.

This consideration points out the importance of the transport capacity of a stream for its bed material in determining the behavior of the flow. At a given depth of flow and velocity, perturbation velocities which do not cause significant differential deposition of one sand can be sufficient to form antidunes of appreciable magnitude on a bed of finer, more easily transported sand. Likewise, the transport capacity is important in determining how frequently antidunes form, their rate of growth, and whether the limiting height of the antidunes will be such that the waves break.

5-3. Criteria for the Formation of Antidunes and Breaking Waves

a. Discussion of criteria. If the depth of flow, velocity, and

sand size are such that only minimal differential deposition occurs, the largest antidunes that form will be of vanishingly small amplitude. As the depth and/or velocity are changed to increase the rate of differential deposition, a point will be reached at which antidunes can be discerned. This point is not at all well defined and its detection depends greatly on the eyesight and judgment of the observer. It therefore seems somewhat meaningless to speak of a criterion for the formation of antidunes. A ratio of antidune height to wave length might be defined above which, by definition, antidunes are said to exist, but this would be hard to measure and would serve little useful purpose. A more meaningful criterion, and the one which will be considered here, is the criterion for the occurrence of breaking waves. This condition is more easily recognized.

When speaking of a criterion for the occurrence of breaking waves (or antidunes) it must be borne in mind that over a certain range of depth and velocity the bed and water surface will be flat unless the flow is disturbed to form an initial wave. In this range, the criterion will tell whether breaking waves (or antidunes) <u>can</u> form.

The formation of antidunes and of breaking waves--indeed, the whole antidune phenomenon--is intimately related to the transport of sediment. As has been pointed out repeatedly in previous chapters, the physical laws governing this transport are unknown. Thus only an empirical criterion can now be given for the occurrence of breaking waves. Assumed transport laws can be used in connection with the potential flow theory of chapter 2 and section 5-2 to investigate the behavior of the flow. However, the results of such analyses are at

best only qualitatively correct and they may actually be misleading.

b. Criterion for the occurrence of breaking waves. In the depth range investigated ($0.074 < d < 0.356$ ft), wave breaking appeared to be related to Froude number, as shown in figures 4-21, 4-22 and 4-23. For Sand 1 ($D_g = 0.549$ mm), breaking waves in the Froude number range $0.7 < F < 1.0$ were induced by the dunes which formed. The waves also broke if the Froude number was greater than 1.8, provided the depth was larger than 0.10 ft. For Sand 2 ($D_g = 0.233$ mm), breaking waves could occur if the Froude number was greater than about 0.9.

Over a wide range of depth, these values of Froude number can not be expected to be the correct criterion for the occurrence of breaking waves. The Froude number partially describes the hydraulic properties and magnitude of the perturbation velocities of a given flow (see equation 5-7) but it says nothing about the transport characteristics over a wide range of depth. Any criterion which does not include the transport capacity of a stream for its bed material cannot be valid except for a limited range of depth.

For example, consider a flow which is much deeper than those of this investigation. The velocity increases as the square root of the depth for constant Froude number and the sediment transport rate generally increases as some higher power of the velocity (usually greater than three). Equation 5-7 shows that the magnitude of the horizontal perturbation velocity at the level of the bed also increases with velocity. Consequently, an increase in depth at constant Froude number leads to a relatively large increase in the sediment transport

rate and the differential deposition caused by the perturbation velocity. Thus a flow at one depth with a certain Froude number might not have breaking waves while another flow with the same Froude number but a larger depth could have active wave breaking. It would be expected then that the critical Froude number for a given sand above which breaking waves can occur would decrease as the depth increases.

Conversely, as the depth decreases, the Froude number above which breaking waves can form would be expected to increase for a given sand. This was observed to be the case. Runs 5-11, 5-12, 5-13 and 5-18 had depths less than 0.1 ft and Froude numbers of 2.00, 2.04, 1.86 and 1.82 respectively. In Runs 5-11, 5-12 and 5-13 the bed and water surface were flat. In Run 5-18, waves and antidunes were induced at the upstream end of the flume. These waves persisted to about station 20 (roughly ten wave lengths from the point where the flow was disturbed) and downstream from this station the bed and water surface were flat.

5-4. Discussion of Gilbert's Experiments and Langbein's Criterion for Antidunes

The classical experiments by Gilbert (8) were discussed in section 1-2. Gilbert conducted runs in systematic groups, each with a constant discharge. For each of these constant discharges, the depth, velocity, slope and bed configuration were obtained for different rates of sediment transport. As the sediment load was increased, the depth decreased and the velocity increased. At low sediment loads dunes formed. As the transport rate and velocity increased, the dunes gave way to a flat bed which persisted until at still higher velocities,

antidunes formed. A comparison of Gilbert's runs using Sand C (mean diameter = 0.506 mm) with comparable runs of this investigation from Group 1 (D_g = 0.549 mm) indicates that many of Gilbert's flows which had a flat bed would probably have had antidunes if the water surface had been disturbed to initiate surface waves; i.e. many of the flows in which Gilbert observed a flat bed were in the regime where the flow configuration is not unique. Such a comparison is shown in table 5-1.

Table 5-1

Comparison of Flume Experiments

	Gilbert	Author	Author
Run no.	--	5-17*	5-16**
Mean sand size, mm	0.506	0.549	0.549
Flume width, ft	1.32	0.875	0.875
Depth, ft	0.149	0.146	0.154
Velocity, ft/sec	3.73	3.56	3.45
Froude number	1.70	1.64	1.55
Slope	0.0115	0.0154	0.0134
Bed configuration	flat	antidunes	flat

* See example 4, section 4-3 and figures 4-11 and 4-12.

** See example 4, section 4-3 and figure 4-10.

In the flume used by Gilbert, the water entered the channel from a large stilling box and probably received very little disturbance. Thus Gilbert's data cannot be used to determine the minimum Froude number for a given depth above which antidunes <u>can</u> form if the flow is disturbed. If Gilbert had used a different flume entrance, many of the

flows which had a flat bed probably would have had antidunes.

Langbein (10) made a dimensional analysis of Gilbert's data and presented the following criterion for the formation of antidunes:

$$\frac{V}{\sqrt{gr}} > i(Vr)^j \qquad (5\text{-}8)$$

where the constants i and j depend on the sand size and are presented in table 5-2. Gilbert's data covered the range $0.1 < Vr < 0.6$ ft^2/sec.

Table 5-2

Constants for Longbein's Criterion (Equation 5-8)

Mean Sand Size mm	i	j
0.305	1.07	-0.14
0.375	1.13	-0.24
0.506	1.60	-0.06

Langbein's criterion is not valid to the extent that Gilbert's data are misleading in determining the conditions for which antidunes can form. The criterion is valid only for determining the flow conditions for which antidunes formed in Gilbert's flume. Because the entrance to Gilbert's flume gave the flow very little disturbance, antidunes can occur at lower values of $\frac{V}{\sqrt{gr}}$ than indicated by Langbein's criterion. In section 5-7 it is shown that Langbein's criterion does not accurately predict the occurrence of antidunes in natural streams either.

The use of the hydraulic radius, r, instead of the flow depth is not correct since the depth is the important dimension in considerations

of the wave mechanics, energy, and local transport characteristics of a flow. A comparison of results from the two different flumes used in this investigation indicated that the flume width (and thus r for a constant depth) had little effect on the formation and behavior of antidunes.

5-5. Effect of Waves on Sediment Transport Rate

Apparently, surface waves which do not break have little effect on the transport rate of a stream. For example, Run 5-16 (d = 0.154 ft, V = 3.45 ft/sec, F = 1.55, see figure 4-9) had a flat bed and water surface while Run 5-17 (d = 0.146 ft, V = 3.56 ft/sec, F = 1.64, see figure 4-10) had induced antidunes and waves which did not break. The transport rates for these two runs were 22.5 lb/ft-min and 20.6 lb/ft-min respectively. Much of this difference could have been due to experimental error and it is not significant.

Active wave breaking, however, greatly increases the rate of sediment transport since the agitation accompanying breaking is very effective in entraining bed material. For example, Runs 4-27 (d = 0.152 ft, V = 3.29 ft/sec, F = 1.49, see figure 4-19) and Run 4-33 (d = 0.248, V = 3.30 ft/sec, F = 1.17, see figure 4-20) had very nearly the same velocity, but different depths. If both flows had been steady and uniform, the deeper flow, Run 4-33, would have been expected to have a slightly larger sediment discharge, if there were any difference at all. Actually, both runs had antidunes and breaking waves. The waves of Run 4-27 broke much more frequently and violently (compare figures 4-19 and 4-20), giving a sediment transport rate of 65.2 lb/ft-min compared to 30.0 lb/ft-min for Run 4-33 which had much less wave

activity.

5-6. Stationary Waves of Finite Amplitude

In the analytical considerations of chapter 2 from which the velocity-wave length relation was derived, it was assumed that the waves are of vanishingly small amplitude. It was then shown by the minimum energy hypothesis that flow over antidunes corresponds to the top part of a gravity wave in a fluid of infinite depth. The celerity of this wave is equal to the flow velocity so it appears stationary. The experimental results agreed with the velocity-wave length relation of this linearized theory (see section 5-1).

However, the stationary waves which accompany antidunes usually do not have small amplitudes. As soon as antidunes are initiated the amplitudes of both the antidunes and stationary waves increase, and the wave amplitude often reaches the critical value for breaking. The celerity of waves of finite amplitude is given by Keulegan (25) as

$$c^2 = \frac{g\lambda}{2\pi}\left(1 + A^2k^2 + \frac{1}{2}A^4k^4 + \cdots\right) \qquad (5\text{-}9)$$

where A is the wave amplitude and k the wave number. The celerity increases with amplitude and the celerity of the highest wave which can occur $(2A_c = 0.142\lambda)$ is about ten percent greater than one of negligible amplitude.

This consideration leads to an apparent inconsistency. The wave length of the antidunes and stationary waves is determined when they first are initiated. At this stage, the amplitude of the surface waves is very small and the wave length is selected so that the wave celerity is equal to the flow velocity,

$$\lambda = \frac{2\pi V^2}{g}. \qquad (2\text{-}23)$$

As the antidunes become higher, the amplitudes of the surface waves increase but the wave length cannot change since this would displace adjacent waves in the train. Equation 5-9 shows that the wave celerity also increases. This raises the question of how waves of finite amplitude persist over antidunes when the initial velocity-wave length relation is that for waves of negligible amplitude (equation 2-23). The upstream movement of the antidunes is much too slow to account for this difference.

The increase in celerity with amplitude might be instrumental in causing the breaking of the waves. With increasing amplitude, the wave configuration has a stronger tendency to move upstream relative to the antidunes. This tendency of the wave crests to move toward the antidune troughs might possibly precipitate breaking. The close agreement between the theoretical value of critical wave height given in section 2-5 and the measured values given in the fifth column of table 4-1 indicates in any event that waves break when their height is at or near the maximum possible value.

5-7. Antidunes and Stationary Waves in Natural Streams

a. General. Most natural streams have cross-sections which are quite irregular. A typical example is shown in figure 5-2. In sections of this form the local depth and velocity vary across the section and consequently dunes, flat bed, and antidunes often occur simultaneously in different parts of the stream. For example at the location on the Virgin River shown by figures 5-2 and 5-3, dunes

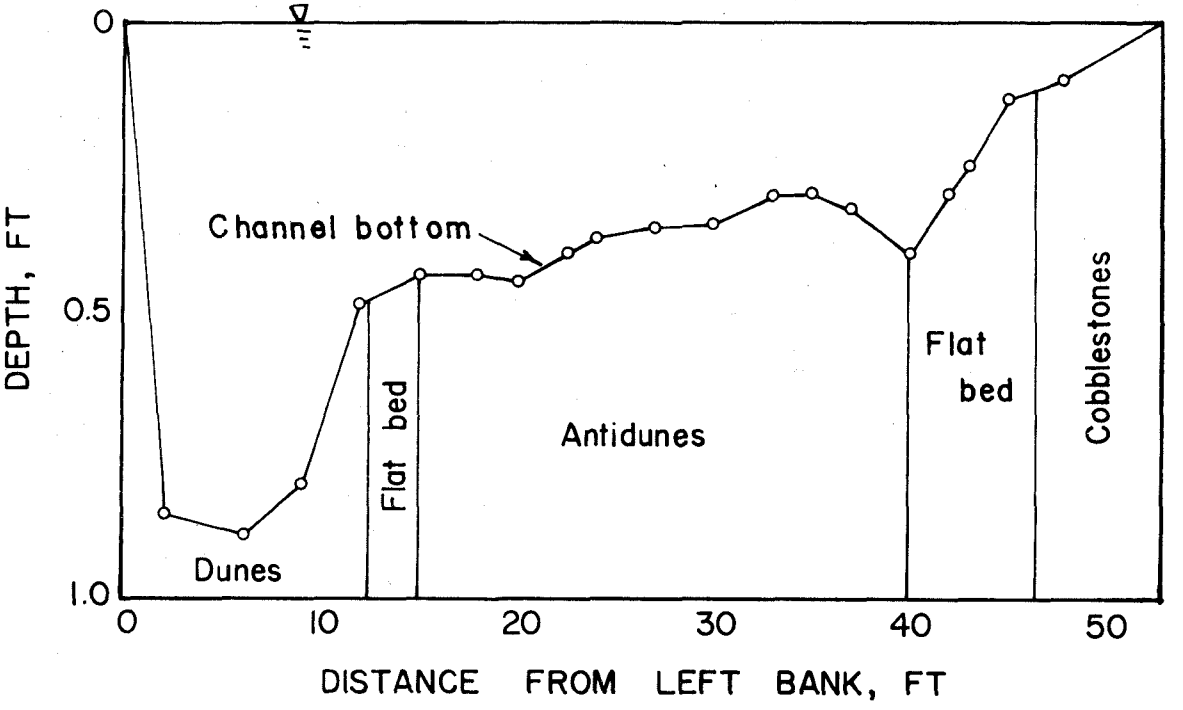

Fig. 5-2. Cross section (looking downstream) of Virgin River near St. George, Utah.

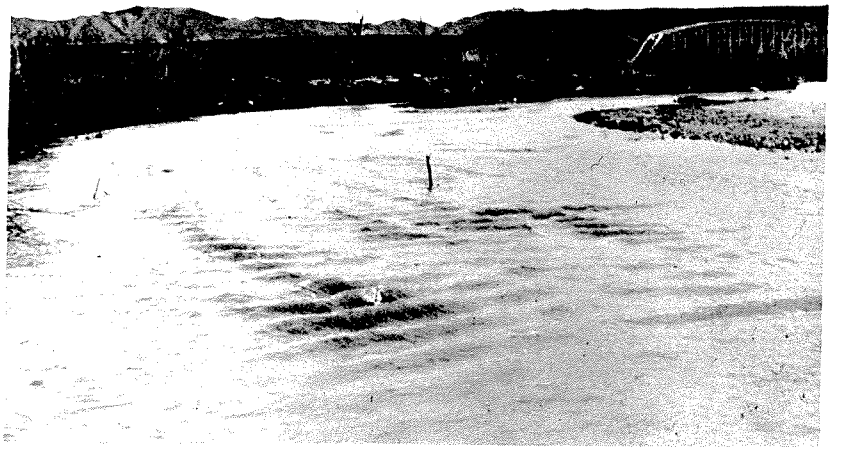

Fig. 5-3. Downstream view of Virgin River at location of cross section shown in figure 5-2.

occurred in the deep part at the left, while antidunes occupied the shallower central portion. The bed was flat in the regions adjacent to the antidunes and the region at the far right was covered with cobblestones.

The occurrence and characteristics of antidunes and their stationary waves depend only on the local depth, velocity, and size of bed material; consequently it is these local parameters which must be used in all considerations involving antidunes and stationary waves. Any analysis pertaining to antidunes which is based on the mean velocity (Q/A) and the mean depth (area divided by surface width) for the whole section will invariably lead to erroneous conclusions unless the stream is rectangular or very nearly so.

b. Summary of field data. Very little quantitative information on antidunes and stationary waves is available. Table 5-3 summarizes all of the data presently available to the writer. The depths and velocities given in columns 1 and 2 respectively are the mean values in the region where antidunes occurred. An estimate of the accuracy of the data, based on the conditions under which it was obtained, is included for each flow in column 6. The stationary waves of the Virgin and Little Colorado Rivers were actively breaking. The exact details of the surface configurations for the other rivers are not known but the field notes gave the impression that the waves were breaking.

The velocity-wave length data of table 5-3 for the natural streams are plotted in figure 5-4. The agreement with the theoretical relation derived in section 2-4 is good considering the poor accuracy of much of the data.

Table 5-3

Summary of Data for Flow over Antidunes in Natural Streams [a]

No.	1 d Depth ft.	2 V Velocity ft/sec	3 F Froude Number	4 λ Wave Length ft	5 D_g Bed Material Size mm	6 Estimated Accuracy	7 River	8 Location
1	0.23	2.48	0.91	1.25	0.157	Good	Little Colorado	Cameron, Arizona
2	0.40	3.25	0.91	2.10	0.185	Good	Virgin [b]	St. George, Utah
3	0.18	3.2	1.33	1.5	0.45	Poor	Gravel Pit Runoff	Byhalia, Miss.
4	0.2	2.1	0.8	1.1	0.32	Fair	Laboratory Creek	Pigeon Roost Watershed, Miss.
5	0.47	3.80	0.98	2.6	0.41	Good	Pigeon Roost Creek	ARS Sta. 12, Pigeon Roost Watershed, Miss.
6	0.62	4.32	0.97	3.2	0.41	Good	Pigeon Roost Creek	ARS Sta. 12, Pigeon Roost Watershed, Miss.
7	0.8	4.9	0.97	4.0	0.38	Good	Dry Fork Creek	ARS Sta. 10, Pigeon Roost Watershed, Miss.
8	1.3	5.4	0.83	7.1	0.38	Fair	Dry Fork Creek	ARS Sta. 10, Pigeon Roost Watershed, Miss.
9	1.38	6.56	0.98	11.	0.38	Good [c]	Dry Fork Creek	ARS Sta. 10, Pigeon Roost Watershed, Miss.
10	3.0	8.0	0.81	10.	0.46	Poor	Cuffawa Creek	ARS Sta. 32, Pigeon Roost Watershed, Miss.
11	3.1	6.5	0.65	15.	0.41	Poor	Pigeon Roost Creek	ARS Sta. 17, Pigeon Roost Watershed, Miss.
12	4.0	7.7	0.68	14	0.41	Poor	Pigeon Roost Creek	ARS Sta. 34, Pigeon Roost Watershed, Miss.

(a) Data on streams of the Pigeon Roost Watershed was supplied by the Agricultural Research Service (ARS) of the U. S. Department of Agriculture.

(b) See figures 5-2 and 5-3.

(c) This value of wave length is open to some question as there was a discrepancy in the field notes.

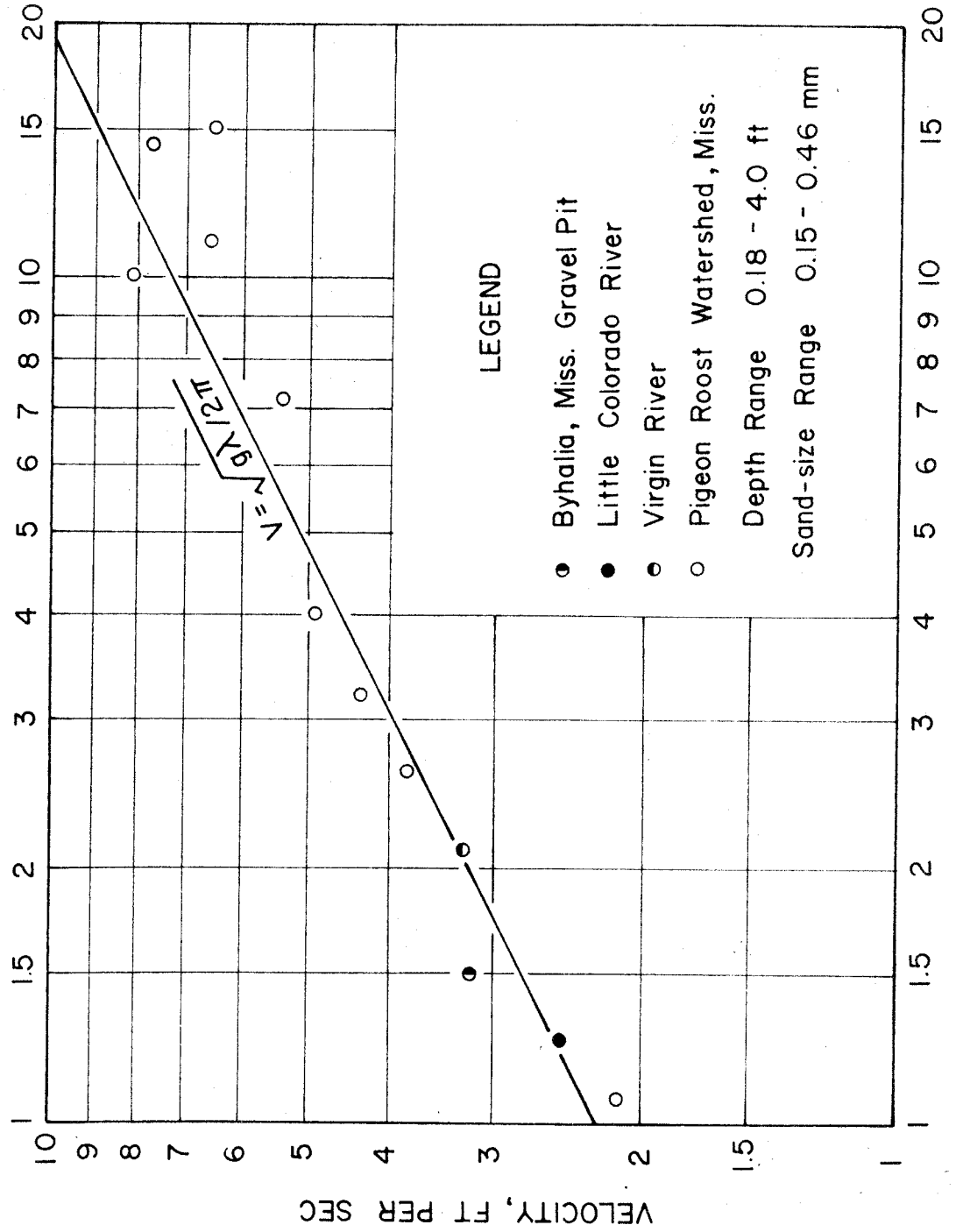

Fig. 5-4. Measured and computed values of wave length as a function of velocity for data from natural streams.

In the discussion of section 5-3, it was hypothesized that the critical Froude numbers for the formation of antidunes and stationary waves decrease as depth increases. The flows of table 5-3 which had depths greater than three feet (Nos. 10, 11 and 12) had antidunes and stationary waves at Froude numbers of only 0.81, 0.65 and 0.68 respectively. In laboratory flows at smaller depths using a finer sand (D_g = 0.233 mm) breaking waves did not occur at Froude numbers less than 0.9. This indicates that the hypothesis may be correct.

The sand sizes of flows No. 3 through 12 are in the range covered by Langbein's criterion. According to this criterion, assuming the depth can be used as the hydraulic radius for these wide flows, none of these flows would have had antidunes.

CHAPTER 6

SUMMARY OF CONCLUSIONS

The following conclusions are based on a comprehensive theoretical and experimental study of the occurrence and characteristics of antidunes and associated stationary waves, including their effects on the friction factor and sediment transport capacity of alluvial streams. The two different sands used in the laboratory investigation had geometric mean sieve diameters of 0.55 mm and 0.23 mm.

The principal conclusions may be summarized as follows:

1. It was shown that potential flow over a wavy bed is the same as the segment of flow above an intermediate streamline at mean depth d of the fluid motion accompanying a train of stationary gravity waves in a fluid with a horizontal bottom at mean depth H. The wave is made stationary by imposing on the fluid a uniform velocity equal and opposite to the wave celerity. For a given velocity, the wave length is related only to the depth to the horizontal bottom, H.

2. In the case of flow over an erodible sand bed, the flow deforms the bed by scour and deposition. Since there is theoretically an infinite number of possible wave lengths and shapes for the waves and antidunes, it was hypothesized that, for a given flow velocity, the flow shapes the sand bed to conform to a streamline of the fluid motion accompanying the stationary gravity wave with the minimum energy. It was also assumed that the potential flow solution is applicable to the real fluid flow over a deformable sand bed. The minimum energy flow corresponds to the case $H = \infty$ in the solution mentioned in conclusion 1. Thus, under this representation, flow over antidunes is the same as the segment of flow above an intermediate streamline of the fluid motion

associated with a stationary gravity wave in a fluid of infinite depth.

3. It follows from this representation of flow over antidunes that the relation between the mean flow velocity, V, and the wave length, λ, of the stationary waves and antidunes is given by

$$V^2 = \frac{g\lambda}{2\pi}. \qquad (2\text{-}23)$$

The wave length is independent of the depth of flow, d, and thus of the Froude number also. Measured values of velocity and wave length from laboratory and field data were in good agreement with this relation when the waves were two-dimensional.

4. When three-dimensional surface waves (rooster tails) formed, the wave length was smaller than that of two-dimensional waves for a given flow velocity.

5. Two-dimensional waves broke when the ratio of wave height to wave length (wave steepness) reached a value of approximately 0.14. This agrees with the theoretical value for deep water waves.

6. Over a limited range of depth and velocity, stationary waves and antidunes formed only if an initial surface wave was induced; i.e., the flow configuration was not unique. If the flow was undisturbed, the bed and water surface were flat over the whole length of the flume. If a disturbance was induced to form an initial surface wave, stationary waves and antidunes propagated downstream and occurred in all parts of the flume. When the disturbance was removed, the bed and water surface again became flat.

7. Antidunes are the result of a pattern of scour and deposition which is caused by the perturbation velocities accompanying stationary waves. The frequency of antidune formation, the rate of antidune growth,

and the breaking of the waves all depend on the local rate of sediment transport. Therefore, no general criterion for the formation of antidunes or the occurence of breaking waves can be given until the laws governing the transport of sediment are known. Further, any criterion which does not include the transport capacity of a stream for its bed material is not adequate. At the present time, only empirical criteria are reliable.

8. The results of this investigation, a study of available field data, and considerations of the mechanism of antidune formation and growth indicated that the critical Froude number for the occurrence of breaking waves (a) decreases as the depth of flow is increased, and (b) decreases as the sand size is decreased and the sediment becomes more easily transported.

9. Stationary waves which did not break had little effect on the sediment transport capacity or the friction factor of the stream.

10. Stationary waves which broke increased the gross sediment transport capacity and the friction factor of the stream. The increase in transport capacity was due to the sediment entrainment caused by the agitation accompanying breaking. The increase in friction factor was due to the energy dissipation in wave breaking. These effects became more pronounced as the breaking became more frequent and violent.

11. The following observations are based on the laboratory experiments with the 0.55 mm sand with flows in the depth range $0.123 < d < 0.346$ ft:

(a) Three-dimensional waves were the dominant wave form.

(b) The effective roughness of the stream generally decreased

with increasing Froude number.

(c) Wave breaking had relatively little effect on the transport capacity or the effective roughness of the stream.

12. The following observations are based on the laboratory experiments with the 0.23 mm sand with flows in the depth range between 0.145 and 0.356 ft.

(a) Two-dimensional waves were the dominant wave form.

(b) Breaking waves could occur if the Froude number was greater than approximately 0.9.

(c) The effective roughness of the stream generally increased with Froude number.

(d) Wave breaking caused relatively large increases in the transport capacity and effective roughness of the stream.

(e) For a given depth and velocity, waves formed more frequently and broke more violently with the 0.23 mm sand than with the 0.55 mm sand.

APPENDIX

SUMMARY OF NOTATION

The following summary omits, for simplicity, definitions of letters of secondary importance which appear only in a single section. The symbols used in chapter 4 to describe the bed and water surface configurations and the conditions under which the runs were carried out are defined in connection with table 4-1 and are not repeated here.

The page numbers listed refer to the page on which each symbol first appears.

			Page
a	=	amplitude of antidunes.	18
A	=	amplitude of surface waves.	17
$2A_c$	=	critical height for breaking of surface waves.	25
A	=	cross sectional area of the stream.	69
A_b	=	part of cross sectional area associated with the bed.	71
A_w	=	part of cross sectional area associated with the walls.	71
b	=	width of rectangular channel.	28
b	=	transverse wave length of three-dimensional waves.	28
c	=	wave celerity.	15
$\overline{C}$	=	sediment discharge concentration.	131
d	=	depth of flow.	13
D_g	=	geometric mean sieve diameter.	76
f	=	complex potential = $\phi + i\psi$.	17
f	=	Darcy-Weisbach friction factor for channel = $8\left(\frac{U_*}{V}\right)^2$.	70
f'_b	=	friction factor determined from pipe-friction diagram using r_b as the characteristic length and D_g as the size of the roughness elements.	131

Page

f_b = friction factor for bed alone calculated from side-wall correction procedure = $8\left(\frac{U^* b}{V}\right)^2$. 72

f_w = friction factor for walls. 72

F = Froude number = $\frac{V}{\sqrt{gd}}$. 58

g = acceleration due to gravity. 14

G = total sediment discharge per unit width. 15

$G(x)$ = local sediment transport rate per unit width. 26

H = distance from water surface to virtual horizontal bottom. 15

k = wave number = $\frac{2\pi}{\lambda}$. 15

m, n = constants in the assumed and observed transport relations, $G(x) = m\left[V(x)\right]^n$ and $G = mV^n$. 26

p = wetted perimeter of the stream. 69

p_b = wetted perimeter of the bed section. 72

p_w = wetted perimeter of the wall section. 72

P = potential energy per wave length. 20

$\overline{P}$ = average potential energy per unit length. 20

q = discharge per unit width = Vd. 14

$\vec{q}$ = vectorial velocity = $\nabla \phi$. 13

Q = total discharge. 60

r = hydraulic radius = A/p. 69

r_b = bed hydraulic radius = A_b/p_b. 72

r_w = wall hydraulic radius = A_w/p_w. 72

R = Reynolds number = $\frac{4Vr}{\nu}$. 72

R_w = Reynolds number for wall section = $\frac{4Vr_w}{\nu}$. 72

S = slope of energy grade line. 58

S_f = slope of flume 58

T	=	water temperature.	131
T	=	kinetic energy per wave length.	21
$\overline{T}$	=	average kinetic energy per unit length.	21
u	=	horizontal perturbation velocity at the level of the bed.	147
U_*	=	shear velocity for whole channel $= \sqrt{grS}$.	61
U_{*_b}	=	shear velocity for bed $= \sqrt{gr_b S}$.	73
V	=	mean velocity.	13
V_a	=	velocity of antidune movement.	25
x	=	horizontal coordinate.	13
y	=	vertical coordinate.	13
y	=	elevation of water surface relative to carriage rails.	55
y_b	=	elevation of bed relative to carriage rails.	58
z	=	complex number $= x+iy$.	17
β	=	bulk specific weight of sand in bed.	15
γ	=	unit weight of water $= \rho g$.	69
η	=	form of bed profile.	14
ζ	=	form of water surface profile.	14
λ	=	wave length.	17
ν	=	kinematic viscosity of water.	72
ρ	=	mass density of water.	20
σ_g	=	geometric standard deviation of the sand-size distribution.	76
τ_o	=	shear stress on the boundary.	69
$\overline{\tau}_o$	=	average shear stress on the entire boundary.	69
ϕ	=	velocity potential.	13
$\overline{\phi}$	=	velocity potential of perturbation velocities.	13
ψ	=	stream function.	17

REFERENCES

1. Vanoni, Vito A., and Brooks, Norman H., "Laboratory Studies of the Roughness and Suspended Load of Alluvial Streams," Sedimentation Laboratory, California Institute of Technology, Pasadena, Calif., Report No. E-68, Dec. 1957.

2. Simons, D. B., and Richardson, E. V., Discussion of Reference 19, Proc. Am. Soc. Civ. Engrs., J. of the Hydraulics Division, Vol. 85, No. HY 12, Paper 2271, Dec. 1959, pp. 110-112.

3. Lamb, Horace, Hydrodynamics, Dover Publications, New York, 1945.

4. Milne-Thomson, L. M., Theoretical Hydrodynamics, MacMillan Co., New York, 1955.

5. Cornish, Vaughan, "On Kumatology: The Study of Waves and Wave Structures of the Atmosphere, Hydrosphere, and Lithosphere," Geophysical Journal, Vol. 13, 1899, pp. 624-625.

6. Owens, John S., "Experiments of the Transporting Power of Sea Currents," Geographical Journal, Vol. 31, 1908, pp. 421-425.

7. Murphy, E. C., "The Behavior of a Stream Carrying Sand and the Effect of Sand on the Measurement of Bottom Velocity," Engineering News, Vol. 63, No. 20, 1910, pp. 580-581.

8. Gilbert, Grove Karl, "The Transportation of Debris by Running Water," U. S. Geological Survey, Professional Paper No. 86, 1914.

9. Pierce, Raymond C., "The Measurement of Silt-Laden Streams," U. S. Geological Survey, Water-Supply Paper No. 400, 1916, pp. 42-43.

10. Langbein, Walter B., "Hydraulic Criteria for Sand-Waves," Trans. Am. Geophys. Un., Part II, 1942, pp. 615-621.

11. Ursell, F., "Wave Generation by Wind," Surveys in Mechanics, G. I. Taylor 70th Anniversary Volume, ed. by G. K. Batchelor and R. M. Davies, Cambridge Press, London, 1956, pp. 216-249.

12. Vitousek, Martin J., "Some Flows in a Gravity Field Satisfying the Exact Free Surface Condition," Applied Mathematics and Statistics Laboratory, Stanford Univ., Calif., Tech. Rep. No. 25, Nov. 1954.

13. Lewy, H., "On Steady Free Surface Flow in a Gravity Field," Comm. Pure and Appl. Math., Vol. 5, 1952, pp. 413-414.

14. Michell, J. H., "The Highest Waves in Water," Phil. Mag., Vol. 36, 1893, pp. 430-437.

15. Fuchs, Robert A., "On the Theory of Short-Crested Oscillatory Waves," Gravity Waves, National Bureau of Standards Circular 521, 1952, pp. 187-200.

16. Vanoni, Vito A., "Transportation of Suspended Sediment by Water," Trans. Am. Soc. Civ. Engrs., Vol. 111, 1946, pp. 67-133.

17. Ismail, Hassan, "Turbulent Transfer Mechanism and Suspended Sediment in Closed Channels," Trans. Am. Soc. Civ. Engrs., Vol. 117, 1952, pp. 409-446.

18. Brooks, Norman H., "Mechanics of Streams with Movable Beds of Fine Sand," Trans. Am. Soc. Civ. Engrs., Vol. 123, 1958, pp. 526-549.

19. Vanoni, Vito A., and Nomicos, George N., "Resistance Properties of Sediment-Laden Streams," Proc. Am. Soc. Civ. Engrs., J. of the Hydraulics Division, Vol. 85, No. HY 5, Paper 2020, May 1959, pp. 77-107.

20. Brooks, Norman H., "Laboratory Studies of the Mechanics of Streams Flowing over a Movable Bed of Fine Sand," Ph.D. Thesis, California Institute of Technology, Pasadena, Calif., 1954.

21. Nomicos, George N., "Effects of Sediment Load on the Velocity Field and Friction Factor of Turbulent Flow in an Open Channel," Ph.D. Thesis, California Institute of Technology, Pasadena, Calif., 1956.

22. Johnson, J. W., "The Importance of Side-Wall Friction in Bed-Load Investigations," Civil Engineering, Vol. 12, No. 6, June 1942, pp. 329-331.

23. Otto, George H., "A Modified Logarithmic Probability Graph for the Interpretation of Mechanical Analysis of Sediments," J. of Sedimentary Petrology, Vol. 9, No. 2, 1939, pp. 62-76.

24. Taylor, G. I., "An Experimental Study of Standing Waves," Proc. Royal Soc. of London, Series A, Vol. 218, June-July 1953, pp. 44-59.

25. Keulegan, G. H., "Wave Motion," Engineering Hydraulics, ed. by H. Rouse, Wiley and Sons, New York, 1950, pp. 711-768.